WHOI-2008-03

Woods Hole Oceanographic Institution

NPAL04 OBS Data Analysis Part 1: Kinematics of Deep Seafloor Arrivals

by

Stephen, R.A., Bolmer, S.T., Udovydchenkov, I., WHOI
Worcester, P.F., Dzieciuch, M.A., Van Uffelen, L., SIO
Mercer, J.A., Andrew, R.K., Buck, L.J. APL/UW
Colosi, J.A., NPGS
Howe, B.M., SOEST/UH

December 2008

Technical Report

Funding was provided by the Office of Naval Research
through Contract No. N00014-06-1-0222.

WHOI-2008-03

NPAL04 OBS Data Analysis Part 1: Kinematics of Deep Seafloor Arrivals

by

Stephen, R.A., Bolmer, S.T., Udovydchenkov, I., WHOI
Worcester, P.F., Dzieciuch, M.A., Van Uffelen, L., SIO
Mercer, J.A., Andrew, R.K., Buck, L.J. APL/UW
Colosi, J.A., NPGS
Howe, B.M., SOEST/UH

December 2008

Technical Report

Funding was provided by the Office of Naval Research through
Contract No. N00014-06-1-0022.

Approved for Distribution:

Maurice Tivey

Maurice Tivey, Chair

Department of Geology and Geophysics

Abstract

These notes provide supporting information for a JASA (Journal of the Acoustical Society of America) LttE (Letter to the Editor) manuscript, "Deep seafloor arrivals: A new class of arrivals in long-range ocean acoustic propagation" (Stephen *et al.*, submitted). It addresses five issues raised by the co-authors: 1) incorrect processing for the time-compressed traces at T2300 and T3200 that appeared in an early version of the LttE (T2300, T3200 … refer to transmissions at 2300, 3200km etc from the DVLA (Deep Vertical Line Array)), 2) processing issues, including the trade-offs between coherent and incoherent stacking and corrections for the effects of moving sources and receivers and tidal currents (Doppler), 4) the distinction between "deep shadow zone arrivals", which occur below the turning points in Parabolic Equation (PE) models, and "deep seafloor arrivals", which appear dominantly on the Ocean Bottom Seismometer (OBS) but are either very weak or absent on the deepest element in the DVLA and do not coincide with turning points in the PE model (some of these OBS late arrivals occur after the finale region), 4) the role of surface-reflected bottom-reflected (SRBR) paths in explaining the late arriving energy, and 5) generally reconciling the OBS analysis with work by other North Pacific Acoustic Laboratory (NPAL) investigators and Dushaw et al (1999).

Table of Contents

1) Introduction and Summary

These notes provide supporting information for a JASA (Journal of the Acoustical Society of America) LttE (Letter to the Editor) manuscript, "Deep seafloor arrivals: A new class of arrivals in long-range ocean acoustic propagation" (Stephen *et al.*, submitted). (A summary of the acronyms and abbreviations used in this report is given in Table 1-1.) It addresses five issues raised by the co-authors: 1) incorrect processing for the time-compressed traces at T2300 and T3200 that appeared in an early version of the LttE (T2300, T3200 … refer to transmissions at 2300, 3200km etc from the DVLA (Deep Vertical Line Array)), 2) processing issues, including the trade-offs between coherent and incoherent stacking and corrections for the effects of moving sources and receivers and tidal currents (Doppler), 4) the distinction between "deep shadow zone arrivals", which occur below the turning points in Parabolic Equation (PE) models, and "deep seafloor arrivals", which appear dominantly on the Ocean Bottom Seismometer (OBS) but are either very weak or absent on the deepest element in the DVLA and do not coincide with turning points in the PE model (some of these OBS late arrivals occur after the finale region), 4) the role of surface-reflected bottom-reflected (SRBR) paths in explaining the late arriving energy, and 5) generally reconciling the OBS analysis with work by other North Pacific Acoustic Laboratory (NPAL) investigators and Dushaw et al (1999).

This is essentially a progress report up to November 2008. There are a number of issues that need to be studied more carefully. Particularly these include: i) What are the absolute signal levels and signal-to-noise ratios on the various receivers, including the geophone channels on the East and West OBSs as well as the hydrophone channels on the East, South and West OBSs? ii) We need to do a more careful analysis of the existence and characteristics of SRBR arrivals on the DVLA on the Spice Experiment (SPICEX) (about 250Hz) and on the DVLA and OBSs on the Long-range Ocean Acoustic Propagation Experiment (LOAPEX) (about 75Hz). iii) What is the transmission loss for deep seafloor arrivals and is it predictable? iv) What is the phase relationship between pressure and vertical particle velocity? v) What are the consequences for short range (< 500km) propagation? vi) What is the sensitivity to source depth? vii) What other existing data sets are available that could be used to study this problem?

At this time there is still strong evidence for unexplained, late arrivals in the OBS data and an LttE on this topic is still worthwhile. The LttE is a useful document to focus the discussions among the various NPAL investigators and to point out the differences in the arrival structure between the vertical component of ground motion on one NPAL OBS and the hydrophones on the DVLA.

Some caveats:

i) We focus on the vertical seismometer data from the South OBS (OBS #4) and compare features with the deepest hydrophone (#20) on the lower segment of the DVLA. (For convenience in discussions and figures we use the terms OBS-S-Geo and DVLA-L20-Hyd for these sensors respectively.) There are arrivals to short ranges on the vertical component of the two other "successful" OBSs and on the hydrophones for all three OBSs but the SNR is not as good. Inclusion of the other OBSs and the hydrophone data in the analysis will eventually be worthwhile, when some of the other issues are wrung-

out, but is not necessary for the LttE. Other investigators have studied the Shallow Vertical Line Array (SVLA) and DVLA arrival structure for the LOAPEX sources and it is not necessary to redo this.

ii) Except where otherwise indicated all of the time compressions presented in this paper were computed assuming that the sources and receivers were stationary. Corrections for Doppler effects and the trade-offs between incoherent and coherent stacking are addressed in Section 3.

iii) The geophones and hydrophones on the three OBSs were all self-noise limited so that we can only place upper bounds on the true seafloor ambient noise and the SNRs are minimum values.

iv) To simplify the presentation and the number of variables involved we focus on the LOAPEX M68.2 (an M-sequence centered at 68.2Hz) sequences deployed at 350m depth.

v) For the LttE we have used the PE method to model the arrival structure. The modeling work was done by Matt Dzieciuch. There are other viable modeling approaches (eg Kraken) that we have not used.

1a) The T2300 and T3200 traces on DVLA Lower Channel 20

There were at least two things wrong in the original Figure 3 from the June 27th version of the LttE (Figure 2-1 in this report): 1) The T2300 and T3200 traces on the DVLA show no arrivals and 2) the PE models do not include SRBR paths. An improved version of this figure is given in Figure 2-2.

In summary there appear to be three types of arrivals:

i) The earliest arrivals that appear on both OBS-S-GEO (vertical component) and DVLA-L20-Hyd (deepest hydrophone) and are modeled well by the PE. We call these "PE predicted".

ii) Intermediate arrival time events that appear on DVLA-L20-Hyd but are either very weak or absent on OBS-S-GEO and are not modeled well by the PE. These correspond to "deep shadow zone" arrivals (occurring below shallower turning points).

iii) "Deep seafloor arrivals" that appear on OBS-S-GEO but either are not observed or are very weak on DVLA-L20-Hyd and are not modeled well by the PE.

1b) Coherent versus Incoherent Stacking and "Doppler Corrections"

The traces in the LttE mansucript (Figures 2-1 and 2-2 in this report, for example) were computed by incoherent summing of all acceptable replica correlated sequences. Replica correlation was carried out for each sequence individually and we simply summed the magnitude of the complex output. In this section we do some sanity checks by comparing the arrival structure on individual replica correlated traces, on coherently averaged replica correlated traces over short windows, and over incoherently averaged replica correlated traces. The second sub-section also discusses some results by Rex Andrew on Doppler corrected data.

This is a long and pedantic section with many figures. In short, it shows that the late arrivals on OBS-S-GEO and the absence of late arrivals on DVLA-L20-Hyd are not artifacts of

the processing procedure. They persist through combinations of coherent and incoherent stacking and Doppler corrections.

1c) "Deep Shadow Zone" versus "Deep seafloor arrivals"

We distinguish between "deep shadow zone arrivals" (Dushaw *et al.*, 1999) and "deep seafloor arrivals". The expression "deep shadow zone arrivals" refers to arrivals on deep receivers that occur at about the same time as shallower turning points in the time fronts. There has not been a term for arrivals that appear on deep receivers at times that do not correspond to shallower turning points. We use the term "deep seafloor arrivals" for the new arrivals that we are observing primarily on the OBS vertical geophone.

In this section we compare the DVLA-L20-Hyd and OBS-S-Geo traces with time fronts computed with bottom interaction suppressed. We consider ranges T500, T1000, T1600 and T2300 and we discuss each event in the time series in terms of the three arrival types.

The PE model predicts well the events whose time fronts cross the DVLA-L20-Hyd and OBS-S-Geo depths. We call these "PE predicted". As turning points move shallower across the DVLA-L20-Hyd depth the amplitude of the events increases with time. In the transition to "deep shadow zone arrivals" the turning points move above the DVLA-L20-Hyd depth and the amplitude of the subsequent deep shadow zone events decreases dramatically (over 200 to 300m). These events that we associate with turning points are most often seen better on DVLA-L20-Hyd than on OBS-S-Geo. This is consistent with the notion of energy extending, but still decaying, below the turning points as expected for deep shadow zone arrivals. At all ranges considered (T500, T1000, T1600 and T2300) there are "deep seafloor arrivals" on OBS-S-Geo that are either not observed or are very weak on DVLA-L20-Hyd and these late arrivals do not correspond to turning point times. They appear to decay with height above the seafloor. "Deep seafloor arrivals" are the largest events by far on OBS-S-Geo and "PE predicted" are the largest events by far on DVLA-L20-Hyd.

1d) SRBR Paths and Reconciling Results with Other NPAL Investigators

In this section we consider the hypothesis that the deep seafloor arrivals are SRBR paths (surface-reflected bottom-reflected). In the process we look at results by Lora van Uffelen, Jinshan Xu, and Ilya Udovydchenkov and we look at replica correlated DVLA LOAPEX data provided by Linda Buck at APL/UW (Applied Physics Laboratory – University of Washington). In Section 5e) we do an event-by-event comparison of the DVLA-L20-Hyd and OBS-S-Geo traces with time fronts (provided by Matt Dzieciuch) which include bottom interaction and SRBR. Section 5f) discusses relevant sections of Dushaw et al (1999).

Are the "deep seafloor arrivals" observed on the OBS SRBR? The arrival time of many of the deep seafloor arrivals agrees at least approximately with SRBR. Other aspects of SRBR must be satisfied, however:

i) Deep seafloor arrivals in the OBS data are the largest events by far on the traces. They are much larger than PE predicted and deep shadow zone arrivals.

ii) So far none of the NPAL investigators has observed SRBR arrivals on the DVLA or SVLA for M68.2 LOAPEX transmissions at ranges of T500 and beyond. So for the model SRBR events to agree with the data we need to increase the magnitude of SRBR relative to PE and deep shadow zone arrivals at the seafloor while simultaneously decreasing the magnitude of SRBR relative to PE predicted at SVLA and DVLA depths (particularly above 3000m). This is a tall order.

iii) In contrast to deep shadow zone arrivals which decay in amplitude with increasing depth below turning points, the deep seafloor arrivals appear to decay with increasing height above the seafloor. It would be strange for SRBR to appear louder at the seafloor, except perhaps for up to a six dB gain that could be expected from constructive interference of incident and reflected waves.

iv) The SRBR "events" at the seafloor in the PE models are diffuse clouds of slightly stronger energy. The observed deep seafloor arrivals, on the other hand, are large amplitude, discrete events. In many cases the deep seafloor arrivals have the double-peak structure that is characteristic of the PE and deep shadow zone arrivals. The deep seafloor arrivals in the data are not smeared like the arrival clouds in the PE models.

Dushaw et al's (1999) preferred explanation for the arrival structure of long range acoustic propagation on bottom-mounted receivers was "leakage" below caustics occurring shallower in the sound channel. They called these "deep shadow zone" arrivals. Dushaw et al state clearly, however, that there are a number of instances where the "deep shadow zone arrival" explanation breaks down. The NPAL04 (North Pacific Acoustic Laboratory 2004) OBS data are another case where the "deep shadow zone arrival" explanation is not the whole story, but we have the simultaneous water column data and the multiple range data, which Dushaw et al did not have, to help resolve the issues. It is important to sort out the physical mechanisms responsible for the additional deep seafloor arrivals. Deep seafloor arrivals that are not associated with caustics could complicate the tomography work based on seafloor sensors.

1e) Outstanding Issues

Since this is a work in progress we include a section that discusses issues that need further work.

Table 1-1: Acronyms and Abbreviations Used in This Report (in alphabetical order)

2-D	Two Dimensional
Angle Rec	Azimuthal arrival Angle at the Receiver
APL/UW	Applied Physics Laboratory – University of Washington
Del	Difference between nominal and actual ranges
Diff	Difference between old (drop) positions and new (seafloor) positions
Dir	Direction
DOEI	Deep Ocean Exploration Institute at WHOI
DVD	Digital Video Disk – used as a data exchange medium
DVLA	Deep Vertical Line Array*
DVLA-L20-Hyd	The 20th hydrophone in the lowest section of the DVLA
Geo	Geophone
GPS	Global Positioning System
Hyd	Hydrophone
IRIS-DMC	Incorporated Research Institutions for Seismology - Data Management Center.
JASA	Journal of the Acoustical Society of America
JOE	Journal of Oceanic Engineering
jpeg	Joint Photographic Experts Group – a standard figure format
Lat	Latitude
LOAPEX	Long-range Ocean Acoustic Propagation Experiment*
Lon	Longitude
LttE	Letter to the Editor
M68.2, M75	Format of swept frequency acoustic sources centered at 68.2 and 75Hz.*
M-sequence	Particular format of a swept frequency source *
NPAL	North Pacific Acoustic Laboratory*
NPAL04	North Pacific Acoustic Laboratory 2004*
NSF	National Science Foundation
OBS	Ocean Bottom Seismometer
OBS/H	Ocean Bottom Seismometer and Hydrophone
OBS-S-Geo	The geophone in the South OBS
ONR	Office of Naval Research
P-wave	Primary wave, compressional wave
pdf	Portable Document Format
PE	Parabolic Equation
RR	Refracted Refracted**
RSR	Refracted Surface-Reflected**
SIO-OBSIP	Scripps Institution of Oceanography Ocean Bottom Seismic Instrumentation Pool
SRBR	Surface-Reflected Bottom-Reflected**

SN69, SN61 etc	Seismometer Number 69, 61 etc
SNR	Signal-to-Noise Ratio
SPICEX	Spice Experiment*
SPICE04	The Spice Experiment in 2004*
sqrt	Square root
sqrt(sum(Residual2)/N)	Root mean square of the data residuals
SSP	Sound Speed Profile
SVLA	Shallow Vertical Line Array*
T50, T250,…	Refer to transmission stations at 50, 250km etc from the DVLA*
TL	Transmission loss
Vp	Compressional wave speed
WGS-84	World Geodetic System 1984
WHOI	Woods Hole Oceanographic Institution
WOA2204	World Ocean Atlas 2004
zsrc	Source depth

* These terms are discussed in more detail in the NPAL04 reports (Mercer *et al.*, 2005; Mercer *et al.*, submitted; Worcester, 2005a; b).
** These terms are discussed in Munk et al (1995).

2) The T2300 and T3200 traces on DVLA Lower Channel 20

Figure 2-1 shows the original Figure 3 from the June 27th version of LttE manuscript. At least two things are wrong in this figure: 1) The T2300 and T3200 traces on the DVLA show no arrivals and 2) the PE models do not include SRBR paths. An improved version of this figure is given in Figure 2-2. The DVLA section now has the corrected traces for T2300 and T3200. (I had originally hardwired my DVLA processing to 1200sps and had not noticed that T2300 and T3200 were sampled at 300sps - finger trouble.) All of the DVLA-L20-Hyd traces agree pretty well with the traces in Rex Andrew's report (Andrew, 2008; Stephen *et al.*, submitted). So although I am still showing incoherent stacks of all available traces, the existence, location and relative amplitude of the major peaks does not change dramatically with more clever processing (coherent stacking over short groups and doppler corrections, for example). This is discussed further in Section 3. The basic story, that OBS-S-Geo sees large amplitude late arrivals that are not seen on DVLA-L20-Hyd, persists.

The T2300 and T3200 traces do confirm the existence of later arrivals (after line B) on DVLA-L20-Hyd that are not modeled with the PE. These are genuine "deep shadow zone" arrivals (occurring below shallower turning points) and are discussed further in Section 5.

In summary there appear to be three types of arrivals:

i) The earliest arrivals that appear on both OBS-S-GEO (vertical component) and DVLA-L20-Hyd (deepest hydrophone) and are modeled well by the PE. In general they occur between a velocity of 1.487km/s (line C on Figures 2-1 and 2-2) and a velocity of 1.485km/s (line B). These correspond to the earliest and deepest arrivals in the time fronts. We call these "PE predicted".

ii) Events that appear on DVLA-L20-Hyd but are either very weak or absent on OBS-S-GEO and are not modeled well by the PE. In general they occur after a velocity of 1.485km/s (line B) and on the furthest ranges, T2300 and T3200. These correspond to "deep shadow zone" arrivals (occurring below shallower turning points).

iii) "Deep seafloor arrivals" that appear on OBS-S-GEO but either are not observed or are very weak on DVLA-L20-Hyd and are not modeled well by the PE. In general they are the largest amplitude events on OBS-S-GEO and occur after a velocity of 1.485km/s (line B) and on all ranges at T500 and beyond. From T500 to T1600 the latest of these appear well-after the finale time at a velocity of about 1.477km/s (line A). They could be SRBR paths but we would need to explain why they do not appear on the DVLA or SVLA. Alternatively they could be a new class of event that propagates as an interface wave at the seafloor and decays exponentially with increasing height off the bottom.

Figure 2-3 is a good summary figure that combines the attributes of Figures 2-1 and 2-2. The OBS and DVLA data (a and c respectively) and the DVLA PE model (d, with bottom interaction) are the same as Figure 2-2. Since the PE results with bottom interaction are so noisy for the OBS we have used Matt's original PE results (without bottom interaction) for b. The arrivals before 1.485km/s (line B) on both the OBS-S-Geo and DVLA_L20_Hyd are "PE predicted" arrivals. The arrivals after 1.485km/s on DVLA_L20_Hyd are "deep shadow arrivals" and the arrivals after 1.485km/s on OBS-S-Geo are "deep seafloor arrivals". The deep

seafloor arrivals are by far the largest magnitude events on OBS-S-Geo and there are many more of them than deep shadow zone arrivals. Although some of the deep seafloor arrivals on OBS-S-Geo could be SRBR (surface-reflected bottom-reflected) we would need to explain why they do not appear on DVLA_L20_Hyd.

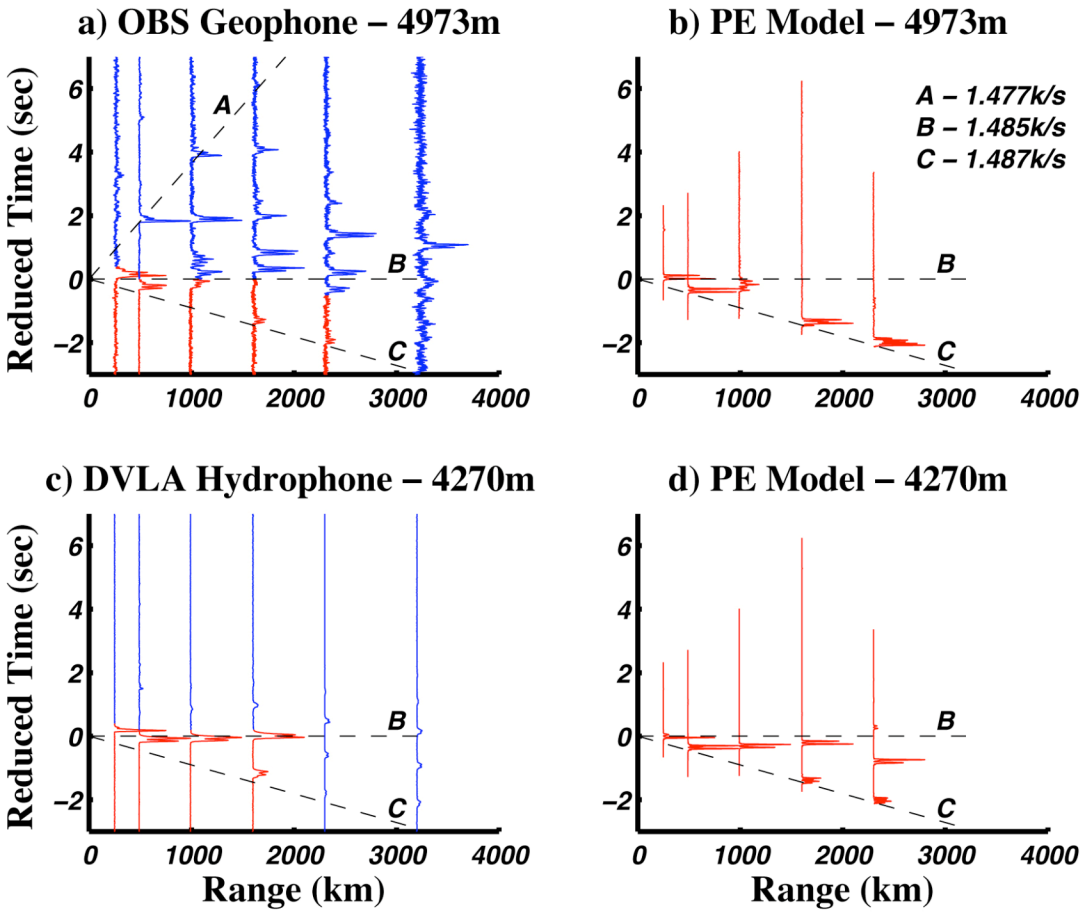

Figure 2-1: This is the original Figure 3 from the June 27th version of LttE mansucript. The caption was: " The stacked traces from the OBS vertical geophone on the seafloor (a) show many more arrivals than the deepest DVLA hydrophone (c) or the parabolic equation (PE) models (b and d). For the OBS geophone traces (a), events occurring with a sound speed faster than about 1.485km/s (roughly earlier than line B) are predicted by the PE but there are many "late arrivals". The late arrivals are not bottom bounce paths because they are not observed on the DVLA hydrophone. From left to right the number of traces that contributed to each stacked trace are 421, 690, 1345, 975, 606 and 599 for the OBS geophone and 27, 480, 1080. 930, 144 and 144 for the DVLA hydrophone. All traces have been amplitude normalized to the maximum value on the trace except for the 2300 and 3200km DVLA traces which show no apparent signal. The time axis has been reduced by subtracting the range divided by 1.485km/s. Dashed lines correspond to three relevant velocities: A- the apparent sound speed of the latest arrival at T500, T1000 and T1600, B - the apparent sound speed of the largest PE predicted at the deepest hydrophone of the DVLA which seems to separate the known early arrivals from the late unknown arrivals and C - the apparent sound speed of the earliest arriving energy at the OBS and DVLA, which corresponds to the deepest turning rays (see Figure 4). The arrival from 3200km shown in Figure 2 is a "late arrival". " At least two things are wrong in this figure: 1) The T2300 and T3200 traces on the DVLA (c) show no arrivals and 2) the PE models (b and d) do not include SRBR paths. [Fig_3_h1.jpg]

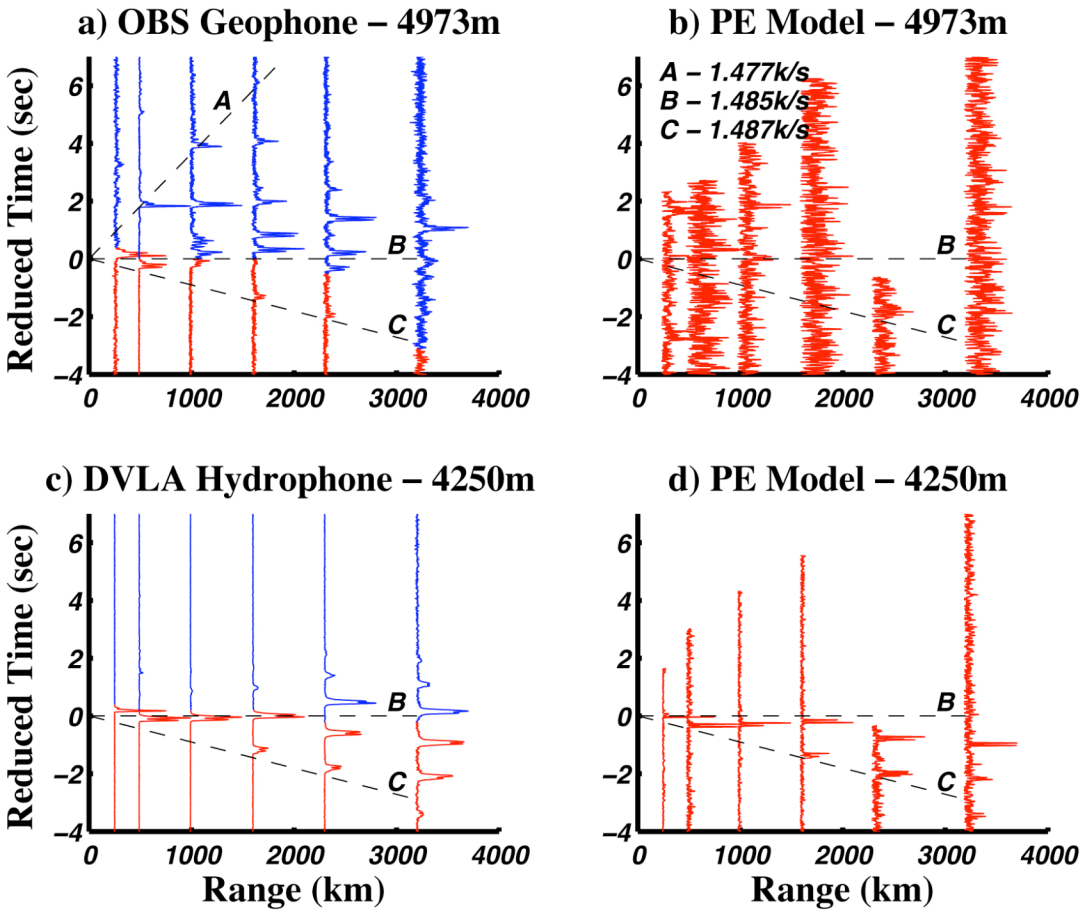

Figure 2-2: This new version of Figure 3 for the LttE mansucript has two changes. 1) The traces for T2300 and T3200 on DVLA-L20-Hyd show clear arrivals. 2) The PE models, which have been provided by Matt Dzieciuch, include the effects of bottom bounce paths (SRBR). The DVLA-L20-Hyd stacks at T2300 and T3200 are the sum of 576 sequences each. [Fig_3_h1_4.jpg]

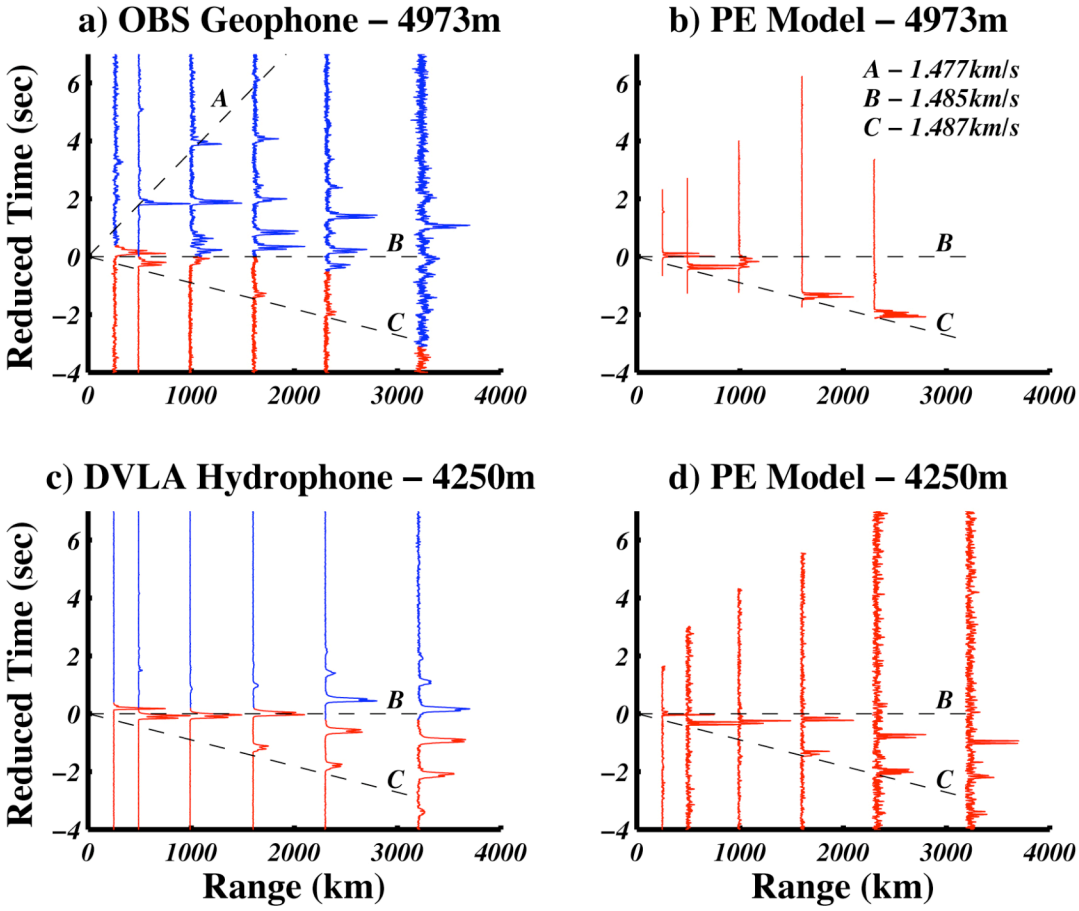

Figure 2-3: This figure is a compromise of PE results. The OBS and DVLA data (a and c respectively) and the DVLA PE model (d, with bottom interaction) are the same as Figure 2-2. Since the PE results with bottom interaction are so noisy for the OBS we have used Matt's original PE results (without bottom interaction) for b.

The arrivals before 1.485km/s (line B) on both the OBS-S-Geo and DVLA_L20_Hyd are "PE predicted" arrivals. The arrivals after 1.485km/s on DVLA_L20_Hyd are "deep shadow arrivals" and the arrivals after 1.485km/s on OBS-S-Geo are "deep seafloor arrivals". The deep seafloor arrivals are by far the largest magnitude events on OBS-S-Geo and there are many more of them than deep shadow zone arrivals. Although some of the deep seafloor arrivals on OBS-S-Geo could be SRBR (surface-reflected bottom-reflected) we would need to explain why they do not appear on DVLA_L20_Hyd. [Fig_3_h1_5.jpg]

3) Coherent versus Incoherent Stacking and "Doppler Corrections"

The traces in the LttE mansucript (Figures 2-1 and 2-2, for example) were computed by incoherent summing of all acceptable replica correlated sequences. Replica correlation was carried out for each sequence individually and we simply summed the magnitude of the complex output. (Note that strictly speaking "incoherent summing" sums the magnitude of the intensity. Intensity is a vector and for spherical and plane waves in an acoustic medium (no shear) its magnitude is proportional to pressure squared (Morse and Feshbach, 1953; Pierce, 1989). Perhaps we should be summing the magnitude of the complex output squared, but we are not.) Since the plotted traces are normalized to the maximum amplitude on the trace the "sum" and the "average" plot the same. The OBS-S-GEO data particularly had some noisy and spiky traces which were not included in the stacks. The number of "good" sequences (NN__) used for each trace and the total elapsed time at each station (for Figure 2-2) are:

T250 - 9hours, NN_OBS = 421, NN_DVLA = 27
T500 - 15hours, NN_OBS = 690, NN_DVLA = 480
T1000 - 34hours, NN_OBS = 1345, NN_DVLA = 1080
T1600 - 28hours, NN_OBS = 975, NN_DVLA = 930
T2300 - 14hours, NN_OBS = 606, NN_DVLA = 576
T3200 - 15hours, NN_OBS = 599, NN_DVLA = 576

Because the LOAPEX sources and DVLA hydrophones move during transmission and because there are tidally generated currents along the propagation path, there can be differences between the transmitted and received frequencies that will affect the replica correlation. One assumption is to assume that the speeds involved are constant over the period of a transmission sequence (30sec for M68.2 transmissions), change the sample rate over a range of values, carry out the replica correlation, and then assume that the sample rate with the largest peak magnitude gives the "correct, Doppler shifted" result.

There are many approaches to stacking strategies and Doppler corrections and these are both active fields of research. Even among the NPAL investigators there is not a commonly accepted approach or set of parameters to either issue. Some of the approaches and results are discussed in Section 5.

There is evidence for strong variability in the arrival structure over as little as 10minutes (Figure 3-1 for example). By carrying out the incoherent stack of all available traces we are emphasizing the most robust arrivals. It is possible that some arrivals are being enhanced (on OBS-S-GEO for example) at the expense of diminishing others (on DVLA-L20-Hyd for example). An exhaustive study of all possible effects is beyond the scope of this report and may not be necessary to demonstrate the existence and relevance of deep seafloor arrivals. As a compromise we suggest using the "incoherent sum of all sequences" as a reference and then compare the arrival structure from other processing procedures to it. So far there have been no surprises.

This is a long and pedantic section with many figures. In short, it shows that the late arrivals on OBS-S-GEO and the absence of late arrivals on DVLA-L20-Hyd are not artifacts of the processing procedure. They persist through combinations of coherent and incoherent stacking and Doppler corrections.

3a) Incoherent versus coherent stacks

This section shows that the arrival structure (the relative amplitude, separation and timing of arrivals) on OBS-S-GEO and DVLA-L20-HYD is not an artifact of the stacking procedure. In a number of examples, the arrival structure can be seen in just a single sequence without stacking.

The traces in Figures 2, 3 and 4 of the LttE were incoherent stacks of the magnitude of the complex output of the replica correlator for all of the acceptable sequences. I have done a quick check of the stack issue - stacking the magnitude of the complex series versus taking the magnitude of the stacked complex series. (Another procedure, stacking the time series before replica correlation, was studied by Rex Andrew (Andrew, 2008) and is discussed in section 3b.)

i) T3200 on OBS-S-Geo

I focused first on the T3200 traces in Figure 2 of the LttE. This is given here as Figure 3-2 for completeness. The event at 18.25sec is the largest event on OBS-S-GEO for the T3200 source. It appears on the incoherent stack as well as a few individual replica correlated sequences. It is one example of a deep seafloor arrival.

I started by looking at the real and imaginary parts of single, unstacked time series. Figures 3-3 and 3-4 correspond to the top two single sequence traces in Figure 3-2. In each case the magnitude, real part and imaginary part of the complex output are displayed (from top to bottom respectively). You would miss the arrival at about 18.25sec entirely if you just looked at the real part. And you would miss the arrival at about 17.4sec entirely if you just looked at the imaginary part. Sometimes the arrival is on the real trace, sometimes on the imaginary trace, and sometimes on both. So looking at the magnitude of the complex output makes sense.

The top trace in Figure 3-5 shows an expanded time axis for the stacked trace at the bottom of Figure 3-2. This is the same trace as the T3200 trace for the OBS in Figures 2-1a and 2-2a. This is the "stack of the magnitudes of the complex time series" or "incoherent stack". The next two traces are stacks of the real and imaginary time series. The bottom trace shows the "magnitude of the stacks of the real and imaginary time series or "coherent stack". Oddly enough the top trace (what I have been doing all along by accident) shows the clearest arrival, but there is still an arrival on the bottom trace. The arrival at about 17.4sec in Figure 3-3 did not survive either stack.

ii) T1600 on OBS-S-Geo

I have done a similar analysis for the T1600 geophone with similar results. The incoherent stack is the T1600 trace in Figures 2-1a and 2-2a and is the geophone trace used in Figure 4 of the draft LttE. This is given here as Figure 3-6 for completeness. The earliest arrival at 1076sec in Figure 3-6 corresponds to the earliest and deepest time front in the PE. The other four arrivals do not coincide well with the turning points. Since these are not modeled well in the PE and since they do not appear on DVLA-L20-Hyd they are candidates for "deep seafloor arrivals". The latest arrival occurs after the finale region.

The real part, imaginary part and magnitude for two single sequence examples are given in Figures 3-7 and 3-8. The five-arrival pattern is perceptible in the magnitude trace of each figure but would be difficult to see on either the real or imaginary parts by themselves. The top trace in Figure 3-9 is the incoherent stack displayed at the bottom of Figure 3-6. The next two traces are stacks of the real and imaginary time series and the bottom trace shows the "coherent stack" of all acceptable arrivals. The five-arrival pattern is evident in the coherent stack as well as is the incoherent stack, although the fourth arrival about 23.7sec is much weaker in the coherent stack.

iii) T500 on OBS-S-Geo

As a third example of an OBS-S-Geo trace we chose the T500 trace in Figures 2-1a and 2-2a. This is the shortest range that shows both a PE predictable early arrival on OBS-S-Geo and DVLA-L20-Hyd and an unpredictable late arrival on OBS-S-Geo and not on DVLA-L20-Hyd. The SNR of these arrivals is better at T500 than on the later traces. Since it is possible that the late arrival is not observed on DVLA-L20-Hyd because it is just falling beneath the noise floor, it would be useful to know if there is any indication of it at all on the traces with the best SNR.

The real part, imaginary part and magnitude for two single sequence examples are given in Figures 3-10 and 3-11. The two-arrival pattern is evident in the magnitude and imaginary part traces of each figure but the early arrival is difficult to see on the real part alone. Figure 3-12 compares the incoherent stack with the stacks of the real part and imaginary part and the magnitude of the complex stack (the "coherent stack"). The two-arrival pattern is quite clear on all traces.

iv) T500 on DVLA-L20-Hyd

This section looks at the DVLA-L20-Hyd trace at T500 in Figures 2-1c and 2-2c. The traces can be compared to the OBS-S-Geo T500 results in the earlier section. The real part, imaginary part and magnitude for two single sequence examples are given in Figures 3-13 and 3-14. Only the early arrival is evident in the traces. There is no indication of the second arrival on the corresponding geophone trace that comes in about 2.1sec later. Figure 3-15 compares the incoherent stack with the stacks of the real part and imaginary part and the magnitude of the complex stack (the "coherent stack"). The PE predictable early arrival (near 24.7sec) is quite

clear. There are a number of later, much smaller arrivals but the event corresponding to the second arrival on OBS-S-Geo, which should appear near 26.8sec is barely perceptible on either the coherent or incoherent stacks. The near-absence of the second arrival on DVLA-L20-Hyd is a ubiquitous feature that is observed for individual sequences as well as for any manner of stacking strategy.

3b) "Doppler Corrections"

Rex Andrew has done a preliminary study of various processing sequences, with and without correcting for Doppler effects, of the bottom channel of the DVLA lower subarray (our DVLA-20-Hyd) for the M68.2Hz sequences at 350m source depth (Andrew, 2008). He considered three processing sequences:

i) This involved Doppler correction/coherent averaging followed by incoherent averaging. For the Doppler correction: adjust the original 1200 or 300sps data sequences for a range of dilations, resample the data to 272.8sps, stack (average) as many M-sequences as possible (to a maximum of 36, call this a group) within a 20 or 80 minute transmission reception, and pulse compress (replica correlate) the stack. Of the various replica correlated results, the one with the largest peak magnitude is chosen as the "correct" Doppler processed result. The magnitudes of the replica correlated results are incoherently averaged across all available transmission receptions.

A transmission reception is either 20 or 80 min long and may have consisted originally of 1 or more raw data capture files. The first 28 or 36 whole M-sequences (depending on what is available) are chosen for the coherent stack. Only the first group in each transmission reception is used in the incoherent stack. For example, for an 80minute transmission window, the first 36 M-sequences are used (18min) and the remaining 62minutes is not included.

ii) A processing sequence similar to i) but not considering the range of dilations - no Doppler corrections. The available M-sequences were averaged prior to replica correlation. This differs from the processing done in Sections 3a) and 5d) in that the coherent averaging within a transmission receptions is applied prior to replica correlation. In Sections 3a) and 5d) the coherent averaging is done after replica correlation. (Since the operations of replica correlation and stacking commute the results should be identical.) Furthermore the coherent stacking in Sections 5b) and 5d) (Jinshan's thesis and the APL/UW analysis) was carried out over only 10 M-sequences.

iii) Replica correlating each M-sequence and then averaging the magnitudes of the complex output of the correlation process. This is incoherent stacking without Doppler corrections and is roughly the same as the process used for the traces in Figures 2-1 and 2-2. One difference is that the traces in Figures 2-1 and 2-2 use all available M-sequences within a transmission reception but here only the first 28 or 36 M-sequences within a transmission reception were used.

In general the differences between the various processing sequences in Rex's figures are quite small and the appearance of the traces, by eye, is very similar to traces for DVLA-L20-Hyd shown in Figures 2-1 and 2-2. The number and relative magnitude of the events is essentially unchanged.

In Rex's own words:

"In all cases, the deDopplerized result shows a noticible but small improvement in the peak value of the most prominent peak. This is to be expected because the Doppler search yields (as a by-product) the time series with the greatest maximum absolute value. This "best dilation correction" was usually very close to $\beta = 1$, generally just a few search points to one side of the other. Conversely, the result for $\beta = 1$ (i.e., no Doppler processing) is generally quite good by itself.

"For the most distant sites (T2300 and T3200), both non-Doppler processed and deDopplerized coherent averaging show considerable increase in SNR (i.e., the "background" has been knocked down a lot), particularly with respect to the incoherently averaged case. Nevertheless, the dominant arrivals remain robust and readily identifiable for all three processing recipes.

"At first glance, it does not appear that too many arrivals are missing should one forego doppler processing and simply incoherently average all possible M-sequences. "

In Figures 3-16 and 3-17 the results of Rex' s processing are compared with the processing described in Section 3a). The five traces are respectively: i) Doppler corrected with coherent averaging over 18minutes (either 28 or 36 periods because of recording gaps) and then incoherent averaging over 12 groups, ii) the same as i) but without Doppler corrections, and iii) incoherently summing the magnitudes of the individual replica correlated traces (between 12*28=336 and 12*36=432), iv) incoherent averaging over all available traces (510, upper trace in Figure 3-15) and v) coherent averaging over all available traces (510, lower trace in Figure 3-15). With the exception of coherently averaging over the whole available data set, the results of the various processing scenarios are very similar. Note that the amplitudes and times in Rex's processing (top three traces) agree very well with the amplitudes and times of the processing in this report (fourth trace). This is a useful sanity check since the processing was done independently.

Even after expanding both the time and amplitude scales (Figure 3-17) the top four processing scenarios give remarkably similar results. Arguably the straight incoherent stack of the magnitude of all available individual traces (trace iv) gives the cleanest and most easily picked events. This is the trace that was used in Figures 2-1 and 2-2 and in the arrival discussions in Sections 4) and 5e). It would seem that for the purposes of identifying arrival structure, more involved processing including Doppler corrections is not necessary.

In conclusion, the arrival patterns for DVLA-L20-Hyd and OBS-S-Geo are not sensitive to the details of the processing - either Doppler corrections or various combinations of coherent and incoherent stacking. Nonetheless it would be good to use a common processing sequence that all NPAL investigators agree is acceptable. Some issues:

i) Since Doppler corrections do not seem to cause large changes in the traces and since Doppler corrections have not been applied yet to the OBS data, I would prefer that Doppler corrections not be included in the common processing sequence.

ii) Personally any combination of coherent versus incoherent stacking would be acceptable. Details of the processing sequence do not significantly affect the distribution and

relative amplitude of arrivals on either the DVLA or OBS.

iii) Over what time (or over how many M-sequence periods) should coherent stacking be carried out? Jinshan used 10 periods (5 minutes) and Rex used 28 or 36 (18 minutes).

iv) Should the incoherent stacking be done over magnitude or intensity (magnitude squared)?

v) Should the incoherent stacking be carried out for just the first groups (of 10 or 36 periods, 5 or 18minutes) in an M-sequence transmission (20 or 80minutes long) or over as many groups as possible? For example, for an 80minute transmission do we consider 1 group or 4?

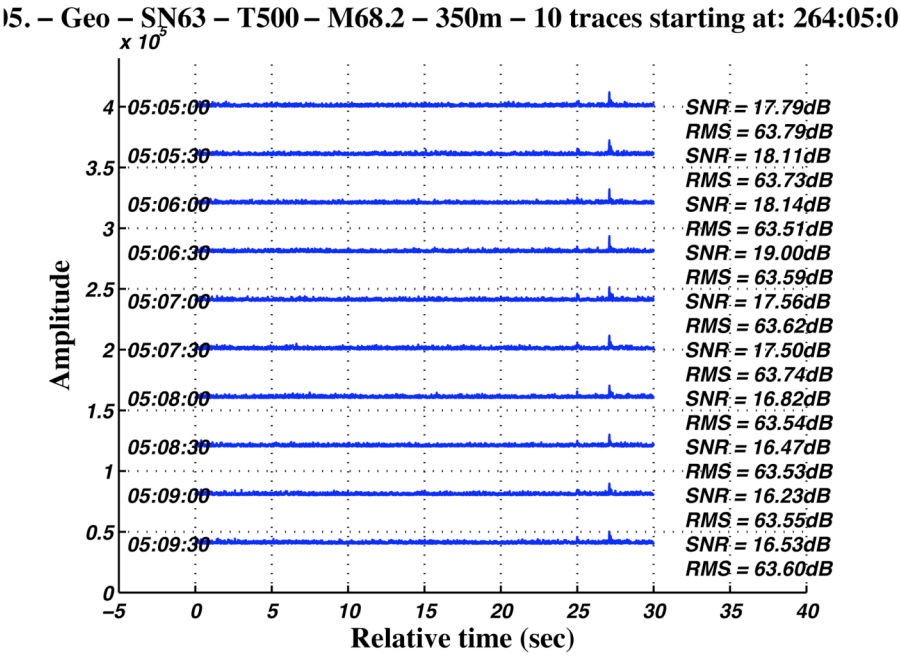

Figure 3-1a

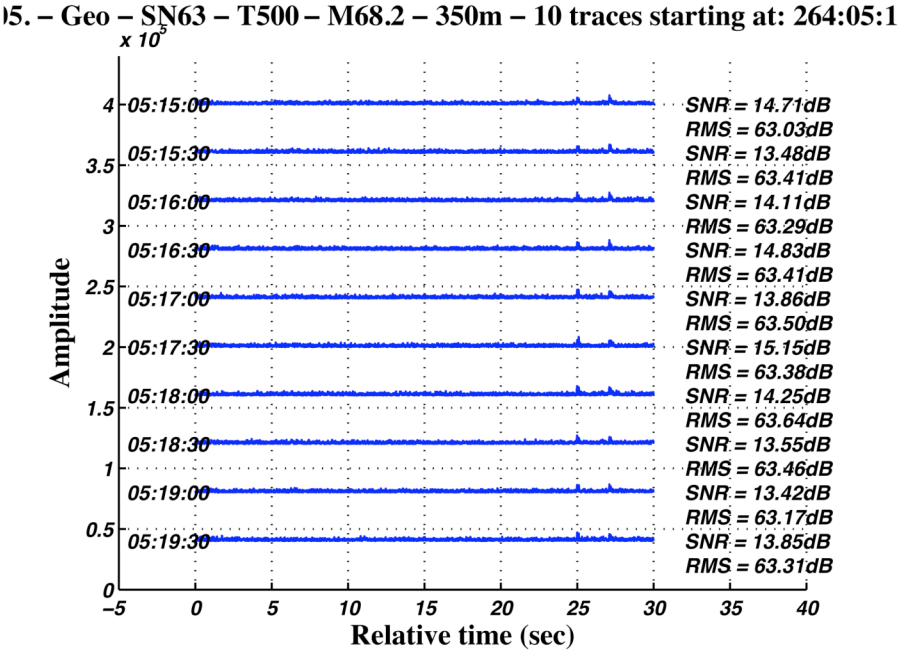

Figure 3-1b

Figure 3-1: These examples of single replica correlated sequences at T500 show the variability of some arrivals over just 15minutes. The first ten sequences after 264:05:05 (Figure 3-1a) show a single dominant arrival around 27sec but 10 minutes later (Figure 3-1b) the arrivals at 25 and 27sec are similar. [Pulse_Geo_SN63_T500__M68.2_350m_264_04_50_04.jpg and Pulse_Geo_SN63_T500__M68.2_350m_264_04_50_06.jpg]

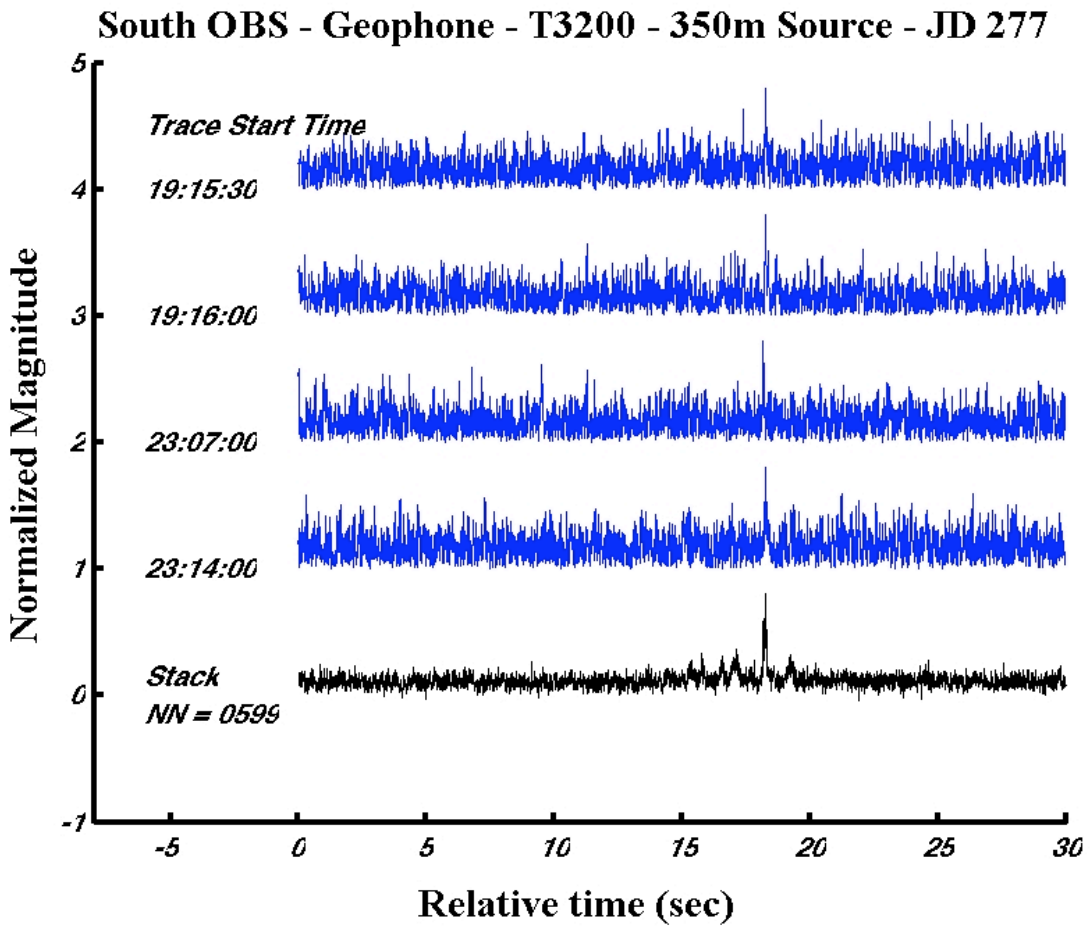

Figure 3-2: This is Figure 2 of the June 27 draft of the LttE. The caption was: " Four samples of unstacked traces (top) and the stack of 599 traces (bottom) are shown for propagation over 3200km range from the LOAPEX source at 350m depth as received on the vertical geophone on the "south" OBS in the deep shadow zone at 4,973m depth. It is remarkable that transmissions are observed (at about 18sec) on single, unstacked traces in the deep shadow zone at this range. "Unstacked traces" are the magnitude of the complex output of the replica correlation; all "stacked traces" in this paper are simply the point-wise sum of the unstacked traces." [Fig_2_TC_Geo_T3200.jpg]

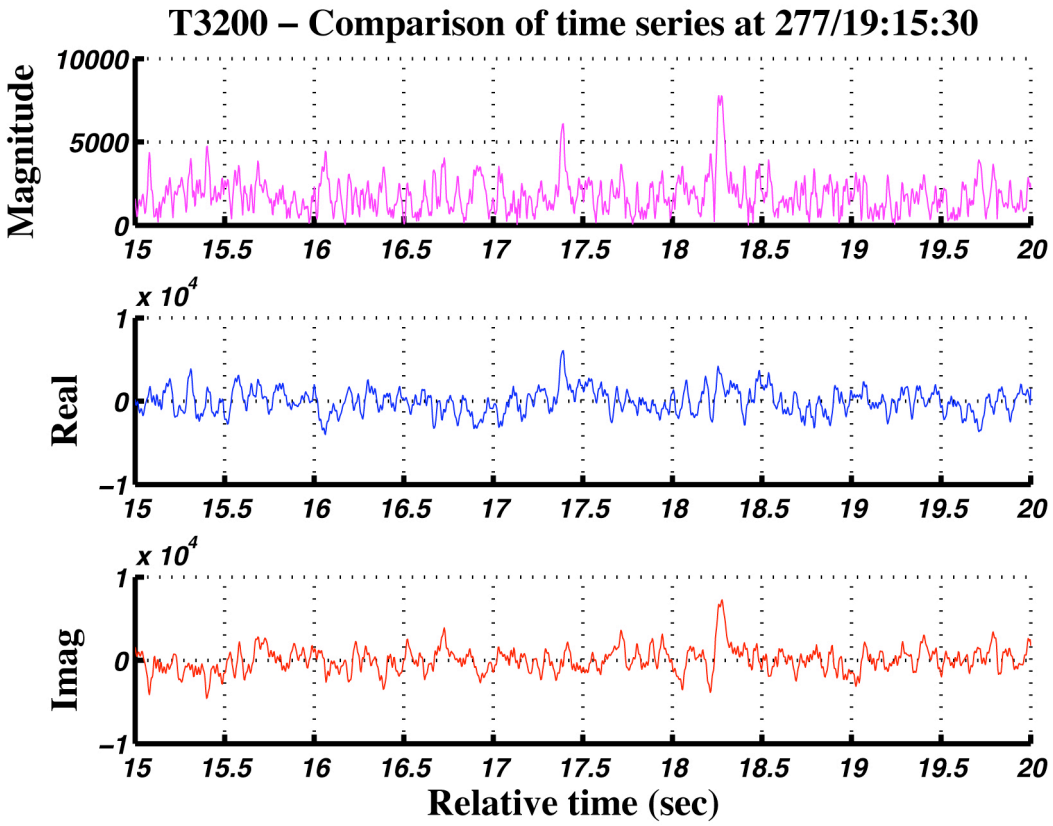

Figure 3-3: The real and imaginary components are compared with the magnitude of the replica correlator for a single sequence on OBS-S-Geo at T3200 (the top time series in Figure 3-2). Since arrivals sometimes occur on the real part and sometimes on the imaginary part it is convenient to look at the magnitude of the complex output. [Stack_Study_T3200_3.jpg]

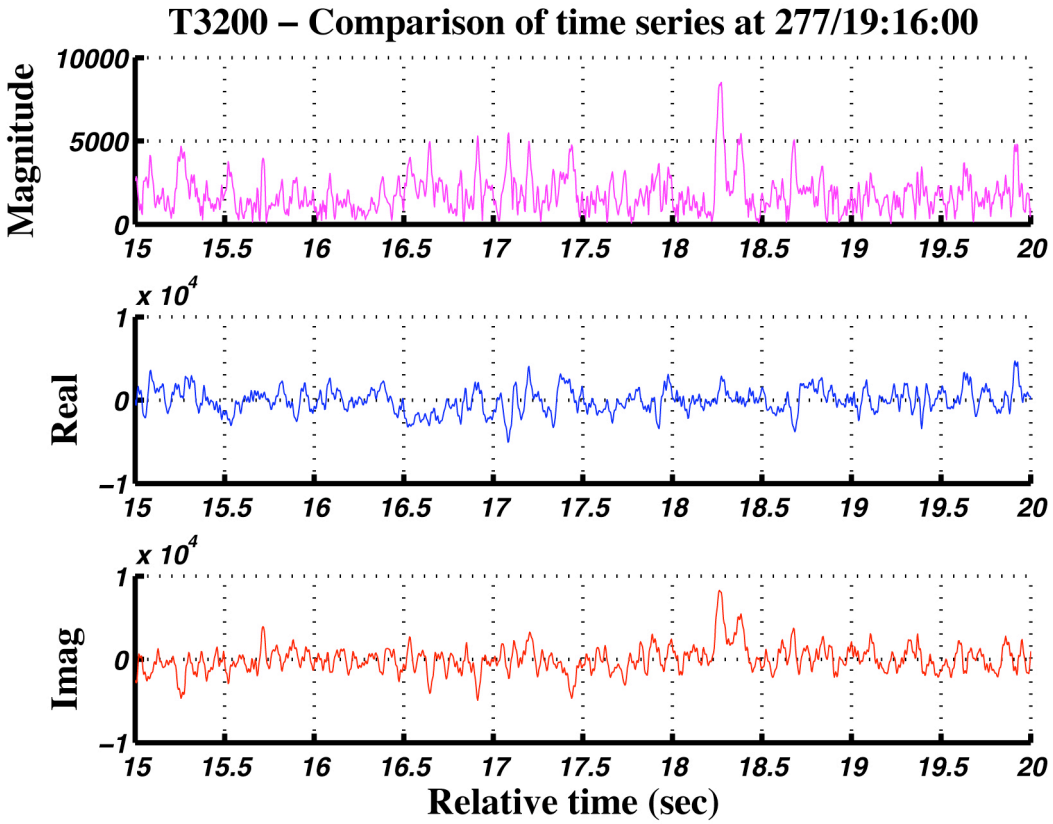

Figure 3-4: The real and imaginary components are compared with the magnitude of the replica correlator for another single sequence on OBS-S-Geo at T3200 (the second from the top time series in Figure 3-2). [Stack_Study_T3200_4.jpg]

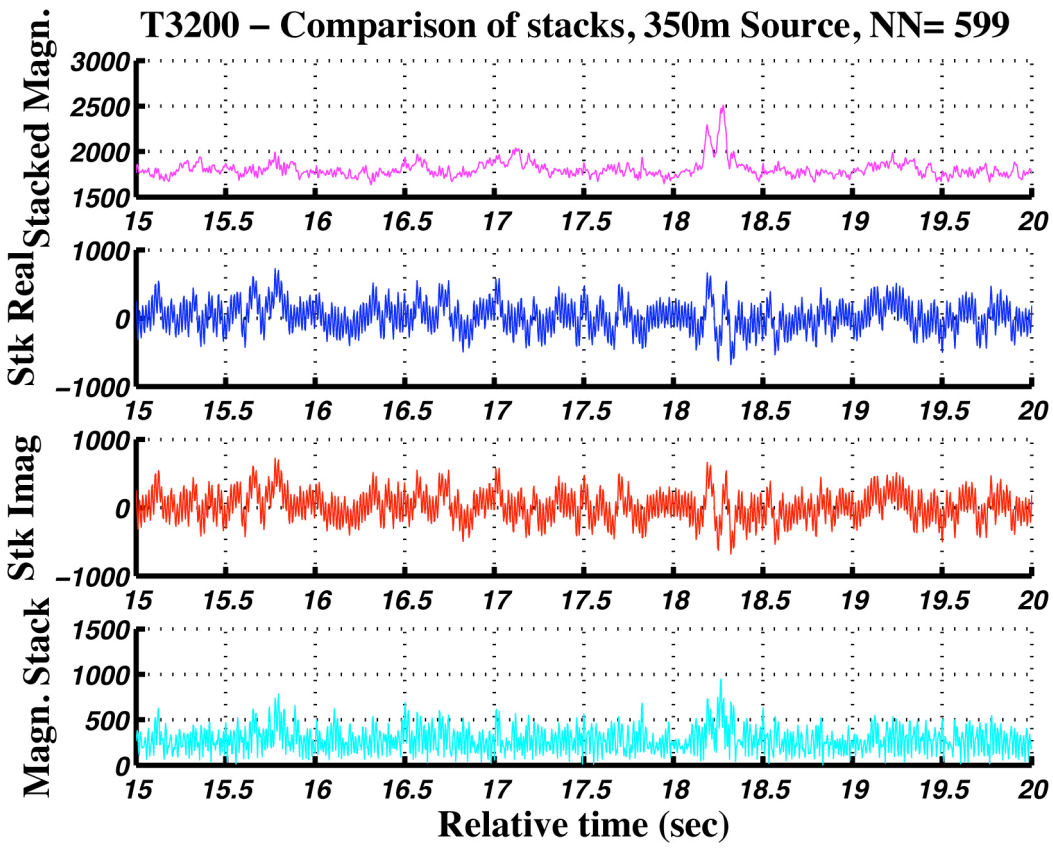

Figure 3-5: The incoherent stack (the sum of the magnitudes of the complex output of the replica correlator) of all 599 sequences to OBS-S-Geo from T3200 is shown in the top trace. This is the same as the bottom trace in Figure 3-2 and the T3200 trace in Figures 2-1a and 2-2a. The coherent stack (the magnitude of the stacks of the real and imaginary parts of the complex output of the replica correlator) of all 599 sequences to OBS-S-Geo from T3200 is shown in the bottom trace. The middle two traces are the stacks of the real and imaginary parts. The major arrival at about 18.25sec, an example of a late bottom arrival, appears on coherent and incoherent stacks as well as some individual traces. It is not an artifact of the stacking procedure. [Stack_Study_T3200_7.jpg]

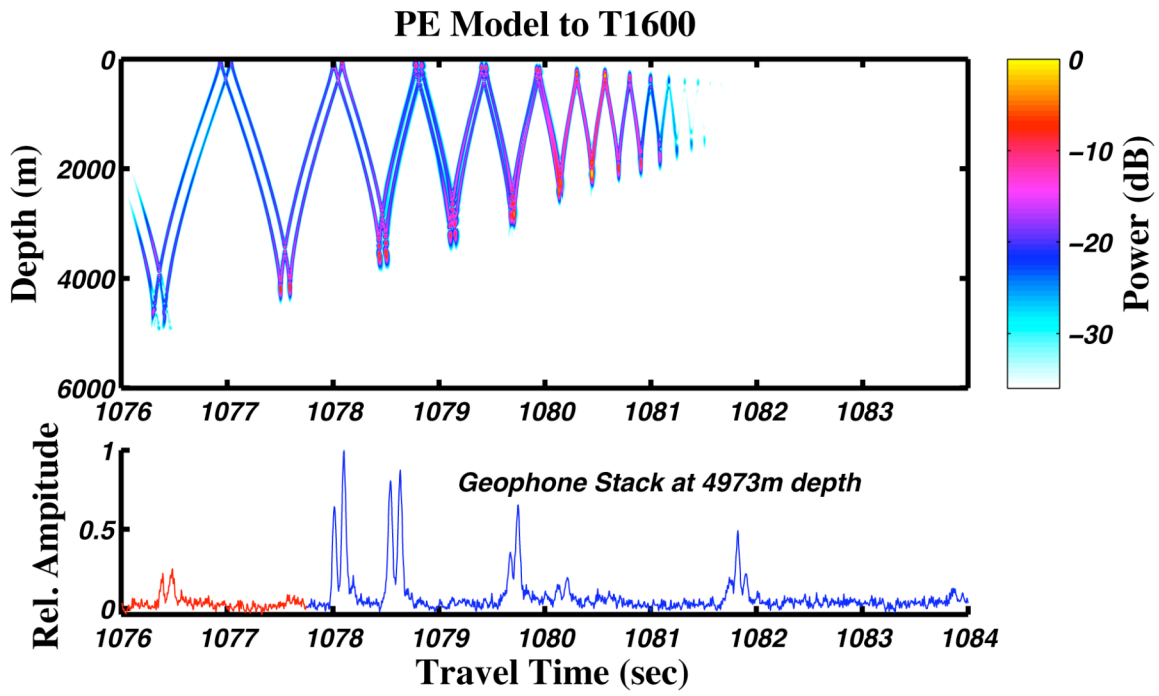

Figure 3-6: This is Figure 4 of the draft LttE. It compares the incoherent stack on OBS-S-Geo at T1600 with a PE model which does not include bottom interaction (no SRBR). The original caption is: "The predicted time front to 1600km range based on the parabolic equation (PE) model is compared to the stacked vertical velocity trace from an OBS on the seafloor. The earliest arriving doublet between 1076 and 1077sec corresponds to the deepest and earliest arriving rays. Of the four large amplitude late arrivals occurring after 1078sec only the arrivals near 1078.5sec and 1079.5sec appear to correspond to a cusp or caustic. This could be a coincidence. Since we do not see evidence for any of the late arrivals on the deepest hydrophone in the DVLA, we postulate that the late arrivals are interface waves whose amplitude decays exponentially away from the seafloor." [Fig_4.jpg]

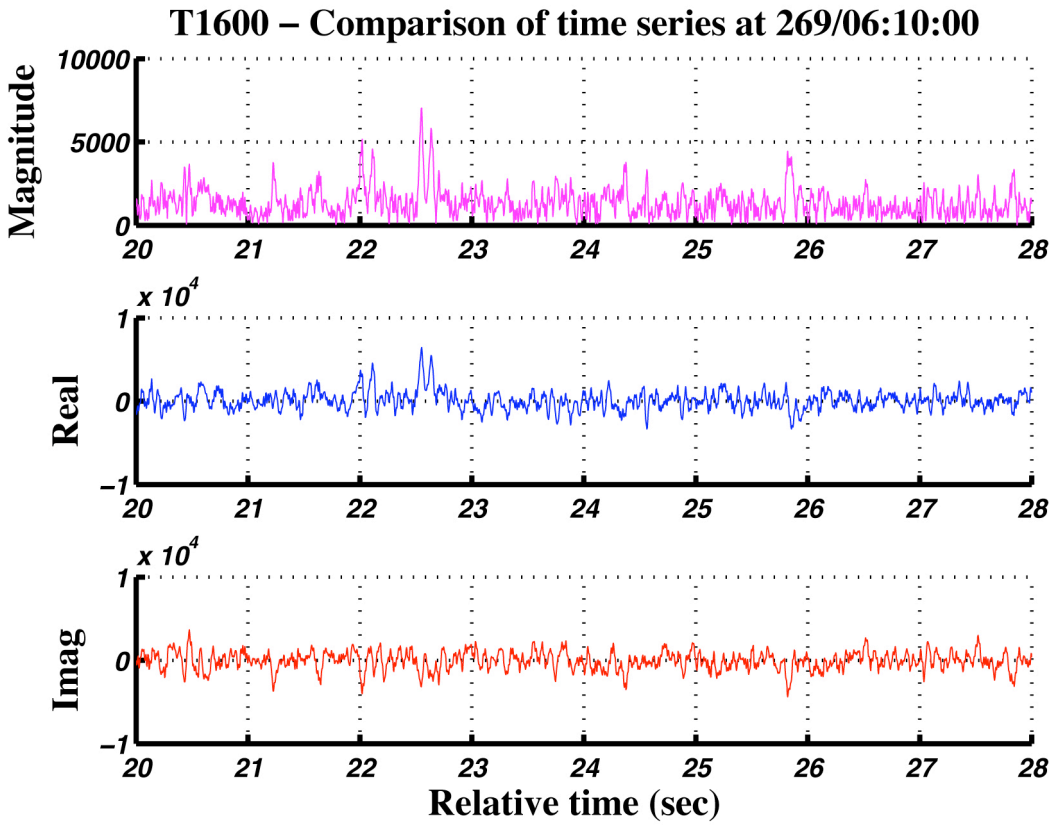

Figure 3-7: The real and imaginary components are compared with the magnitude of the replica correlator for a single sequence on OBS-S-Geo at T1600. At this range the SNR is much better than at T3200 and there are detectable arrivals. [Stack_Study_T1600_3.jpg]

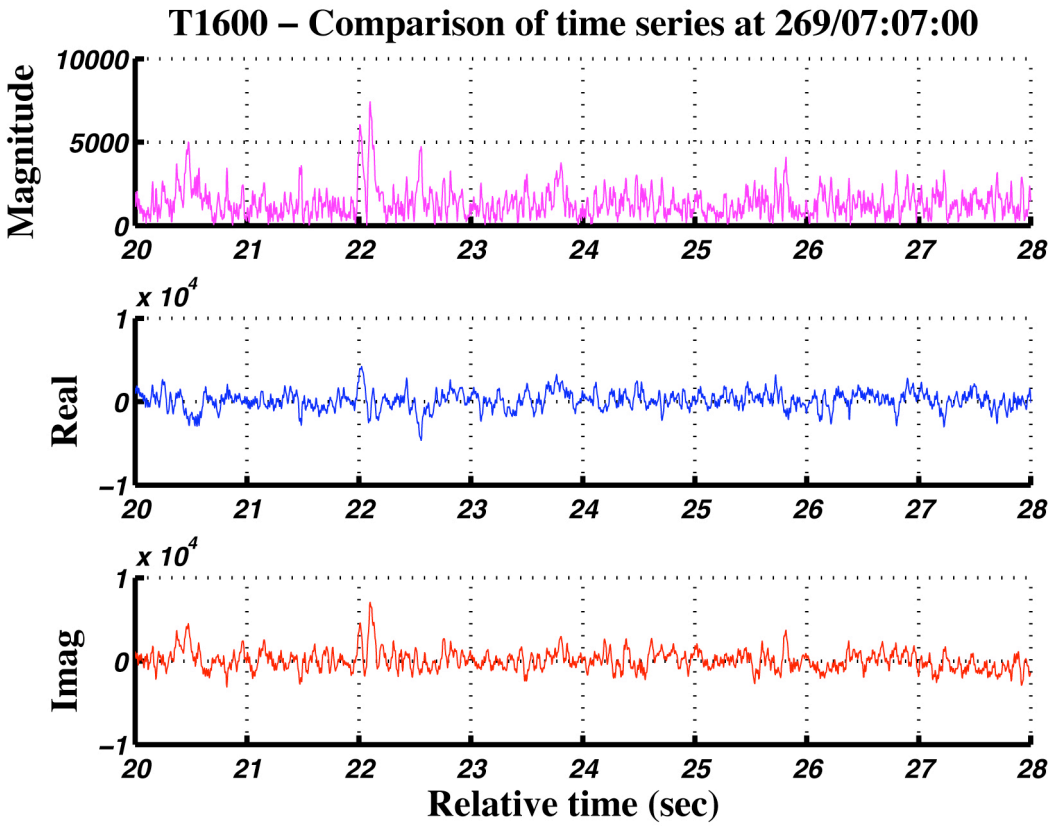

Figure 3-8: The real and imaginary components are compared with the magnitude of the replica correlator for another single sequence on OBS-S-Geo at T1600. At this range the SNR is much better than at T3200 and there are detectable arrivals. [Stack_Study_T1600_4.jpg]

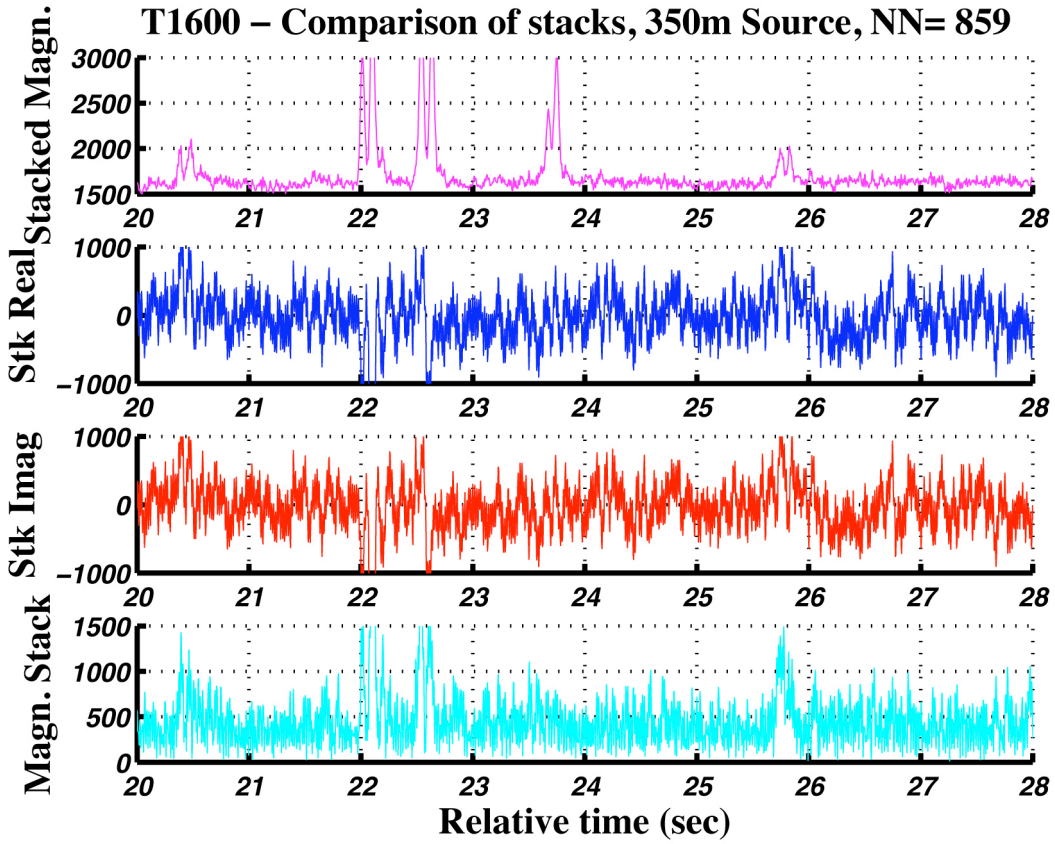

Figure 3-9: The incoherent stack (the sum of the magnitudes of the complex output of the replica correlator) of 859 sequences to OBS-S-Geo from T1600 is shown in the top trace. This is the same as the T1600 trace in Figure 3a of the LttE. The coherent stack (the magnitude of the stacks of the real and imaginary parts of the complex output of the replica correlator) of all 859 sequences to the South OBS from T1600 is shown in the bottom trace. The middle two traces are the stacks of the real and imaginary parts. The major arrival pattern is the same on the coherent and incoherent stacks and can even be seen in the single sequences in Figures 3-7 and 3-8. These arrivals are not artifacts of the stacking procedure. [Stack_Study_T1600_7.jpg]

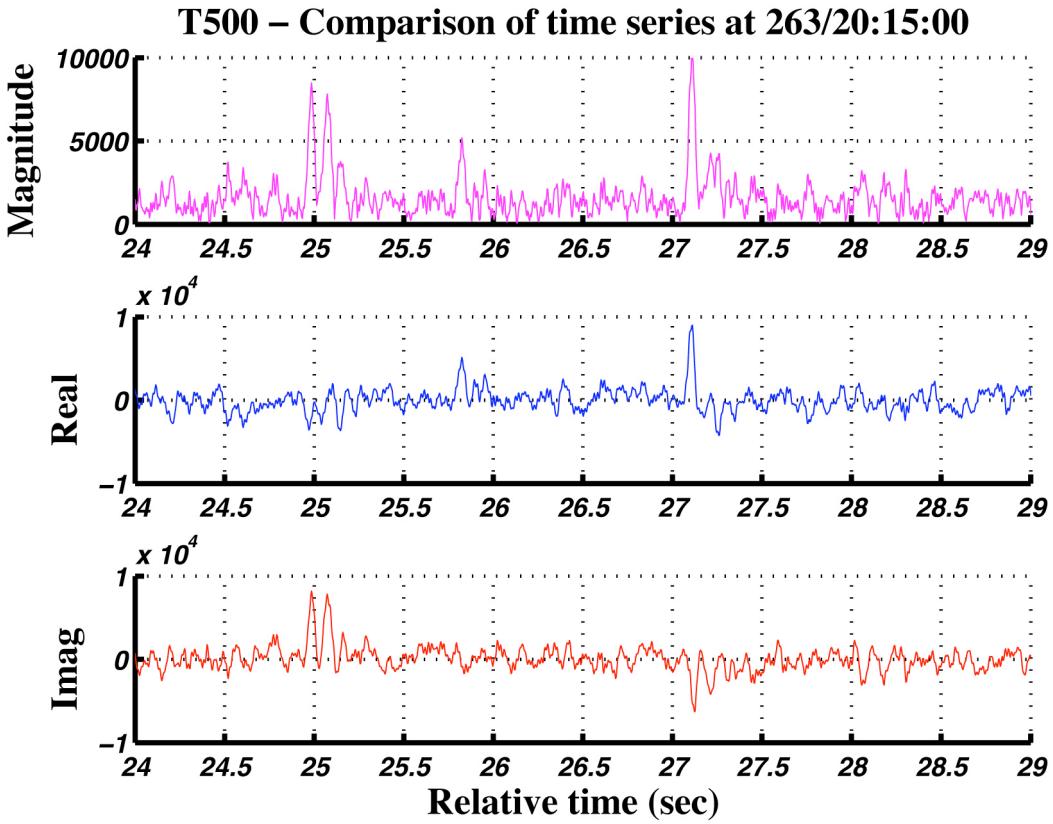

Figure 3-10: The real and imaginary components are compared with the magnitude of the replica correlator for a single sequence on OBS-S-Geo at T500. This range has the best SNR on both OBS-S-Geo and DVLA-L20-Hyd for both early and late arrivals. In this example both the early (near 25sec) and late (near 27.1sec) arrivals are quite clear in the magnitude trace. The arrival near 25.8sec is not consistent on other sequences and does not survive the stacking process. [Stack_Study_T500_3.jpg]

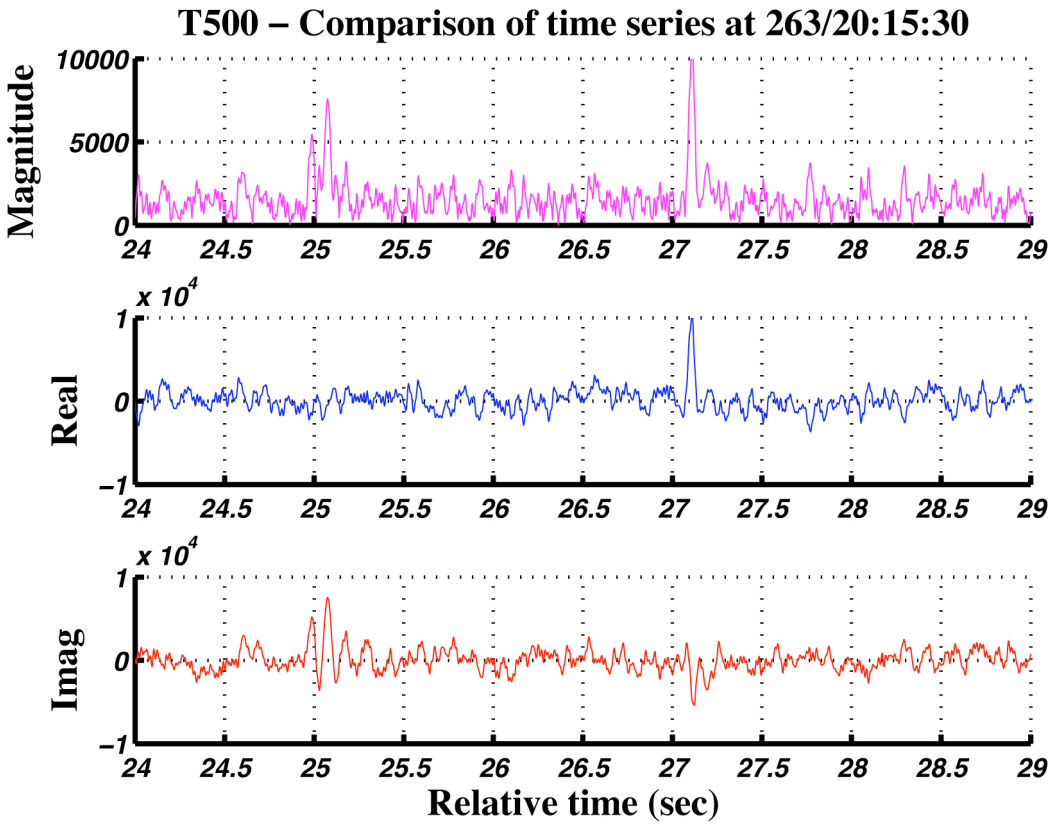

Figure 3-11: The real and imaginary components are compared with the magnitude of the replica correlator for another single sequence on OBS-S-Geo at T500. This range has the best SNR on both OBS-S-Geo and DVLA-L20-Hyd for both early and late arrivals. In this example both the early (near 25sec) and late (near 27.1sec) arrivals are quite clear in the magnitude trace. [Stack_Study_T500_4.jpg]

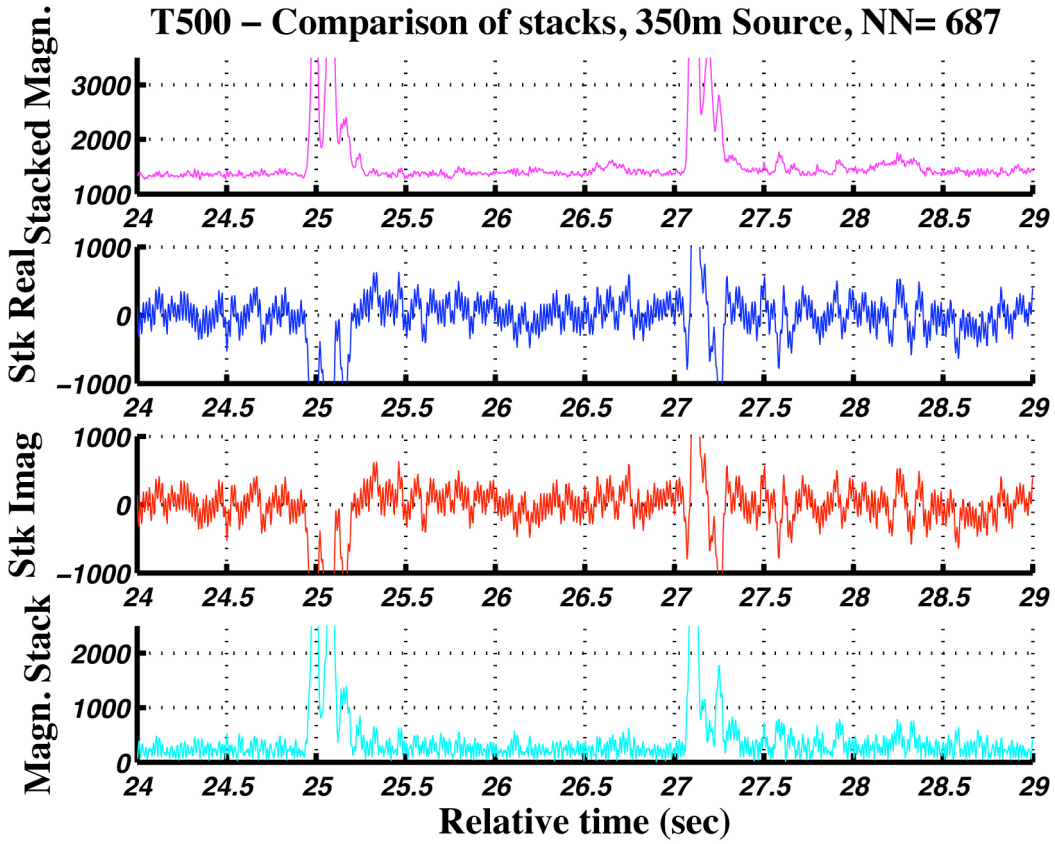

Figure 3-12: The incoherent stack (the sum of the magnitudes of the complex output of the replica correlator) of 687 sequences to OBS-S-Geo from T500 is shown in the top trace. This is the same as the T500 trace in Figure 3a of the Junje 27 version of the LttE (Figures 2-1a and 2-2a). The coherent stack (the magnitude of the stacks of the real and imaginary parts of the complex output of the replica correlator) of all 687 sequences is shown in the bottom trace. The middle two traces are the stacks of the real and imaginary parts. Both the PE predictable early arrival and the unpredictable late arrival on the OBS are not artifacts of the stacking procedure. They are ubiquitous features that are observed for individual sequences as well as for any manner of stacking strategy. [Stack_Study_T500_7.jpg]

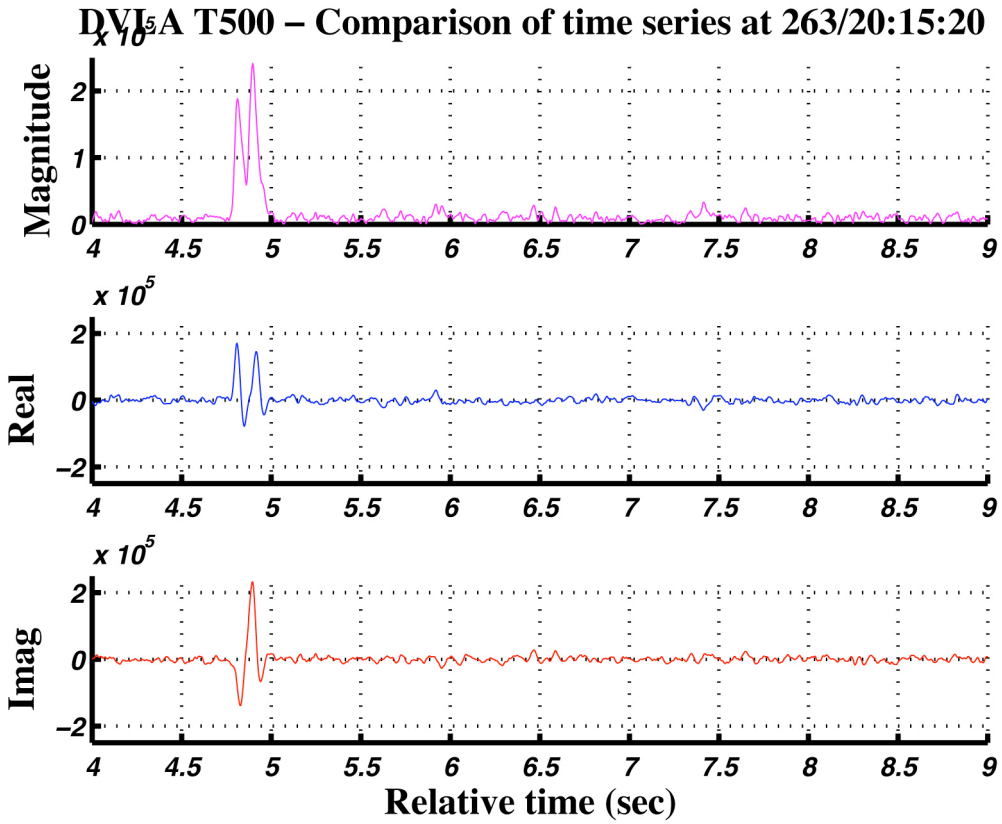

Figure 3-13: The real and imaginary components are compared with the magnitude of the replica correlator for a single sequence on DVLA-L20-Hyd at T500. This range has the best SNR on both OBS-S-Geo and DVLA-L20-Hyd for both early and late arrivals. In this example the early (near 4.75sec) arrival is quite clear all traces but the second arrival which appears on the OBS geophone about 2.1sec later is not observable. [Stack_Study_T500_DVLA_3.jpg]

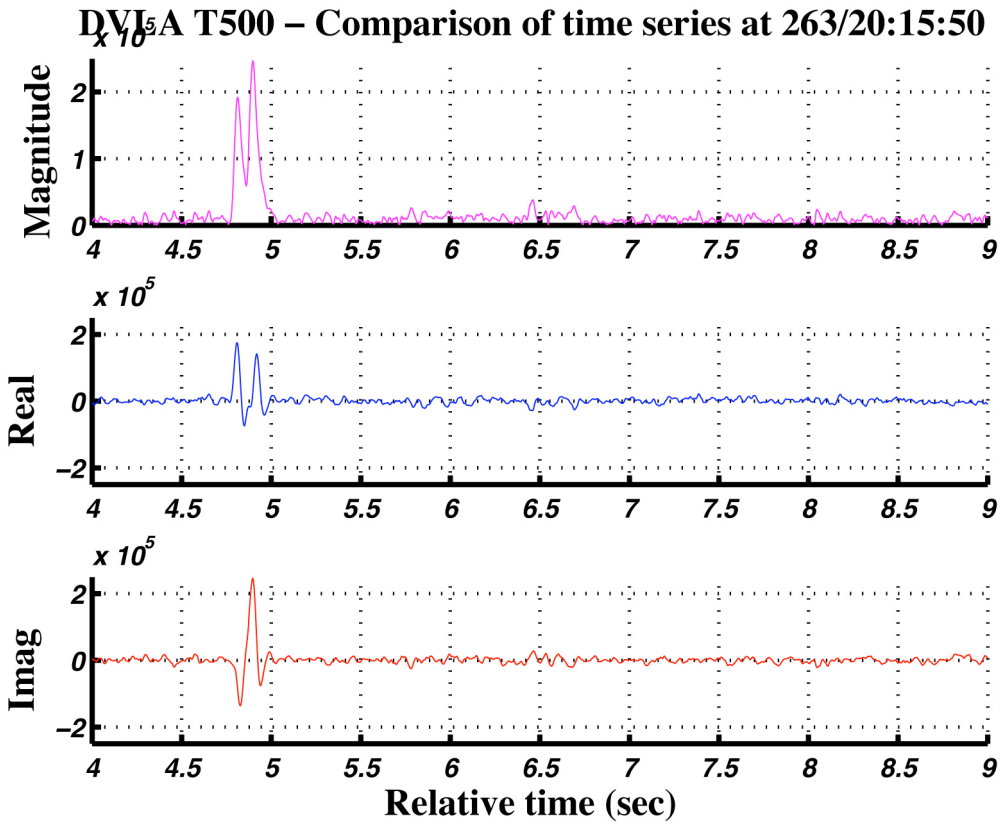

Figure 3-14: The real and imaginary components are compared with the magnitude of the replica correlator for another single sequence on DVLA-L20-Hyd at T500. This range has the best SNR on both OBS-S-Geo and DVLA-L20-Hyd for both early and late arrivals. In this example the early (near 4.75sec) arrival is quite clear all traces but the second arrival which appears on the OBS geophone about 2.1sec later is not observable.
[Stack_Study_T500_DVLA_4.jpg]

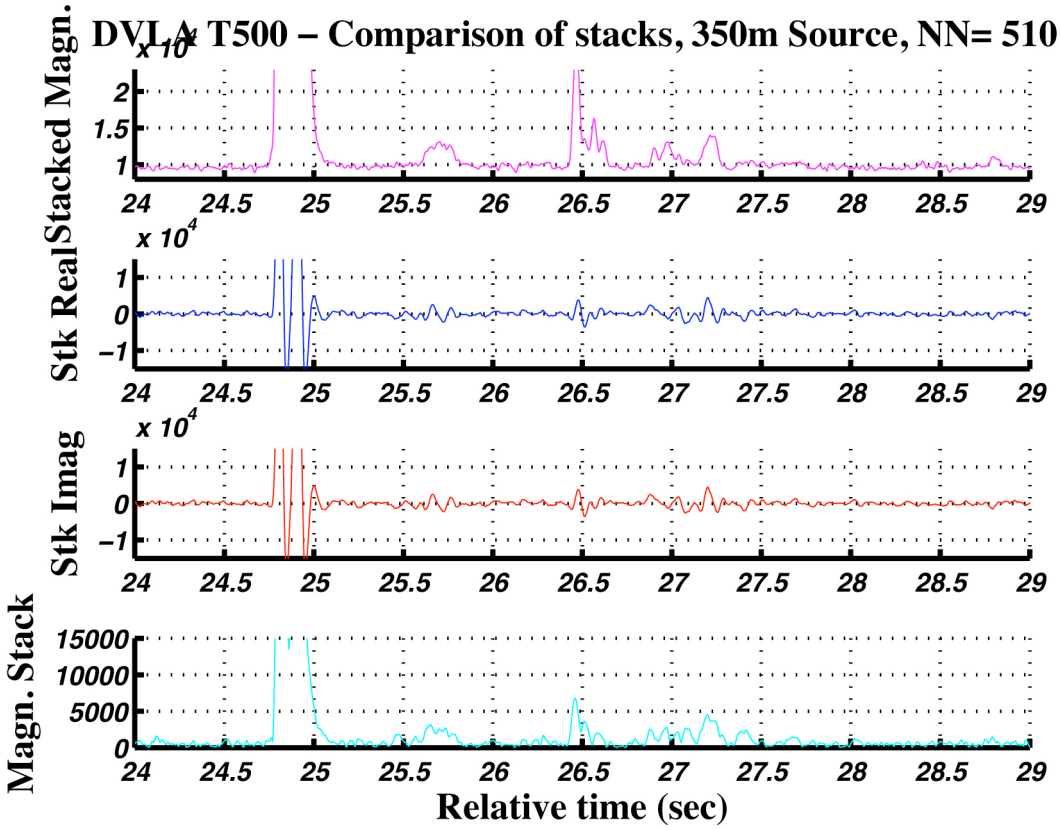

Figure 3-15: The incoherent stack (the sum of the magnitudes of the complex output of the replica correlator) of 510 sequences to DVLA-L20-Hyd from T500 is shown in the top trace. This is the same as the T500 trace in Figure 3c of the LttE (Figures 2-1c and 2-2c). The coherent stack (the magnitude of the stacks of the real and imaginary parts of the complex output of the replica correlator) of all 510 sequences is shown in the bottom trace. The middle two traces are the stacks of the real and imaginary parts. The PE predictable early arrival (near 24.7sec) is quite clear. There are a number of later, much smaller arrivals but the event corresponding to the second arrival on OBS-S-Geo, which should appear near 26.8sec is barely perceptible on either the coherent or incoherent stacks. The near-absence of the second arrival on DVLA-L20-Hyd is a ubiquitous feature that is observed for individual sequences as well as for any manner of stacking strategy. [Stack_Study_T500_DVLA_7.jpg]

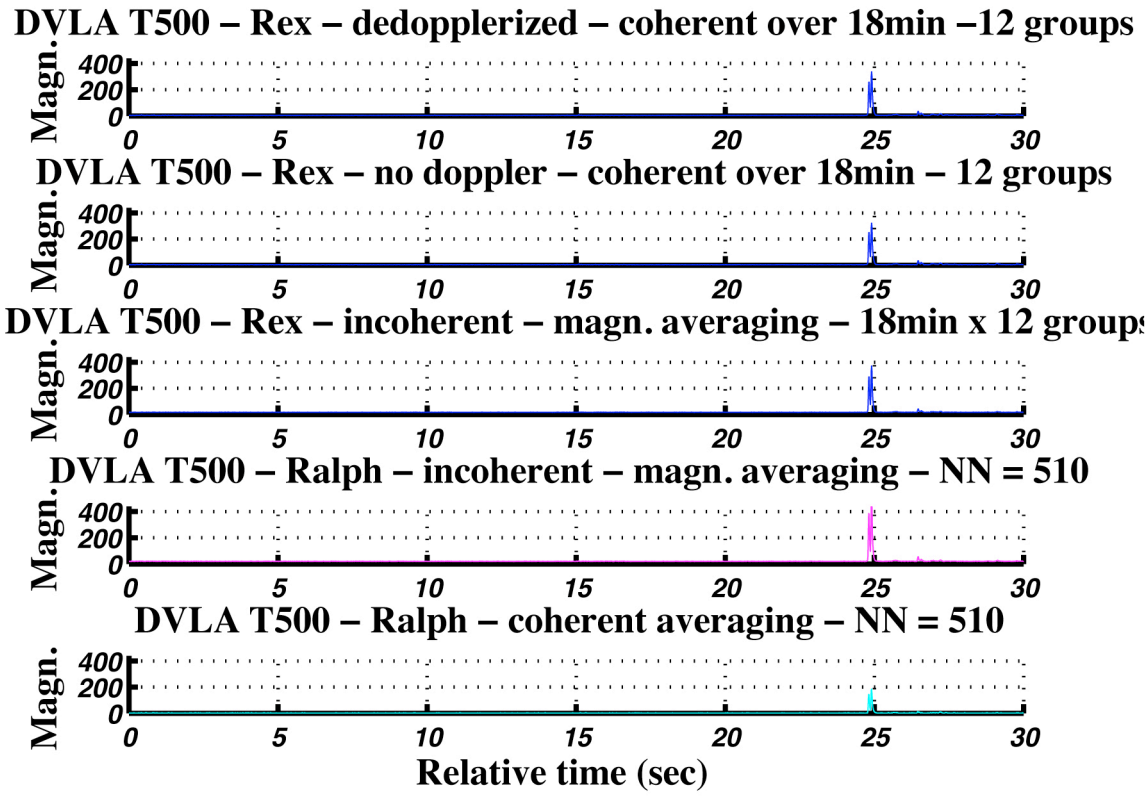

Figure 3-16: The top three traces are the results of Rex Andrew's processing for the lowermost hydrophone in the DVLA for T500 (Andrew, 2008). From top to bottom the three traces are: i) Doppler corrected with coherent averaging over 18minutes (either 28 or 36 periods because of recording gaps) and then incoherent averaging over 12 groups, ii) the same as i) but without Doppler corrections, and iii) incoherently summing the magnitudes of the individual replica correlated traces (between 12*28=336 and 12*36=432). The bottom two traces are from the processing described in Section 3a): iv) incoherent averaging over all available traces (510, upper trace in Figure 3-15) and v) coherent averaging over all available traces (510, lower trace in Figure 3-15). Results are discussed in the text. [Rex_Study_T500_DVLA_1.jpg]

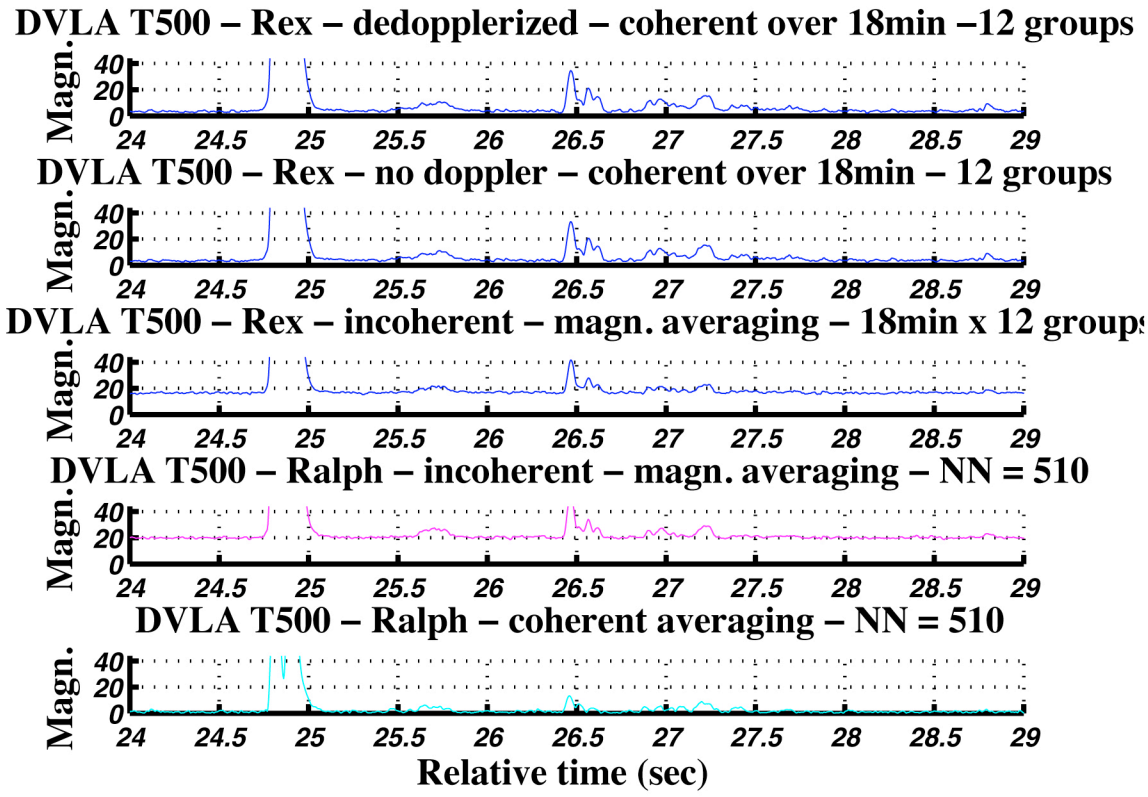

Figure 3-17: This is an expanded view in time and magnitude of the traces in Figure 3-16. The top four processing scenarios give remarkably similar results. Arguably the straight incoherent stack of the magnitude of all available individual traces (trace iv) gives the cleanest and most easily picked events. This is the trace that was used in Figures 2-1 and 2-2 and in the arrival discussions in Sections 4) and 5e). It would seem that for the purposes of identifying arrival structure, more involved processing including Doppler corrections is not necessary. [Rex_Study_T500_DVLA_3.jpg]

4) "Deep Shadow Zone" versus "Deep seafloor arrivals"

We distinguish between "deep shadow zone arrivals" (Dushaw *et al.*, 1999) and "deep seafloor arrivals". The expression "deep shadow zone arrivals" refers to arrivals on deep receivers that occur at about the same time as shallower turning points in the time fronts. There has not been a term for arrivals that appear on deep receivers at times that do not correspond to shallower turning points. We use the term "deep seafloor arrivals" for the new arrivals that we are observing primarily on the OBS vertical geophone. As discussed in Section 5, at least some of the deep seafloor arrivals could be SRBR but their characteristics have not yet been satisfactorily predicted by PE modeling with bottom interaction. For convenience we refer to the traditional, successfully predicted arrivals as "PE predicted" arrivals.

Examples of these three arrival types are demonstrated in Figures 4-1 to 4-4 for T500, T1000, T1600 and T2300 respectively. The top plot in each figure is the PE time front computed without bottom interaction (by Matt Dzieciuch). The second plot is the incoherent stack for DVLA-L20-Hyd (the same traces as in Figures 2-1c and 2-2c). The third plot is an expanded view of the DVLA-L20-Hyd trace. The bottom plot is the incoherent stack for OBS-S-Geo (the same traces as in Figures 2-1a and 2-2a).

Figure 4-1 summarizes the arrival structure for T500. The event at about 330sec (propagation speed of 1.487km/s, C in Figures 2-1 ands 2-2) is an example of a "PE predicted" arrival. The PE model time front shows that energy reaches the depths of DVLA-L20-Hyd and OBS-S-Geo at this time.

The event on DVLA-L20-Hyd just before 331sec is an example of a "deep shadow zone" arrival. This event occurs at the time of a turning point shallower than the receiver. These arrivals can be imagined as extensions of the turning point to depths deeper than expected. There is a very weak indication of it on OBS-S-Geo. Typically later "deep shadow zone arrivals" have progressively weaker amplitude as the turning points move to shallower depths. For example the later turning points are not observed in this case. The large event after 331.5sec on DVLA-L20-Hyd occurs at about the finale time in the PE model and appears weakly on OBS-S-Geo. This could be the "deep shadow zone arrival" of the finale, but arrivals like this at the finale time are not seen on DVLA-L20-Hyd or OBS-S-Geo at further ranges (T1000 and further).

The largest event on OBS-S-Geo, which appears at 332sec (propagation speed of 1.477km/s, A in Figures 2-1 ands 2-2) and which appears weakly on DVLA-L20-Hyd is an example of a "late seafloor" arrival. These events occur on OBS-S-Geo at times other than turning point times and are not predicted by PE modeling without bottom interaction. Deep seafloor arrivals do not necessarily get progressively weaker at later times. Bottom bounce paths (surface reflected - bottom reflected, SRBR) are a possible explanation for these arrivals and are discussed in Section 5. At T500 the deep seafloor arrival is a dominant event occurring well after the finale time and it appears weakly on DVLA-L20-Hyd. There are also very weak late arrivals at about 332.25sec on DVLA-L20-Hyd (not on OBS-S-Geo) and at about 332.5 and 332.9sec on OBS-S-Geo (not on DVLA-L20-Hyd).

At T1000 (Figure 4-2) the earliest PE arrival predicted at a time of about 665.3sec is not observed on DVLA-L20-Hyd. The next PE arrival at about 666.6sec is the largest event by far on DVLA-L20-Hyd. In the model time front this event does not extend to the OBS-S-Geo depth, but it is weakly observed on the OBS. It could be called a deep shadow arrival on the OBS.

Deep shadow zone arrivals from the next two turning points are clearly observed on DVLA-L20-Hyd at about 667.5 and 668.2sec. There is an indication of the first one on the OBS. This figure is an example of the deep shadow zone arrivals occurring progressively weaker at later times and being less clearly observed on OBS-S-Geo than on DVLA-L20-Hyd. Both of these effects are expected for energy that is decaying away from the turning points.

T1000 is the shortest range where we see a strong OBS arrival occurring between deep shadow zone arrivals, at about 667.0sec. In this case there is a weak indication of this event on DVLA-L20-Hyd as well. Since we do not have an explanation for this event yet we include it in the category of deep seafloor arrivals. Although all traces are displayed in relative magnitudes there is an indication here that this event is weaker on DVLA-L20-Hyd than on OBS-S-Geo, that is it decays with height above the seafloor. The other two deep seafloor arrivals, at about 668.7 and 670.8sec are prominent on OBS-S-Geo but there is no indication of them on DVLA-L20-Hyd. The second one (propagation speed of 1.477km/s, A in Figures 2-1 ands 2-2) is occurring over a second after the finale time.

At T1600 (Figure 4-4) two PE predicted at about 1076.2 and 1077.5sec are observed clearly on DVLA-L20-Hyd. The first of these (propagation speed of 1.487km/s, C in Figures 2-1 ands 2-2) is also clearly observed on OBS-S-Geo. In the model time front the second event does not extend to the OBS depth, but it is weakly observed on OBS-S-Geo. It could be called a deep shadow zone arrival on the OBS.

Deep shadow zone arrivals from the next two turning points are clearly observed on DVLA-L20-Hyd at about 1078.5 and 1079.1sec. The first one is clearly seen on OBS-S-Geo. There is an indication of a deep shadow zone arrival on DVLA-L20-Hyd for the next (fifth) turning point, near 1079.8sec but, oddly enough there is a very prominent event on the OBS at this time. There is also an indication of an arrival on OBS-S-Geo at the 6th turning point at 1080.1sec. Since they are more prominent on OBS-S-Geo than on DVLA-L20-Hyd, these could be deep seafloor arrivals but we will include them in the deep shadow zone class for now. Except for the 1079.8 and 1080.1sec events, this figure is an example of the deep shadow zone arrivals occurring progressively weaker at later times and being less clearly observed on the OBS than on the DVLA. Both of these effects are expected for energy that is decaying away from the turning points.

The unexplained events, that we are calling deep seafloor arrivals, at T1600 occur just before 1078sec and at about 1081.6sec. There is no way the first of these can be associated with a turning point. The second event is occurring at or just after the finale time. There is no indication of either one on DVLA-L20-Hyd. Since the near-finale arrival is not seen on DVLA-L20-Hyd it is a different type of event than the near-finale arrival discussed for T500. The very weak event just before 1084sec corresponds to the latest events seen at T500 and T1000 and has a propagation speed of 1.477km/s (A in Figures 2-1 ands 2-2).

At T2300 (Figure 4-4) the earliest PE arrival predicted at a time of about 1545.8 is not observed on the deepest hydrophone on DVLA-L20-Hyd or OBS-S-Geo. The next three PE predicted at about 1547.0, 1548.5, and 1549.5sec are the largest events on DVLA-L20-Hyd and get progressively larger with time. In the model time front only the first of these three extends to the OBS depth and a weak arrival is observed on OBS-S-Geo at this time. The other two PE events are not observed on OBS-S-Geo.

Deep shadow zone arrivals from the next two turning points (the fifth and sixth overall) are clearly observed on DVLA-L20-Hyd at about 1550.5 and 1551.0sec. There is no indication of these on OBS-S-Geo. There is a weak event on OBS-S-Geo corresponding to the ninth turning point at 1552.5sec but there is nothing at this time on DVLA-L20-Hyd. With the exception of the 1552.5sec event, this figure is an example of the deep shadow zone arrivals occurring progressively weaker at later times and being less clearly observed on OBS-S-Geo than on DVLA-L20-Hyd. Both of these effects are expected for energy that is decaying away from the turning points.

There are four deep seafloor arrivals for T2300 on OBS-S-Geo at about 1548.7, 1549.0, 1550.5 and 1551.5sec. The first and fourth of these are clearly not observed on DVLA-L20-Hyd. The second and third are close to events on DVLA-L20-Hyd but do not line-up well. For now we are considering them as OBS only events. There is no indication at T2300 for arrivals at propagation speeds of 1.477km/s (line A in Figures 2-1 and 2-2) that were seen at T500, T1000 and weakly at T1600.

The combination of PE predicted and deep shadow zone arrivals (those events associated with time fronts and turning points in PE models without bottom interaction) explains 3, 3, 5 and 5 arrivals on DVLA-L20-Hyd at T500, T1000, T1600 and T2300 respectively and 3, 2, 5, and 2 arrivals on OBS-S-Geo. There is one unexplained deep seafloor arrival observed on both DVLA-L20-Hyd and OBS-S-Geo at T500. There are no other unexplained arrivals on DVLA-L20-Hyd, but there are 3, 2, and 4 unexplained deep seafloor arrivals observed on OBS-S-Geo at T1000, T1600 and T2300 respectively. Of the events interpreted for now as deep shadow zone arrivals some of these are controversial because their pattern of relative magnitudes is not consistent. (For example, rather than progressively decreasing in magnitude with increasing time of the associated turning point, later turning points actually have dramatically increased magnitudes. As another example they appear on OBS-S-Geo but not on DVLA-L20-Hyd.) There are 1, 0, 2, and 1 of these respectively at T500, T1000, T1600 and T2300. The unexplained late arrivals and the controversial deep shadow zone arrivals are discussed further in Section 5e.

In conclusion the PE model predicts well the events whose time fronts cross the DVLA-L20-Hyd and OBS-S-Geo depths. We call these "PE predicted". As turning points move shallower across the DVLA-L20-Hyd depth the amplitude of the events increases with time. In the transition to "deep shadow zone arrivals" the turning points move above the DVLA-L20-Hyd depth and the amplitude of the subsequent events decreases dramatically. These events that we associate with turning points are most often seen better on DVLA-L20-Hyd than on OBS-S-Geo. This is consistent with the notion of energy extending, but still decaying, below the turning

points as expected for deep shadow zone arrivals. At all ranges considered (T500, T1000, T1600 and T2300) there are "deep seafloor arrivals" on OBS-S-Geo that are either not observed or are very weak on DVLA-L20-Hyd and these late arrivals do not correspond to turning point times. They appear to decay with height above the seafloor. "Deep seafloor arrivals" are the largest events by far on OBS-S-Geo and "PE predicted" are the largest events by far on DVLA-L20-Hyd.

At the very least the title of the draft LttE should be changed to something like "Deep seafloor arrivals: A new class of arrivals in long-range ocean acoustic propagation".

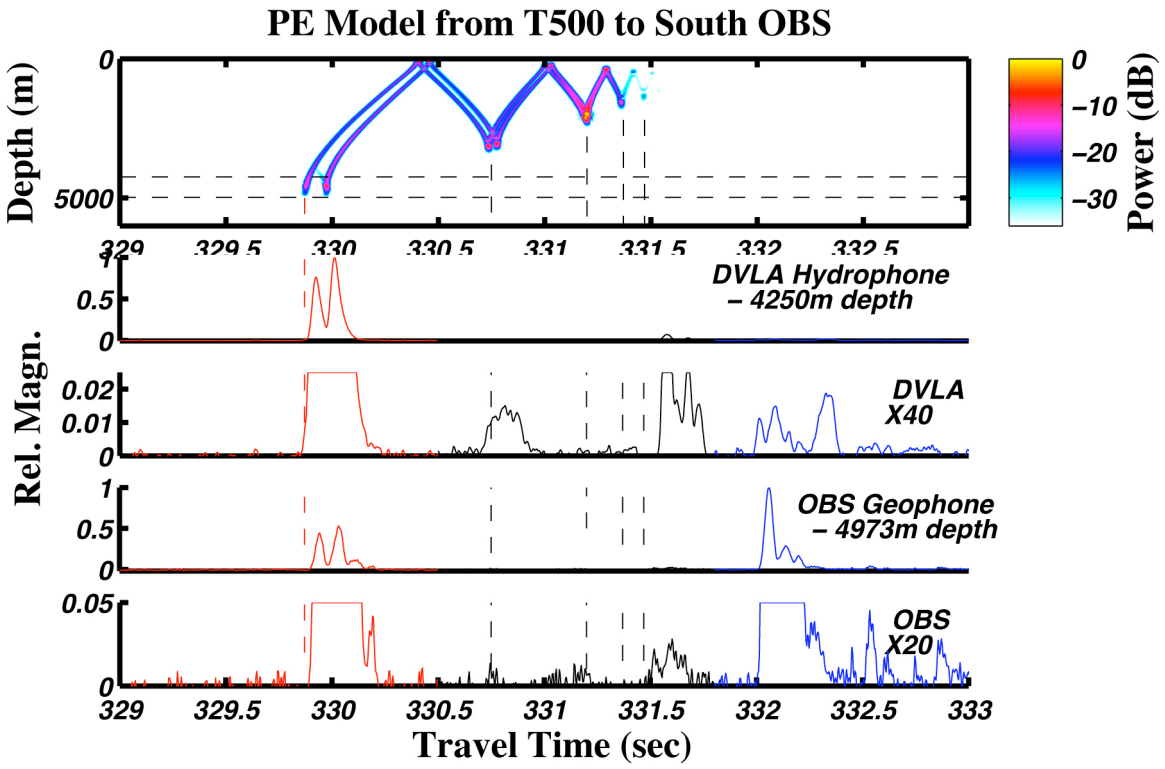

Figure 4-1: The next four figures compare the arrival structure on the deepest hydrophone in the DVLA and the vertical geophone on the South OBS with PE predictions. The top plot in each figure is the PE time front computed without bottom interaction (by Matt Dzieciuch). The upper and lower dashed lines show the depths of the DVLA hydrophone and OBS geophone respectively. The second plot is the incoherent stack for the DVLA hydrophone (the same traces as in Figures 2-1c and 2-2c). The third plot is an expanded view of the DVLA hydrophone trace. (In the DVLA plots the time axis has been stretched to allow for the slight difference in range between the DVLA and the OBS.) The fourth plot (or the bottom plot in later figures) is the incoherent stack for the OBS vertical geophone (the same traces as in Figures 2-1a and 2-2a). The bottom plot is an expanded view of the OBS geophone trace. Vertical dashed lines show the times of the turning points across all of the plots.

For T500 transmissions, examples of a "PE predicted" arrival (red trace at about 330sec), a "deep shadow zone" arrival (black trace just before 331sec) and a "late seafloor" arrival (blue trace at about 332sec) are shown. The event after 331.5sec on the DVLA occurs at about the finale time in the PE model and appears weakly on the OBS. This could be the "deep shadow zone arrival" of the finale. [Fig_4b-500.jpg]

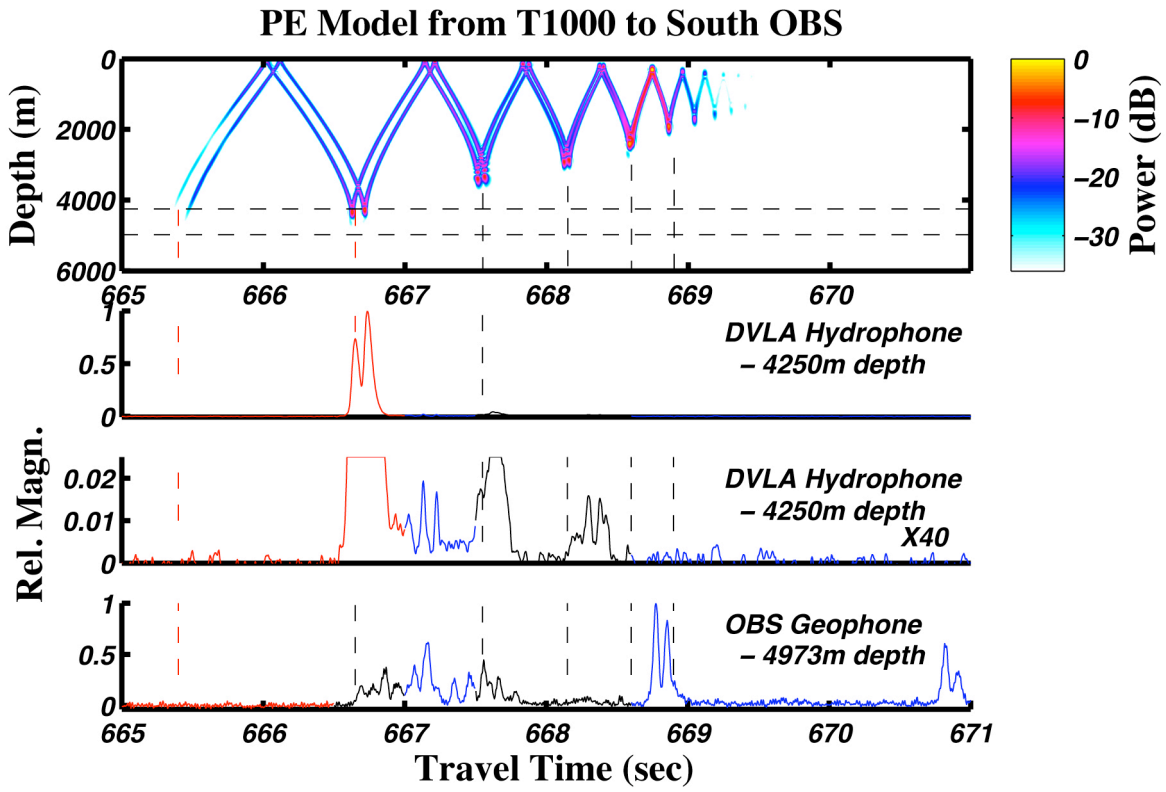

Figure 4-2: The arrival structure for T1000 is displayed in the format described in Figure 4-1.

For T1000 transmissions, examples of a "PE predicted" arrival (red trace at about 666.6sec), "deep shadow zone" arrivals (black traces at about 667.5 and 668.2sec) and "late seafloor" arrivals (blue traces at about 667.0, 668.8 and 670.8sec) are shown. [Fig_4b-1000.jpg]

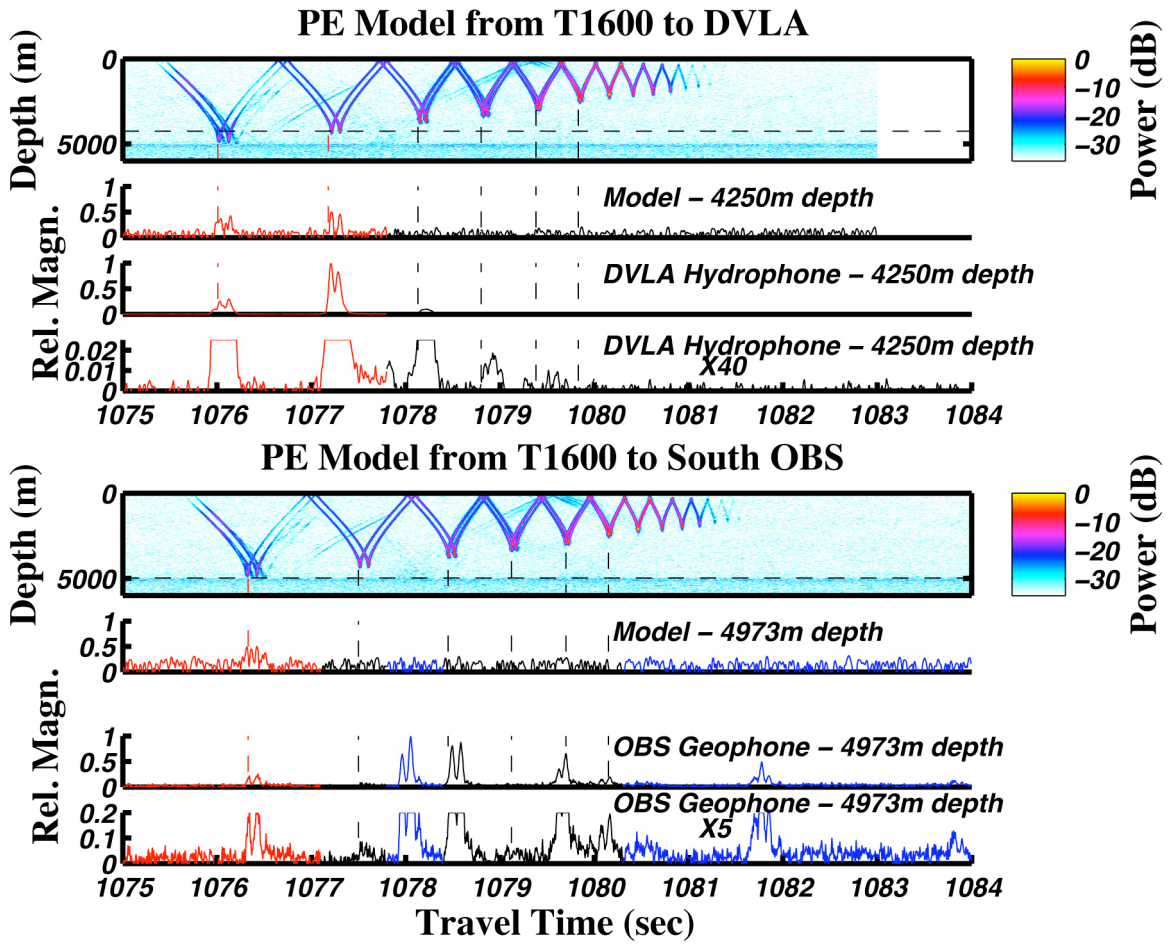

Figure 4-3: The arrival structure for T1600 is displayed in the format described in Figure 4-1.

For T1600 transmissions, examples of "PE predicted" arrivals (red traces at about 1076.3 and 1077.5sec), "deep shadow zone" arrivals (black traces at about 1078.5 and 1079.6sec) and "late seafloor" arrivals (blue traces at about 1078.0 and 1081.7sec) are shown. [Fig_4b-1600.jpg]

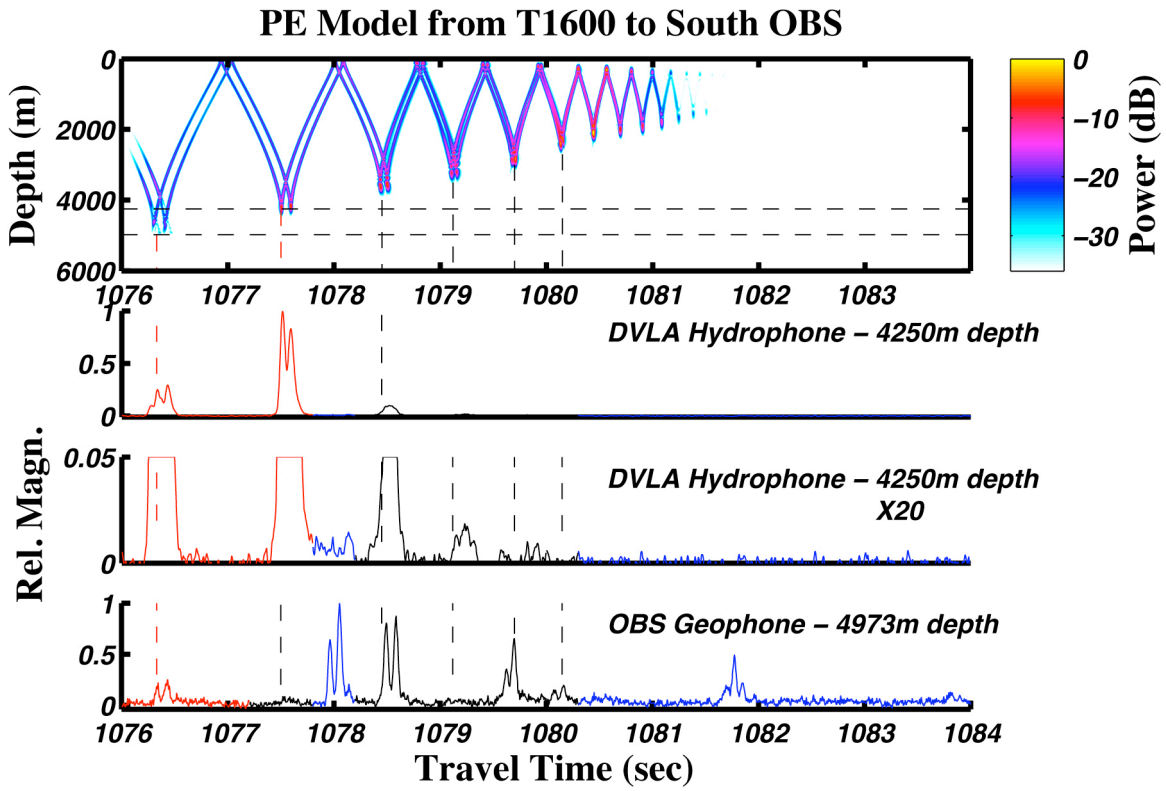

Figure 4-4: The arrival structure for T2300 is displayed in the format described in Figure 4-1.

For T2300 transmissions, examples of "PE predicted" arrivals (red traces at about 1546.6, 1548.1, and 1548.6sec), "deep shadow zone" arrivals (black traces at about 1550.2 and 1550.5sec) and "late seafloor" arrivals (blue traces at about 1548.4,1548.6, 1550.3 and 1550.7sec) are shown. [Fig_4b-2300.jpg]

5) SRBR Paths and Reconciling Results with Other NPAL Investigators

5a) Lora Van Uffelen's SPICE04 Results

Can the deep seafloor arrivals observed on OBS-S-Geo be surface-reflected bottom-reflected (SRBR) paths (water column multiples)? Lora Van Uffelen (Van Uffelen *et al.*, 2008; Van Uffelen *et al.*, submitted) reported clear SRBR's to T500 and T1000 in the SPICE04 data for sources around 250Hz (Figure 5-1). (The data time fronts are the coherent average of 10 periods of a phase coded M-sequence acquired on June 15, 2004 (Julian day 167).) It is curious, however, that up to September 2008 none of the investigators studying the LOAPEX data at 68.2 and 75Hz saw SRBR. In October 2008 Ilya Udovydchenko replotted some of his LOAPEX results (M75 sequences) for T50 and T500 and showed very weak arrivals near the seafloor that could be associated with SRBR (see the discussions in the following sections). A more complete discussion of the SPICE04 results is given in a recent paper submitted to JASA (Van Uffelen *et al.*, submitted).

These studies pose an interesting problem, independent of the OBS data: Why are SRBR paths observed clearly for SPICEX at 250Hz (750m source depth) and only weakly if at all for LOAPEX at 68.2Hz (350m source depth) or 75Hz (800m source depth)? The sound speed profiles could be different in the two cases since the SPICEX example in Figure 5-1 was from the summer (June 15, 2004) and LOAPEX was carried out in the Fall (10 September to 10 October, 2004). In a personal communication (August 27/08) however Lora says that " From a cursory glance at a few Spice receptions in September and October, these SRBR arrivals are present, at least at the 500km range, although they do appear to be slightly less intense than the arrivals seen in the June receptions." This could be an interesting question for a student project that does not involve the OBS data.

5b) Jinshan Xu's LOAPEX Results

Prior to October 2008 none of the investigators studying the LOAPEX sources has observed SRBR at T500 or further. For example Figure 5-2 shows data time fronts for the LOAPEX 68.2Hz source from Jinshan's thesis (Xu, 2007). (Xu did coherent averaging for 10 M-sequence periods in a group and then did an incoherent average over all available groups. Prior to the coherent averaging Doppler effects due to moving sources and receivers and tidal currents were removed.) There is no indication of SRBR in this figure. Furthermore Jinshan did not feel it was necessary to include SRBR in his analysis (for example, see Figure 5-4).

5c) Ilya Udovydchenkov's LOAPEX Results

Similarly, prior to October 2008, Ilya Udovydchenkov (pers.comm., July 31, 2008) did not see any SRBR paths in his analysis of the LOAPEX source data and did not include SRBR in his models (Figure 5-4). Arrivals that are reflected from the surface and refracted near the bottom

below the conjugate depth (Refracted Surface-Reflected - RSR) are included in his models as well as in the PE results in Section 4. [The nomenclature is from Munk et al (1995).]

The upper right panel in Figure 5-4a (for LOAPEX 75Hz transmissions) can be compared with the upper panel in Figure 5-1 (for SPICEX 250Hz transmissions). The 250Hz data shows SRBR arrivals and the 75Hz data does not. There are observable SRBR paths for the LOAPEX source at T50 (Ilya Udovydchenkov, pers.comm., July 31, 2008) (Figure 5-5a), but there is only weak evidence for significant SRBR paths on LOAPEX transmissions at T500.

In October 2008 Ilya regenerated his T500 and T50 plots with a much broader (75dB instead of 35dB) dynamic range. These are shown in Figures 5-4b and 5-5b respectively. The SRBR time fronts are much clearer for T50 (Figure 5-5b). At T500 the SRBR arrivals are very weak, relative to the other time fronts, and they only appear towards the bottom of the DVLA. Further discussion of the significance of SRBR arrivals in the SPICEX and LOAPEX transmissions, and their relevance to the deep seafloor arrivals, should consider absolute signal levels and signal-to-noise ratios.

Also since different investigators use different processing sequences (number of coherent traces in a stack before incoherent stacking, etc) we cannot positively say for sure that LOAPEX is not seeing significant SRBR. (Sections 3 and 6 address this in more detail.) We have seen enough examples with weak or non-existent SRBR, however, that we feel that it is unlikely that clever processing will dramatically enhance SRBR arrivals. This is pursued further in the next two sections involving processed data from APL/UW.

5d) APL/UW LOAPEX Data Provided by Linda Buck

We have checked processing effects further by looking at replica correlated data for every hydrophone in the lower section of the DVLA. The specific goal is to see if SRBR paths can be identified on the DVLA for the LOAPEX transmissions if more sophisticated processing is done. The data were provided by Linda Buck at APL/UW (pers.comm., July 8/08). Doppler processing has not been done on these data. (For a discussion of Doppler processing at APL/UW see Rex Andrew's report (Andrew, 2008) and Section 3b above.) The data set contains the replica correlated traces for the first 10 periods in each transmission window for each of the 20 hydrophones in the lower section of the DVLA. For the M68.2 sequences, for example, a period is 30sec, so 10 periods represents the first 5 minutes of data in either the 20 or 80 minute transmission windows. So only a small portion of the total available data is included here. Nonetheless there seems to be a consensus that coherently stacking over 10 periods (a group) is a reasonable thing to do and then incoherently stacking the coherent stacks for all available groups. This is what Jinshan did for his analysis of the LOAPEX data (Xu, 2007).

Figures 5-6 to 5-8 for T500 and 5-10 to 5-12 for T1000 compare results of APL/UW 0processing of the 20 hydrophones in the lower section of the DVLA (the data time fronts in the top panel) with WHOI processing of DVLA-L20-Hyd and OBS-S-Geo (middle and lower panels respectively). The events on the lower two panels were discussed in Figures 4-1 and 4-2 for T500 and T1000 respectively. These figures accomplish three things: i) They are sanity checks

that the replica correlation done at Woods Hole Oceanographic Institution (WHOI) was done properly. The top panel is APL/UW processing only for the DVLA and the middle panel is WHOI processing only for just DVLA-L20-Hyd. ii) They are sanity checks that the timing done at WHOI was done properly. That the events on the middle trace align with events at the bottom of the time front diagram confirms that the timing processes at the two institutions agree. The DVLA data (top two panels) was acquired with the DVLA clocks and the OBS data (bottom panel) was acquired with the OBS clocks. The apparent delay in the PE arrival at 330sec on the OBS is a consequence of the OBS being at slightly further range (0.46km) than the DVLA. These traces have not been adjusted for the range difference but the traces in Figures 4-1 and 4-2 have. iii) The APL/UW data for the whole lower segment of the DVLA makes time front displays possible. This shows the depth evolution of the arrivals discussed in Section 4. Also SRBR arrivals are clearly resolved in time front diagrams because of their different slope (eg see the SRBR arrivals in Figures 5-1 and 5-5).

Figure 5-6 compares the LOAPEX data time front on the DVLA for a single period of M68.2Hz at 350m source depth for T500 with the corresponding traces from DVLA-L20-Hyd and OBS-S-Geo. Even for a single period the OBS-S-Geo trace shows both the PE arrival (near 330sec) and the deep seafloor arrival (near 332sec) but the DVLA time fronts and DVLA-L20-Hyd trace only show the PE arrival. Since we see deep seafloor arrivals on single replica correlated traces, we can conclude that i) they are not an artifact of the stacking procedure and ii) they are not a subtle effect that requires clever processing to observe.

Figure 5-7 shows the effect of taking the coherent average of the first 10 periods (the first group) and then Figure 5-8 shows the effect of taking the incoherent average of the coherent averages for 12 groups. As the SNR improves clear time fronts emerge across the DVLA and there are three arrivals within 3seconds of the PE arrival on the DVLA-L20-Hyd trace. There is good correspondence between the traces shown here and in Figure 4-1 for the arrivals between 330 and 333sec on both DVLA-L20-Hyd and OBS-S-Geo. (See Section 4 for a discussion of the arrivals on these two traces.)

Figure 5-8 also shows arrivals beyond 3sec after the PE arrival (beyond 333sec including some wrap-around events out to 12sec after the PE arrival) that were not discussed in Section 4. (There is no evidence for these very late events on further stations (T1000 and greater) so they have not been included in the deep seafloor arrival story. I have not looked yet for very late arrivals like this at T50 or T250.) The weak arrival near 334sec on DVLA-L20-Hyd that does not appear on OBS-S-Geo aligns with a time front. This event should be studied further to see if the slope of time front is consistent with an SRBR arrival. New late arrivals also appear on the OBS-S-Geo trace that do not correspond to events on the DVLA-L20-Hyd trace or the DVLA data time fronts. These are occurring from 5 to 12sec after the PE arrival! If these late arrivals are SRBR one would expect to see SRBR on the DVLA as well. Figure 5-9 shows these arrivals in the same format as Figure 4-1 and with the wrap-around removed.

Figures 5-10, 5-11 and 5-12 tell a similar story for T1000. Although OBS arrivals are not observed on this first single period (Figure 5-10), they are observed on some later single periods for T1000. After coherent stacking of the first ten periods (one group), the arrival structure comparable to Figure 4-2 begins to appear. After taking the incoherent average of the coherent

averages within 28 groups, the arrival patterns for both DVLA-L20-Hyd and OBS-S-Geo are very similar to the incoherent stacks in Figure 4-2. It is interesting to see a hint of an arrival on the DVLA corresponding to the earliest turning point at about 665.3sec. It is also interesting to see the decay of the deep shadow zone arrival below the third turning point at about 667.5sec. There is no indication that the more involved processing drew-out more later arrivals at T1000 as at T500.

The work with the APL/UW replica correlated traces (with a partial coherent stack before incoherent stacking but without Doppler processing) confirms i) that the arrival structure on DVLA-L20-Hyd and OBS-S-Geo does not change significantly with slightly more sophisticated processing and ii) there is still no indication of SRBR in the DVLA data time fronts.

5e) Matt Dzieciuch's PE Models with Bottom Interaction

The PE model time fronts in Section 4 were computed with strong absorption in the bottom so that no SRBR paths (water column multiples or seafloor reflections) are included. The time fronts correspond to energy refracted above and below the source in the water column (refracted refracted, RR) and energy reflected from the sea-surface but refracting within the water column above the seafloor (RSR). In this section we consider the effects of bottom interaction and SRBR in the PE model time fronts.

This bottom interaction model consisted of: i) range dependent bathymetry along the geodesic from Smith and Sandwell (1997), ii) a 20m thick layer of homogeneous sediment with Vp = 1.6km/s and attenuation of 0.01dB/meter at 70Hz (all attenuation values are from Hamilton (1976)), iii) a 2km thick layer of basalt with a gradient in P-wave (compressional wave) speed from 4.0km/s to 6.8km/s and attenuation of 0.0025dB/m, iv) a 4km thick layer of gabbro with a gradient in P-wave velocity from 6.8km/s to 8.1km/s and attenuation of 0.0025dB/m and v) a homogeneous half-space for the mantle at 8.1km/s and attenuation of 0.0025dB/m. Density in the sediments (mostly pelagic clay for our experiment) is given by density (g/cc) = 1.35 + (1.80-1.35)/300 * depth (m) (Hamilton, 1976). For the igneous rocks density is related to compressional sound speed (Vp) by: density (g/cc) = 1.91 + Vp *0.158 (Swift *et al.*, 1998). Rigidity and shear wave sound speed are not included in the model.

PE model time fronts for the M68.2Hz source at 350m depth to the South OBS are shown in Figures 5-13 to 5-18 for T50 through T2300. Note that some wrap-around occurs - the weak arrivals on the far left should actually be placed on the right. The plot for T250 (Figure 5-14) is a nice example of water column multiples. One can see the bottom reflected energy (in cyan) below the RR and RSR paths (in blue and maroon) at about 168.8sec. Then three multiples are seen at the seafloor at about 170.3, 172.1 and 174sec (allowing for wrap-around). They are separated by about 1.5 to 1.9sec and the amplitude decays for subsequent arrivals. It is interesting that the amplitude seems to be enhanced by about 6dB near the seafloor. These events decay upward into the water column similar to the deep seafloor arrivals discussed in Section 4. Oddly the SRBR arrivals are relatively very weak at T500 (Figure 5-15), but there is a very weak event near the seafloor just after 332sec which could be SRBR. Two SRBR paths, separated by 2sec, can be seen at the seafloor for T1000 (Figure 5-16) and there are also clear

time fronts shallower than about 3000m. The time fronts are less steep for SRBR, corresponding to steeper ray paths, as expected for SRBR. There is a slight indication of three seafloor SRBR arrivals separated by about 2sec at T1600 (Figure 5-17). Similarly at T2300 (Figure 5-18) there are two SRBR arrivals separated by about 2sec. For T1000, T1600 and T2300 there are larger amplitude SRBR time fronts shallower in the water column. In the PE modeling SRBR arrivals at the seafloor are accompanied with clear time fronts shallower in the water column.

The PE model traces in the right panels of Figure 2-2 are taken from Matt's modeling with bottom interaction. There is good agreement with the DVLA hydrophone data (DVLA-L20-Hyd) for the "PE events" (panels c and d). Unfortunately the PE model traces at the OBS depth are quite noisy.

The correspondence between the PE models with bottom interaction (Figures 5-13 to 5-18) and the observed DVLA-L20-Hyd and OBS-S-Geo traces was checked further by the direct comparisons in Figures 5-19 to 5-22. In these figures the DVLA-L20-Hyd data were compared with the DVLA model time front and the OBS-S-Geo data were compared with the South OBS time front - so stretching the DVLA time series to allow for the slight range difference, as in Figures 4-1 to 4-4 was not necessary.

The data traces here are the incoherent stack of all good replica correlated periods as in the original LttE. At T1000, T1600 and T2300 the DVLA-L20-Hyd traces were advanced 0.20sec to get the first data arrival to align with the first model arrival, and the OBS-S-Geo traces were advanced 0.05sec. At T500 the DVLA-L20-Hyd traces were advanced 0.22sec to get the first data arrival to align with the first model arrival, and the OBS-S-Geo traces were advanced 0.10sec. We assume a resolution of 0.20sec in determining whether arrivals correspond or not. (See the notes on timing, ranges and clock drifts in section 5g.)

The RR and RSR paths in the model time fronts in these figures differ slightly from the RR and RSR paths in the models that did not consider bottom interaction (Figure 4-1 to 4-4). For example the downward branch of the T1000 time front between 665.3 and 666sec in the no bottom interaction case (Figure 4-2) is not observed for the bottom interacting case (Figure 5-20).

The T1000, T1600 and T2300 time fronts (Figures 5-20 to 5-22) have relatively clear, additional time fronts shallower than about 3000m that look like SRBR. The earliest SRBR is relatively stronger than later ones at the seafloor. Although there is an indication that the SRBR events decay upwards to about 500m above the seafloor, the RSBR events at the seafloor are very weak (down about 20dB) compared with the RR and RSR time fronts. The trace just below each time front panel is the model trace at the receiver depth (indicated by a horizontal dashed line in the time front diagram). It is difficult to see any events after the first one or two "PE predicted". The model SRBR events at the seafloor appear as a more dense cloud of color in the time front diagrams. It may be possible to increase the SNR of these events in subsequent processing.

The comparisons in Figures 5-19 to 5-22 have some general characteristics. We define a "PE event" (shown in red) as occurring when the time front diagram crosses or touches the depth

of the receiver. Both DVLA-L20-Hyd and OBS-S-Geo faithfully show all of the "PE predicted". When there are multiple PE predicted (for example, DVLA-L20-Hyd atT2300) subsequent events have larger magnitudes in the data. This observation is not replicated in the model. "Deep shadow zone" events (shown in black) coincide with shallower turning points - the turning points in the PE model do not reach the receiver depth. DVLA-L20-Hyd shows the first two or three of these but their magnitude decreases dramatically with subsequent events. Except for arrivals at T500 after the finale time (between 331.5 and 332.25sec in Figure 5-19) all of the events seen on DVLA-L20-Hyd can be identified as either "PE predicted" or "deep shadow zone" arrivals. The DVLA data can be explained, at least kinematically, by the PE model if one allows for scattering or some diffractive process to extend the turning points below their PE predicted depth. This is not the case for OBS-S-Geo.

OBS-S-Geo only sees the first one or two of the deep shadow zone arrivals (black) confidently, although occasionally there are peaks below much later turning points with gaps in the sequence. These could be aligning with turning points by coincidence, since except at T500 there is no indication of these on DVLA-L20-Hyd. At T500 (Figure 5-19) there is an event at or just after the finale time on both DVLA-L20-Hyd (just before 331.5sec) and OBS-S-Geo (just after 331.5sec). I have no idea what this is but for now I am not including it in the deep seafloor arrival category.

The following is a discussion of the deep seafloor arrivals observed at T500 through T2300 (Figures 5-19 to 5-22):

i) There is a clear deep seafloor arrival at 332sec for T500 on OBS-S-Geo and there is a very weak indication of a similar event on DVLA-L20-Hyd (Figure 5-19). There is a weak indication of this event in the model time front as well between 4000 and 5000m (it can be seen more clearly on Figure 5-15). This event could be SRBR.

ii) At T1000 (Figure 5-20) there is a muddle of energy between the first two turning point times (from about 666.6 to 667.8see) on OBS-S-Geo. The events at the beginning and end of this interval are deep shadow zone arrivals (black). We have identified the energy between these events as deep seafloor arrival energy (blue) and it corresponds to a weak concentration of energy near the seafloor in the PE model (it can be seen more clearly on Figure 5-16).. There is only a slight indication of this in-fill on DVLA-L20-Hyd (just before 667sec). This energy could be SRBR.

iii) The largest amplitude arrival on OBS-S-Geo at T1000 (Figure 5-20) occurs just before 669sec and arrives between the fourth and fifth turning points. It is not a deep shadow zone arrival. There is no indication of it on DVLA-L20-Hyd but it corresponds to a weak concentration of energy near the seafloor in the PE model (this can be seen more clearly on Figure 5-16). This energy could be SRBR.

iv) The second largest amplitude arrival on OBS-S-Geo at T1000 (Figure 5-20) occurs just before 671sec and arrives after the finale. There is no indication of it on DVLA-L20-Hyd but there is a weak concentration of energy just after 671sec near the seafloor in the PE model (this

can be seen on Figure 5-16). Since this arrival is occurring about 0.5sec before the concentration of energy in the PE model, we are tentatively concluding that it is not SRBR.

v) The largest amplitude arrival on OBS-S-Geo at T1600 (Figure 5-21) occurs at about 1078sec and arrives between the second and third turning points. There is no indication of it on DVLA-L20-Hyd but it corresponds to a weak concentration of energy near the seafloor in the PE model (this can be seen more clearly on Figure 5-17). This energy could be SRBR.

vi) The second largest amplitude arrival on OBS-S-Geo at T1600 (Figure 5-21) occurs at about 1078.4sec and coincides well with the third turning point. We have labeled this a deep shadow zone arrival since there is a corresponding event on DVLA-L20-Hyd. This is a curious event because it is much larger than the deep shadow zone arrival below the second turning point. Deep shadow zone arrivals typically get much weaker with subsequent turning points (as on DVLA-L20-Hyd for example). There are strong arrivals for both the second and third turning points on DVLA-L20-Hyd but there is no indication of either event near the seafloor in the PE model (this can be seen on Figure 5-17). This event is not SRBR, we are labeling it as a deep shadow zone arrival, but it could be an unexplained deep seafloor arrival.

vii) The third largest amplitude arrival on OBS-S-Geo at T1600 (Figure 5-21) occurs at about 1079.5sec and coincides well with the fifth turning point. We have labeled this a deep shadow zone arrival but the corresponding event on DVLA-L20-Hyd is extremely weak. (Remember that the DVLA hydrophones have much lower self-noise than the OBS geophones, so the DVLA hydrophones should be more sensitive sensors.) Like vi), this is curious event because it is much larger than the deep shadow zone arrival just before it and deep shadow zone arrivals typically get much weaker with subsequent turning points. There is a weak cloud of energy near the seafloor in the PE model from about 1079.5 to 1080sec (this can be seen on Figure 5-17). This event could be SRBR, we are labeling it as a deep shadow zone arrival, but it could also be an unexplained deep seafloor arrival.

viii) There is a weak arrival on OBS-S-Geo at T1600 (Figure 5-21) just after 1080sec and it coincides well with the sixth turning point. We have labeled this a deep shadow zone arrival but there is no corresponding event on DVLA-L20-Hyd. Like vi) and vii), this is curious event because it is larger than deep shadow zone arrivals before it. It occurs at the time of the weak cloud of energy near the seafloor in the PE model from about 1079.5 to 1080sec (this can be seen on Figure 5-17) so it could be SRBR. We are labeling it as a deep shadow zone arrival, but it could also be an unexplained deep seafloor arrival.

ix) A fairly strong arrival on OBS-S-Geo at T1600 (Figure 5-21) appears just before 1082sec, after the finale. There is no corresponding event on DVLA-L20-Hyd. There is no indication of even a weak cloud of energy near the seafloor in the PE model at this time (this can be seen on Figure 5-17). If one extrapolates the SRBR time front at the surface at 1080sec down to the seafloor, it arrives at about 1082sec, so conceivably this event could be SRBR if parameters could be adjusted to increase its amplitude significantly. We are labeling it as an unexplained deep seafloor arrival.

x) The very weak event just before 1084sec on OBS-S-Geo at T1600 (Figure 5-21) corresponds to the latest events seen at T500 (about 332sec) and T1000 (just before 671sec) and has a propagation speed of 1.477km/s (A in Figures 2-1 ands 2-2). Since the T500 and T1000 events could possibly be SRBR, I guess this event could be as well although there is no indication of an event at this time in the PE model (Figure 5-17). We are labeling it as an unexplained deep seafloor arrival.

xi) A weak arrival on OBS-S-Geo at T2300 (Figure 5-22) appears about 1548.4sec, between the second and third turning points. There is no corresponding event on DVLA-L20-Hyd. There is an indication of a weak cloud of energy near the seafloor in the PE model around 1549sec (this can be seen on Figure 5-18). This energy could be SRBR.

xii) A slightly stronger arrival on OBS-S-Geo at T2300 (Figure 5-22) appears about 1549.1sec, just before the third turning point. There is no corresponding event on DVLA-L20-Hyd. This event could correspond to the same weak cloud of energy as xi), near the seafloor in the PE model around 1549sec (this can be seen on Figure 5-18). This energy could be SRBR.

xiii) There is a very weak event just before 1550sec on OBS-S-Geo at T2300 (Figure 5-22). It occurs between the third and fourth turning points. There is no indication of it on DVLA-L20-Hyd nor on the PE model. It is an unexplained deep seafloor arrival.

xiv) The largest arrival on OBS-S-Geo at T2300 (Figure 5-22) appears about 1550.3sec, slightly too late to correspond to the fourth turning point. There is no indication of it on DVLA-L20-Hyd nor on the PE model (Figure 5-18). It is an unexplained deep seafloor arrival.

xv) A weak arrival on OBS-S-Geo at T2300 (Figure 5-22) appears about 1551.2sec, slightly too early to correspond to the sixth turning point. There is no indication of it on DVLA-L20-Hyd nor on the PE model (Figure 5-18). If one extrapolates the SRBR time front at the surface at 1549sec down to the seafloor, it arrives at about 1551sec, so conceivably this event could be SRBR if parameters could be adjusted to increase its amplitude significantly. We are labeling it as an unexplained deep seafloor arrival.

xvi) There is a weak arrival on OBS-S-Geo at T2300 (Figure 5-22) just after 1552sec and it coincides well with the eighth turning point. We have labeled this a deep shadow zone arrival but there is no corresponding event on DVLA-L20-Hyd. Like vi) and vii), this is curious event because it is larger than deep shadow zone arrivals before it. There is no corresponding event in the PE model (Figure 5-18). If one extrapolates the SRBR time front at the surface at 1550.5sec down to the seafloor, it arrives at about 1552sec, so conceivably this event could be SRBR if parameters could be adjusted to increase its amplitude significantly. We are labeling it as an unexplained deep seafloor arrival.

Of the 16 arrivals discussed above three have been labeled "deep shadow zone" initially (vi, vii and viii) although they are too large in magnitude to be consistent with deep shadow zone events. If we consider these three as deep seafloor arrivals, of the sixteen total, four cannot be SRBR (iv, vi, xiii, and xiv) and twelve could conceivably be SRBR. Of the 12 that could be SRBR, eight correspond to a cloud in the PE model (i, ii, iii, v, vii, viii, xi, and xii), three could

be extrapolated from time fronts at shallower depths (ix, xv and xvi) and one is extrapolated from events at other ranges (x). Although arguments can be made to explain the arrival times of the twelve "SRBR" events in SRBR terms, more modeling would need to be done to explain the relative amplitudes and other characteristics of these events.

At all four ranges the largest magnitude events on OBS-S-Geo do not correspond to either PE predicted (red) or deep shadow zone arrivals (black). These "deep seafloor arrivals" (blue) either occur between turning points or they occur well after the finale time. The earliest of these deep seafloor arrivals occurs between the second and third turning points at T1600 and T2300. The latest occurs at almost 12sec after the PE arrival, 10sec after the finale, at T500 (see Figure 5-9). Quite clearly the arrival structure on OBS-S-Geo is very different from the arrival structure on the DVLA (just look at Figures 2-1 and 2-2) and different physical processes must be invoked to explain them.

5f) Some comments on Dushaw (1999)

Dushaw et al's (1999) explanation for the arrival structure of long range acoustic propagation on bottom-mounted receivers was "leakage" below caustics occurring shallower in the sound channel. They were able to identify several arrivals (peaks) that were associated with caustics (turning points) well above the receiver. Because the spacing in time of the arrivals matched so closely the time spacing of the caustics above, they had confidence in the identification of the ray paths for the tomography problem. They called these "deep shadow zone" arrivals and the model has enjoyed wide-spread acceptance. In our analysis in Section 5e) we see that the arrival structure on DVLA-L20-Hyd (at 4250m depth) matches this model quite well. With few exceptions the peaks correspond to either PE predicted arrivals (the PE time fronts reach the receiver depth) or deep shadow zone arrivals (they occur on the receiver at the same time as shallower turning points). The OBS-S-Geo arrival structure looks completely different although weak arrivals occur at the PE predicted times and occasionally at deep shadow zone arrival times. The large magnitude peaks in the OBS data are either SRBR arrivals (Dushaw et al did not mention this as an option) or some unknown arrival type (possibly a shear or interface wave effect) or both. Dushaw et al do mention that bottom-interacting energy, scattering from bottom features local to the source and receivers, contributes a signal-generated noise that complicates the identification of later arrivals.

A detailed comparison of the NPAL OBS results with Dushaw et al's results could be a lot of work. The 75Hz M-sequence source concept is very similar if not identical. Dushaw et al had much more data in elapsed time, six 20-minute transmission windows per day for almost two years, so tidal and seasonal effects could be addressed. Also the bottom "receivers" were 40 element hydrophone arrays so they could do beam forming in azimuth and presumably the SNR would be much better. (We know for example that our OBS data was self-noise limited. Dushaw et al did coherent averaging over 20minute windows, but suggest that 13-14minutes might be better. As discussed above NPAL04 investigators have used 5minute and 18minute windows. There does not seem to be consensus on the correct window length.) Dushaw et al, however, did not have multiple, in-line receivers as on NPAL04. The move-out, or evolution, of events as a function of range on NPAL04 can be useful in distinguishing arrival types and

propagation paths. Also Dushaw et al did not have a simultaneous and co-located vertical line array in the water column above their bottom receivers. The combination of the DVLA with the OBSs on NPAL04 allows a precise comparison of the arrival times and magnitudes in the water column and on the seafloor.

Dushaw et al's deep receivers, arrays **n** and **o**, appear to be at depths comparable to the NPAL04 DVLA. It is useful to quote Dushaw et al (pages 204-205) here: "...an interesting, and perhaps new, type of "ray arrival" which appears to occur well into the shadow zone of the predicted arrival. We will refer to these arrivals as "shadow-zone arrivals". While all of the stable arrivals can be associated with a cusp [caustic or turning point] of the predicted time front, the later arrivals are 500-1000m below the predicted time front. ... These shadow zone arrivals appear to retain "ray-like" aspects, but the latest arrivals, or those deepest into the shadow zone, are certainly less distinct. ... The apparent stability of these arrivals, together with detection of similar arrivals at several other deep arrays in both the Atlantic and Pacific oceans, rules out bottom interaction as the origin of these arrivals. To date, no known mechanism, e.g. diffraction leakage from caustics or diffusion of acoustic energy by internal wave scattering, can explain the extreme depth diffusion of acoustic energy that must be occurring.

"Because the forward problem for the shadow-zone arrivals is unknown, it is not known how to apply these data correctly to determine ocean temperature changes. For the time being, the ray paths predicted for the time front cusp will be used to represent the sampling associated with these arrivals, even though the time front cusp may be several hundreds of meters above the receiver depth."

I think that our analysis in Section 5e) is consistent with Dushaw et al's reported observations. We see the PE predicted and deep shadow zone arrivals on DVLA-L20-Hyd although the deep shadow zone arrivals seem to decay quickly in 200-300m below the turning point. The largest events that we see on the seafloor OBS that are 500-1000m below the turning points do not align well with the turning point times and with few exceptions do not correspond to arrivals on DVLA-L20-Hyd, as you would expect for energy decaying from the turning point. There seems to be yet another type of arrival that we are calling "deep seafloor arrivals". These could possibly be related to SRBR or they could be associated with shear or interface waves. In the latter case the shear or interface waves could be generated by secondary (deterministic) scattering from features near the receiver. The remarkable observation is that they are by far larger than any of the PE predicted or deep shadow zone arrivals.

Dushaw et al (page 206) mention "the din of bottom interacting energy that appears in the latter part of the reception" and (page 208) "the later arrivals appear to occur well into the shadow zone of the predicted arrival pattern. ... On the one hand, they appear to be stable identifiable arrivals, while, on the other hand, the forward problem is not known, so legitimate inversion of these data is not possible." Furthermore for some of their sensors ray identification was not possible (page 207): "we conclude that no obvious ray identification is available for the receptions at receiver **l**." and (page 212) "The primary complicating factor in these data is the interaction of the acoustic energy with the ocean bottom near the receivers or near the acoustic source." There are a number of instances in Dushaw et al where the "deep shadow zone arrival" explanation breaks down. The NPAL04 OBS data are another case of this, but we have the simultaneous water column data and the multiple range data to help resolve the issues.

It is important to sort out the physical mechanisms responsible for the deep seafloor arrivals. Deep seafloor arrivals that are not associated with caustics could complicate the tomography work based on seafloor sensors.

5g) Timing, Ranges and Clock Drifts

A quantitative analysis of the offset and drift of the DVLA and OBS clocks has not been carried out yet, but it should obviously include stations T50 and T250. Normally the OBS clocks are compared against GPS (Global Positioning System) clocks just before deployment and just after recovery and the appropriate drifts are accounted for. On NPAL04 the OBSs were down so long that the batteries on the clocks ran down so that the clocks could not be checked on recovery. We knew this in advance. The idea was that we could use events recorded on both the OBSs and DVLAs to correct the OBS timing to at least the DVLA accuracy. Drift may not be so bad since the LOAPEX transmissions were made within 4 weeks of deployment (the OBSs were deployed on 13 Sept and the last LOAPEX transmission at T3200 was 4 October and at Kauai was 10 October), although a temperature shock effect on deployment could contribute to an offset. So I believe that the timing in the OBS data set is correct to within a sample (0.002sec) of GPS time on deployment.

In this paragraph and Table 5-1 we assume that the PE model is "correct". Then we log the time shift necessary for each receiver to get the "first PE" arrival to align by eye. This appears to be pretty much constant with respect to range so we express the "time shift" as a range independent "offset" plus a range dependent "drift". These values for the four working receivers and for stations T500 to T2300 are given in Table 5-2.

Inaccuracies in timing can occur in a number of places:

i) The data providers do their best to reduce the data to as accurate a timing as possible. In the case of the OBSs we know that clocks drift and we know they could not check the timing on recovery so there is an obvious reason why the timing may be off but we have no idea how much. We can do some simple sanity checks such as making sure that a 5minute data set has precisely the correct number of samples.

ii) In our (and other NPAL investigators) own processing there are time shifts, etc that need to be properly accounted for. These include the nominal flight times used to offset the recording windows, time shifts associated with the replica correlation and time shifts associated with the Doppler processing. There is a section in the LOAPEX cruise report that discusses timing of the sources and the nominal recording windows. Our agreement with Rex's processing above indicates that we are at least consistent on this for the DVLA.

iii) "Timing offsets" will appear if the ranges used for the PE modeling or flight times are inaccurate. The DVLA drifted about a nominal location and this drift was monitored but we have not included it in our analysis. The OBSs were at least fixed during the experiment and their locations were determined by triangulation from the surface ship prior to recovery. We are

using DVLA and OBS locations and ranges provided by Matt. Since a typical propagation velocity across the array is about 1.5km/s, an offset in time of 0.2sec would correspond to a range offset of 300m and an offset of 0.002sec (one sample on the OBSs) would correspond to 3m. It is very unlikely that the ranges are incorrect by 300m.

iv) Timing in the PE model (or other forward modeling code) needs to be checked and understood.

v) When data sets from different systems (in different locations) are compared, common sense and experience with the physics tells us something about the timing. Certain arrivals should occur at the same time or be offset by a certain amount based on the known physics. If we just accept the timing from i) through iv) then we may be forced to reconsider the physics - so to avoid these situations we go back to i) through iv) to make sure errors were not made or assumptions were valid. Since the OBSs and DVLA were at different ranges (and I guess at a fine scale the DVLA could be blowing in the current) we use something like the PE model to link the arrival structure at different locations.

In Section 5e) at T1000, T1600 and T2300 the DVLA-L20-Hyd traces were advanced 0.20sec to get the first data arrival to align with the first model arrival, and the OBS-S-Geo traces were advanced 0.05sec. At T500 the DVLA-L20-Hyd traces were advanced 0.22sec to get the first data arrival to align with the first model arrival, and the OBS-S-Geo traces were advanced 0.10sec. We assume a resolution of 0.20sec in determining whether arrivals correspond or not. (See the notes on timing, ranges and clock drifts in section 5g.)

So for the purposes of comparing the arrival structure on OBS-S-Geo, DVLA-L20-Hyd and the PE modeling we are getting consistent results to a resolution of 0.20sec and this is OK since the arrivals are seconds apart. This includes the offset with the PE model. The difference between the DVLA and OBS is about 0.12sec (for T500) and 0.15sec (for T1000, T1600 and T2300). (This was just aligning arrivals by eye - getting accurate offsets by correlation of waveforms has not been done yet. Of course this assumes that the waveforms are similar. Since there is stacking and noise involved this could be a complicated process. The dramatic difference between the DVLA and OBS arrival structures does not help.) Now for the OBS at 500sps (sample interval of 0.002sec) this is 60 to 100samples. We expect timing accuracy to within a sample, so our timing is much cruder than the specifications. Whether it is worth the effort to go back and reconsider all of the timing issues depends on available resources and the specific application. For the purposes of our LttE I think we are OK.

Since 2004 there has been some confusion regarding the OBS locations and hence the correct ranges for the propagation modeling. The "OBS locations" in the following documents are all the same and correspond to "drop positions", not the "acoustically navigated actual seafloor positions":

Patricia Cheng's email to Mark Gibaud on June 16, 2005
Table 2.1 in the LOAPEX cruise report (dated April 2005)
Page 9 of the SPICE04 Cruise Report (dated June 25, 2005)

(Also the depth of OBS 1 in Patricia's email is 4995.6m versus 4996.5m on page 9 of Peter's cruise report.)

In an email on June 8, 2007 Jeff Babcock sent "new" OBS locations based on the acoustic triangulation data that had been acquired on the recovery cruise. These are 2-D solutions:

Site 1 (SN69):
==== 2-D ====
Initial Drop: Lat: 33 25.1100 (33.4185), Lon: -137 42.2820 (-137.7047), depth: 4996.5000
Final Drop: Lat: 33 24.9985 (33.4166), Lon: -137 42.2566 (-137.7044), depth: 4996.5000
Number of points (N): 264
sqrt(sum(Residual2)/N) : 11.583163245
Offset Distance: Lat=-206.9000 meters, Lon=39.3000 meters, (r=210.5994 meters, angle=-79.24)

Site 2 (SN61)
==== 2-D ====
Initial Drop: Lat: 33 26.3790 (33.4397), Lon: -137 40.9503 (-137.6825), depth: 5075.9000
Final Drop: Lat: 33 26.1844 (33.4364), Lon: -137 41.0392 (-137.6840), depth: 5075.9000
Number of points (N): 312
sqrt(sum(Residual2)/N) : 100.842095474
Offset Distance: Lat=-361.1000 meters, Lon=-137.7000 meters, (r=386.4641 meters, angle=-110.87)

Site 3 (SN24):
==== 2-D ====
Initial Drop: Lat: 33 25.1100 (33.4185), Lon: -137 39.6300 (-137.6605), depth: 5035.1000
Final Drop: Lat: 33 25.2002 (33.4200), Lon: -137 39.8342 (-137.6639), depth: 5035.1000
Number of points (N): 310
sqrt(sum(Residual2)/N) : 110.195854855
Offset Distance: Lat=167.3000 meters, Lon=-316.2000 meters, (r=357.7314 meters, angle=152.12)

Site 4 (SN64):
==== 2-D ====
Initial Drop: Lat: 33 23.8505 (33.3975), Lon: -137 40.9471 (-137.6825), depth: 4973.4000
Final Drop: Lat: 33 23.9320 (33.3989), Lon: -137 40.9572 (-137.6826), depth: 4973.4000
Number of points (N): 265
sqrt(sum(Residual2)/N) : 117.391372208
Offset Distance: Lat=151.3000 meters, Lon=-15.6000 meters, (r=152.1021 meters, angle=95.89)

I recomputed the OBS ranges to the LOAPEX stations using Matt's range code, obspe.m, the new, final bottom locations from Jeff and the best available time-independent locations for the T stations (but not correcting for doppler or using the acoustically navigated source positions). The matlab subprogram geod.m is used to calculate the geodesic range assuming a

WGS-84 ellipsoid. It is contained in a directory called aoggdr. The code is believed to be accurate to < 1m. The recomputed ranges are given below. "Diff" means the difference between the old (drop) positions and the new (seafloor) positions. This difference was about 250m for the East OBS!

5h) Summary

Are the "deep seafloor arrivals" observed on the OBS SRBR? As we have seen in the PE modeling of Section 5e) the arrival time of many of the deep seafloor arrivals agrees at least approximately with SRBR. Two additional aspects must be satisfied, however:

i) Deep seafloor arrivals (blue) in the OBS data are the largest events by far on the traces. They are much larger than PE predicted (red) and deep shadow zone arrivals (black).

ii) So far none of the NPAL investigators has observed SRBR arrivals on the DVLA or SVLA for M68.2 LOAPEX transmissions at ranges of T500 and beyond (Sections 5b), 5c) and 5d)).

So for the model SRBR events to agree with the data we need to increase the magnitude of SRBR relative to PE predicted and deep shadow zone arrivals at the seafloor while simultaneously decreasing the magnitude of SRBR relative to PE predicted at SVLA and DVLA depths (particularly above 3000m). This is a tall order.

Some other reasons why the deep seafloor arrivals are not SRBR paths:

iii) In contrast to deep shadow zone arrivals which decay in amplitude with increasing depth below turning points, the deep seafloor arrivals discussed in Sections 4) and 5e) appear to decay with increasing height above the seafloor. Deep seafloor arrivals are the largest magnitude events on the OBS-S-Geo traces. It would be strange for SRBR to appear louder at the seafloor, except perhaps for up to a six dB gain that could be expected from constructive interference of incident and reflected waves. The weak clouds of energy near the seafloor that are seen in the PE runs in Section 5e) are consistent with about 6dB of gain. We need to do a quantitative study of the SNRs on the DVLA and OBS, but it appears that the magnitude of the deep seafloor arrivals on OBS-S-Geo is much more than 6dB larger than SRBR events which are not even observed on the DVLA. If anything the effects of the SSP profile seem to concentrate SRBR energy near the sea surface not the seafloor.

iv) The SRBR "events" at the seafloor in the PE models are diffuse clouds of slightly stronger energy. The observed deep seafloor arrivals, on the other hand, are large amplitude, discrete events. In many cases the deep seafloor arrivals have the double-peak structure that is characteristic of the PE and deep shadow zone arrivals. The deep seafloor arrivals in the data are not smeared like the arrival clouds in the PE models.

For now, until there is some evidence for SRBR on the SVLA and/or DVLA for LOAPEX transmissions at T500 and further, we are assuming that SRBR is not a viable explanation for the deep seafloor arrivals that we are seeing on OBS-S-Geo.

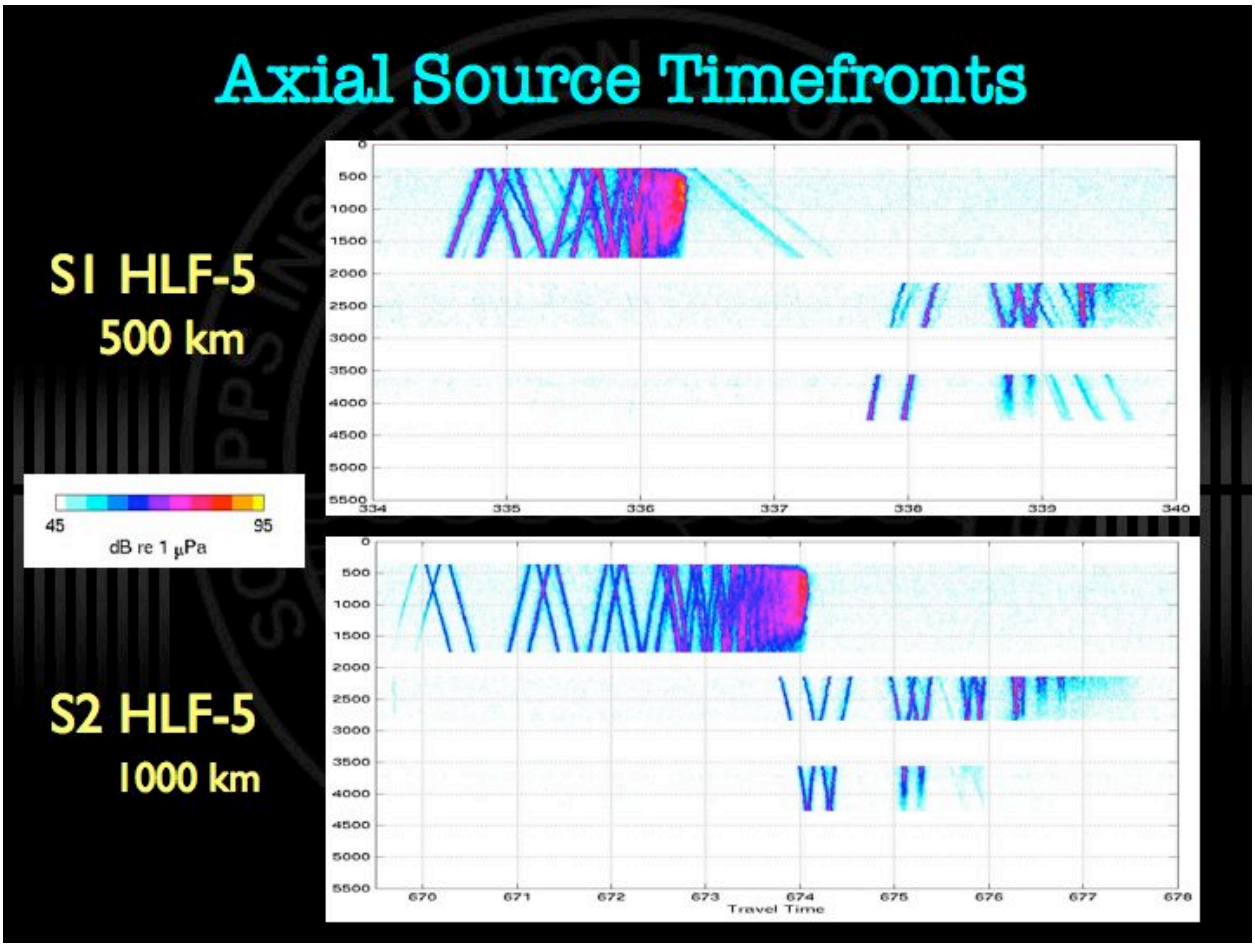

Figure 5-1: This figure from Lora Van Uffelen's presentation at the 2008 Borrego Springs meeting (Van Uffelen *et al.*, 2008) shows SRBR arrivals for 250Hz (750m source depth) transmissions most clearly at T500 but also at T1000. Why are SRBR so clear at 250Hz (SPICE04) but are weak or non-existent at 68.2Hz or 75Hz (LOAPEX)? These figures are also shown in Figure 5 of Van Uffelen et al (submitted).
[VanUffelen_NPAL11_080417_Slide_7.ppt]

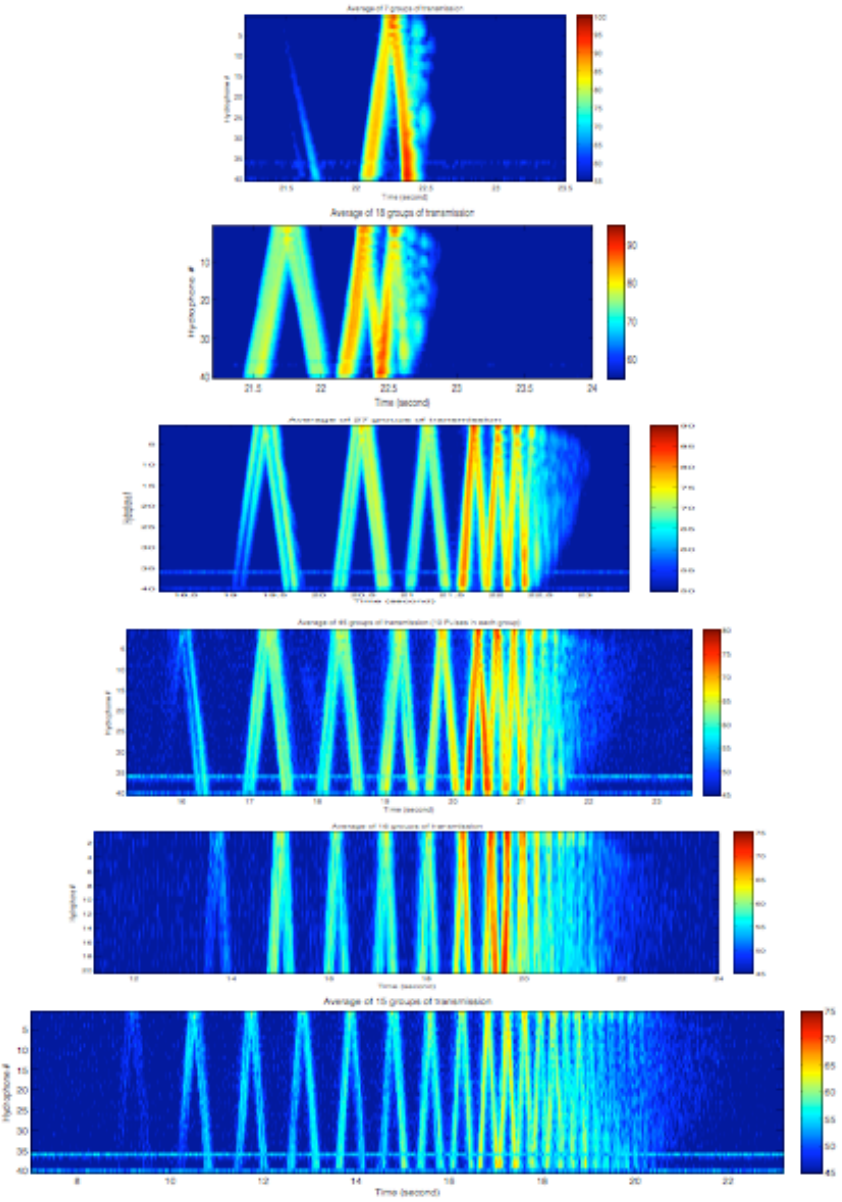

Figure 4-12: The mean wave front intensity at each station: T 250 to T3200 from top to bottom respectively. The colorbars indicate the absolute s ound intensity in unit of dB re 1μPa @ 1m.

Figure 5-2: These data time fronts from Jinshan's thesis (Xu, 2007) do not show any SRBR arrivals. None of the material in Jinshan's thesis for the LOAPEX 68.2Hz source transmitting to the NPAL04 DVLA for ranges at T500 and beyond shows any evidence for SRBR. [Xu_4_12.jpg]

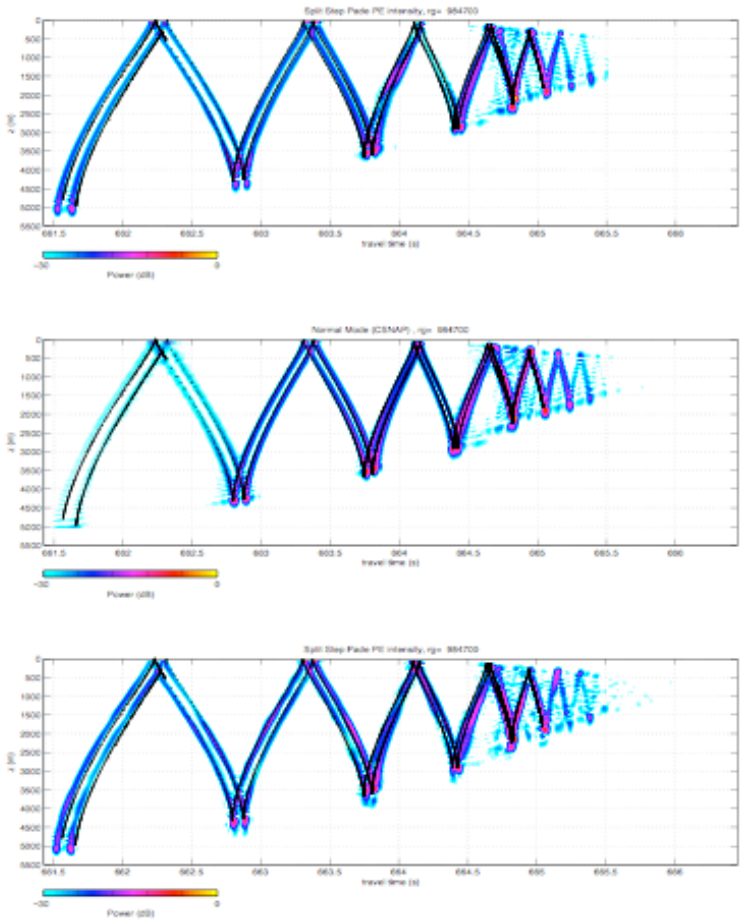

Figure 4-15: The simulations of LOAPEX station T1000 transm ission. From top to bottom, the three panels are PE (RAM) simulations without internal w ave, CSNAP simulations without internal wave, and the PE (RAM) simulations with int ernal wave, respectively. In each simulation, the eigenray simulations are overlapped o n with black dot marks.

Figure 5-3: These model time fronts from Jinshan's thesis for T1000 do not show or consider any SRBR arrivals. [Xu_4_15.jpg]

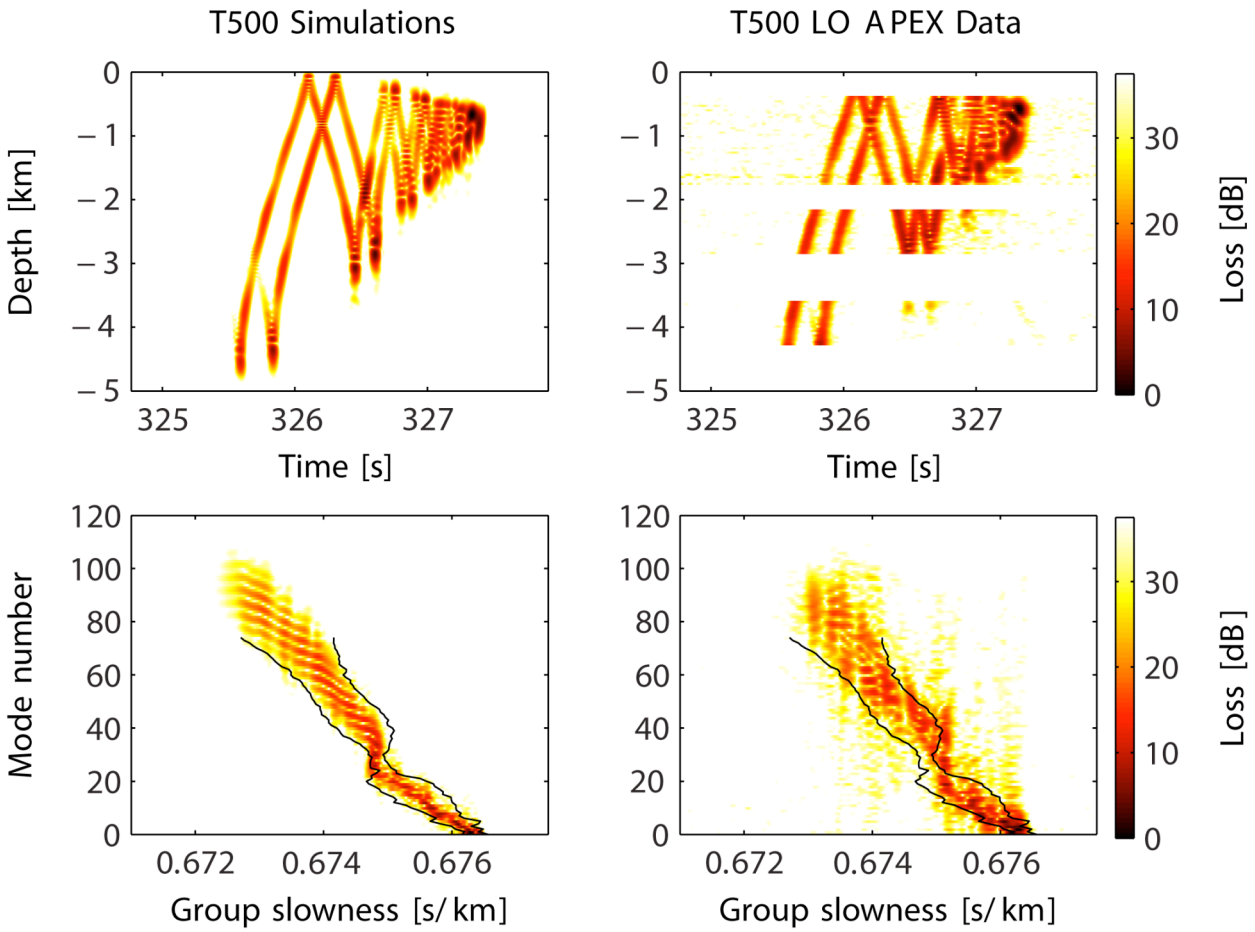

Figure 5-4a: This figure from Ilya Udovydchenkov (pers.comm.) compares the LOAPEX data (top right panel) for T500 on the SVLA and DVLA with model simulations based on PE (top left panel). The mode processing (lower panels) includes the discreet modes with the lower turning depth above the bottom (the upper turning point can be at the surface for large mode numbers). The PE simulation assumes that the bottom is very well attenuating and reflections are not included.

There is no evidence for SRBR paths in the data and the model simulations do not include them. The upper right panel here (for LOAPEX 75 Hz transmissions at 800m source depth) can be compared with the upper panel in Figure 5-1 (for SPICEX 250Hz transmissions at 750m source depth). The 250Hz data shows SRBR arrivals and the 75Hz data does not. [Ilya_fig3_T_500_75_Hz.pdf]

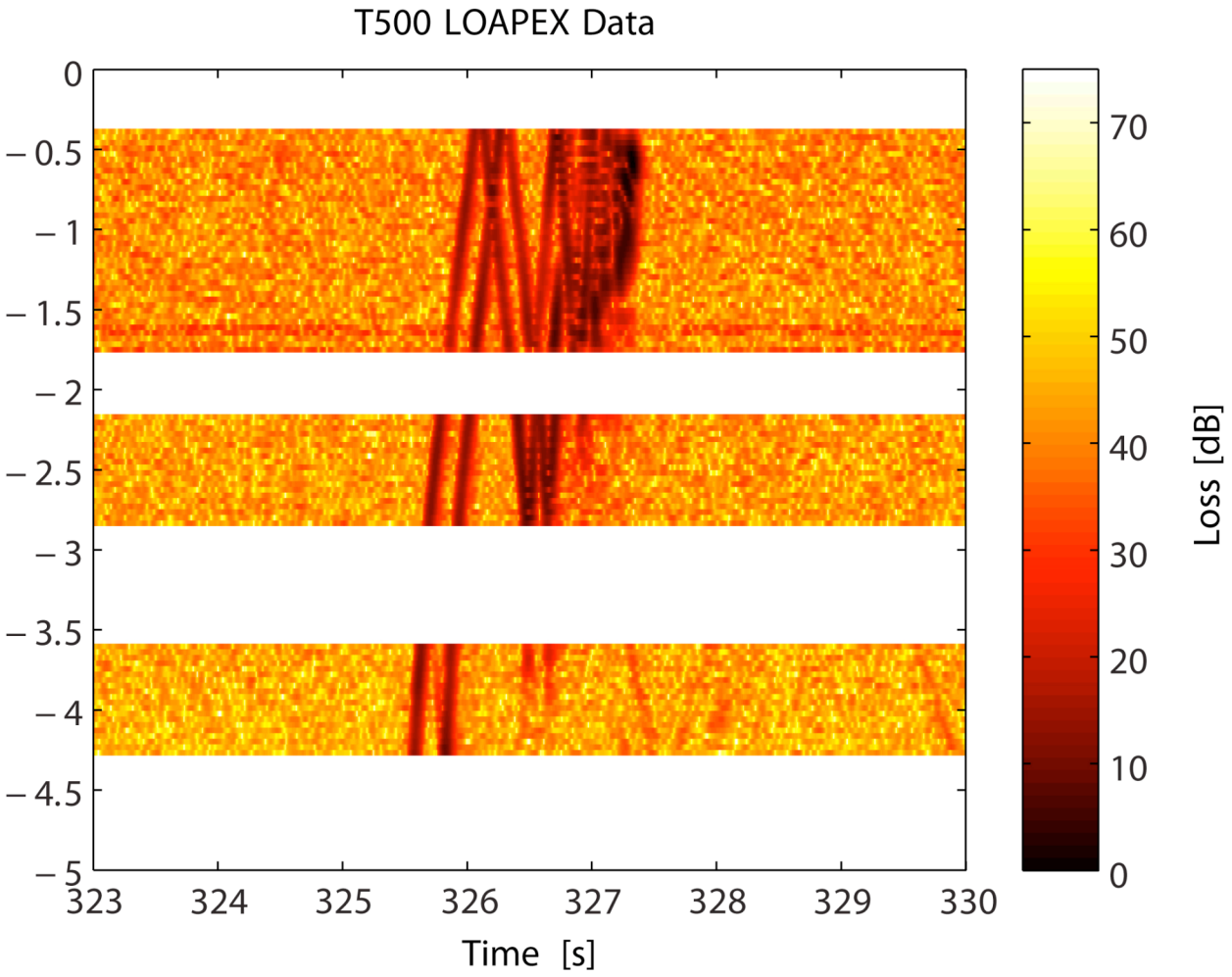

Figure 5-4b: This figure shows the same data as the upper right panel in Figure 5-4a but with a color scale spanning 75dB instead of 35dB. Although the time axes are referenced differently, the arrivals in the bottom panel between 327 and 328sec (for the 75Hz LOAPEX source) are similar to the SRBR arrivals observed in the upper plot of Figure 5-1 between 339 and 340sec (for the 250Hz SPICEX source). The color scale in Figure 5-1 spans only 40dB, so there is an indication that these arrivals at 75HZ are much weaker relative to the other time fronts than at 250Hz. There is also a weak arrival appearing in the lower panel just before 330sec. Unlike Figure 5-1 (at 250Hz), the SRBR time fronts here (at 75Hz) only appear clearly towards the bottom of the DVLA, possibly because the background noise is weaker. [Ilya_T500_LOAPEX_Data_75_dB_scale.pdf]

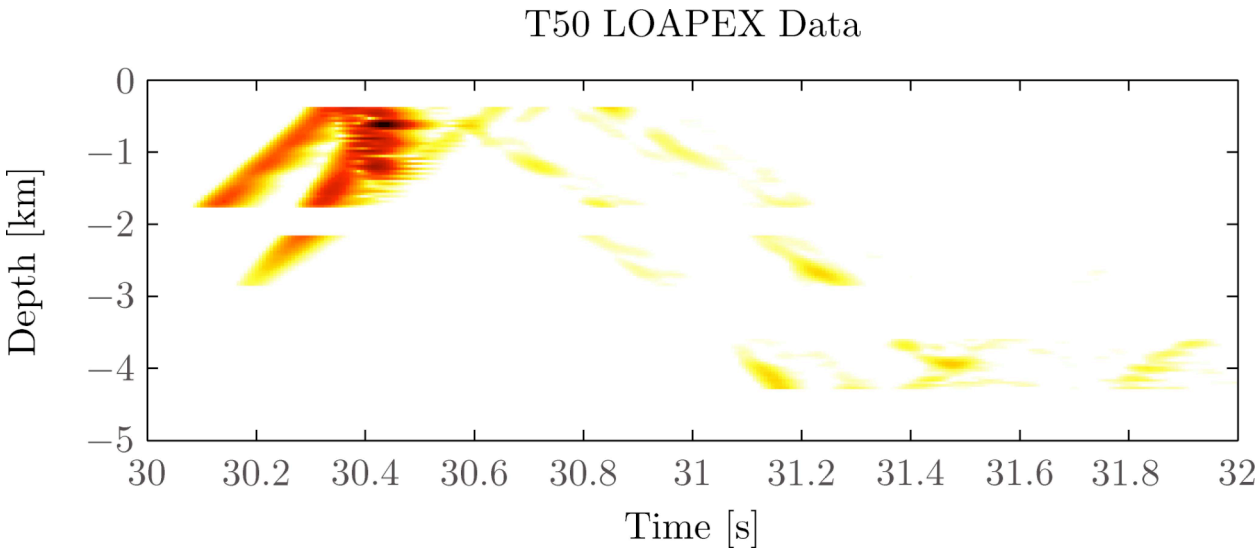

Figure 5-5a: This figure from Ilya Udovydchenkov (pers.comm.) shows the LOAPEX data (75 Hz transmissions at 800m source depth) for T50 on the SVLA and DVLA. The yellow planar arrivals beyond 30.6sec are SRBR arrivals occurring after the finale near 30.4sec. Although observed here at short range, T50, there is only weak evidence for SRBR paths on LOAPEX transmissions at T500. [Ilya_fig_17.jpg]

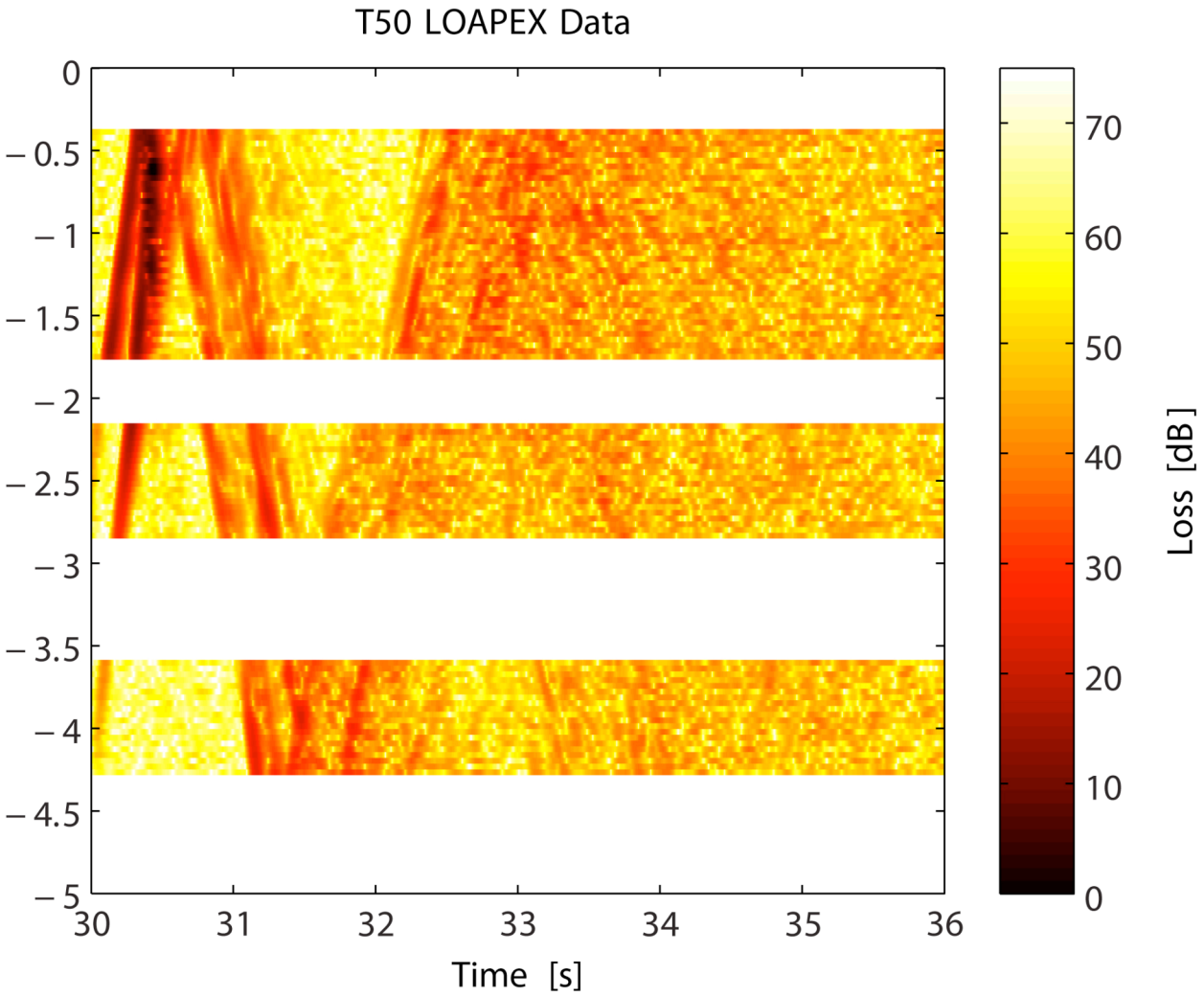

Figure 5-5b: This figure shows the same data as in Figure 5-5a but with a color scale spanning 75dB instead of 35dB. The SRBR time fronts from the first bottom bounce are clearly observed throughout the water column up to about 33sec. There is also weak evidence for SRBR paths from the second bottom bounce between 33 and 36sec.
[Ilya_T50_LOAPEX_Data_75_dB_scale.pdf]

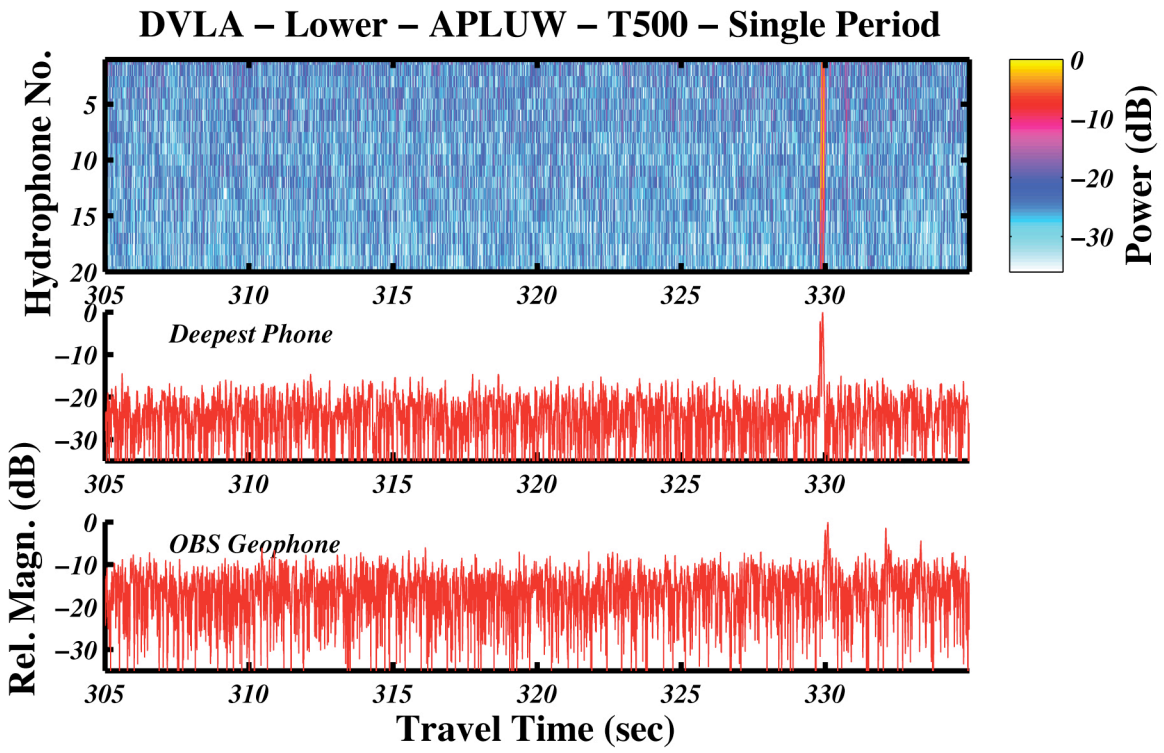

Figure 5-6: This is the first of six figures that compares data time fronts from the APL/UW DVDs (top) with traces from the bottom hydrophone in Linda's data (DVLA-L20-Hyd, middle) and the OBS geophone data (OBS-S-Geo, bottom). As much as possible the same transmissions were used for both the DVLA and OBS data (the OBS had some noisy traces at T1000 that have been excluded - 10 out of 280 traces. Also one whole transmission was noisy at T1000 and this was replaced with a transmission that was missing on the DVD - 267_0100.)

This figure compares data for the first period acquired at T500. Note that there are late arrivals on the OBS even in unstacked data. The late arrivals are not on artifact of the stacking procedure. [APLUW_T500_Fig_1.jpg]

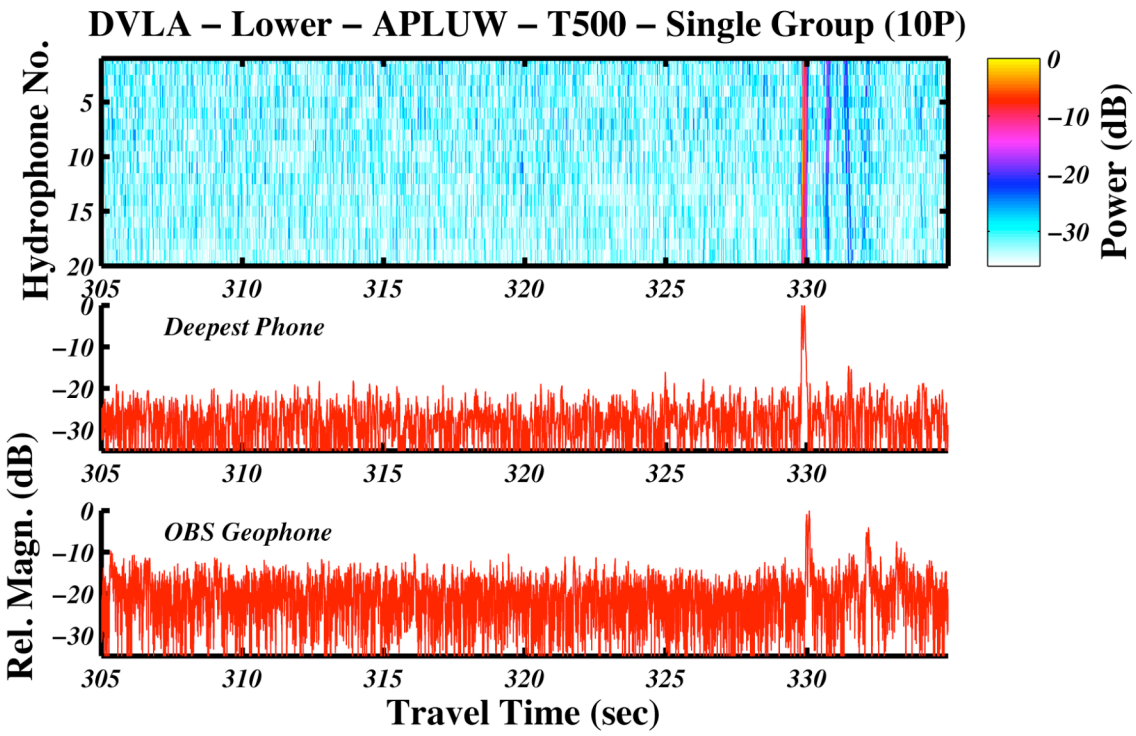

Figure 5-7: This figure compares data for the coherent stack of the first 10 periods at T500. SNR improves. [APLUW_T500_Fig_2.jpg]

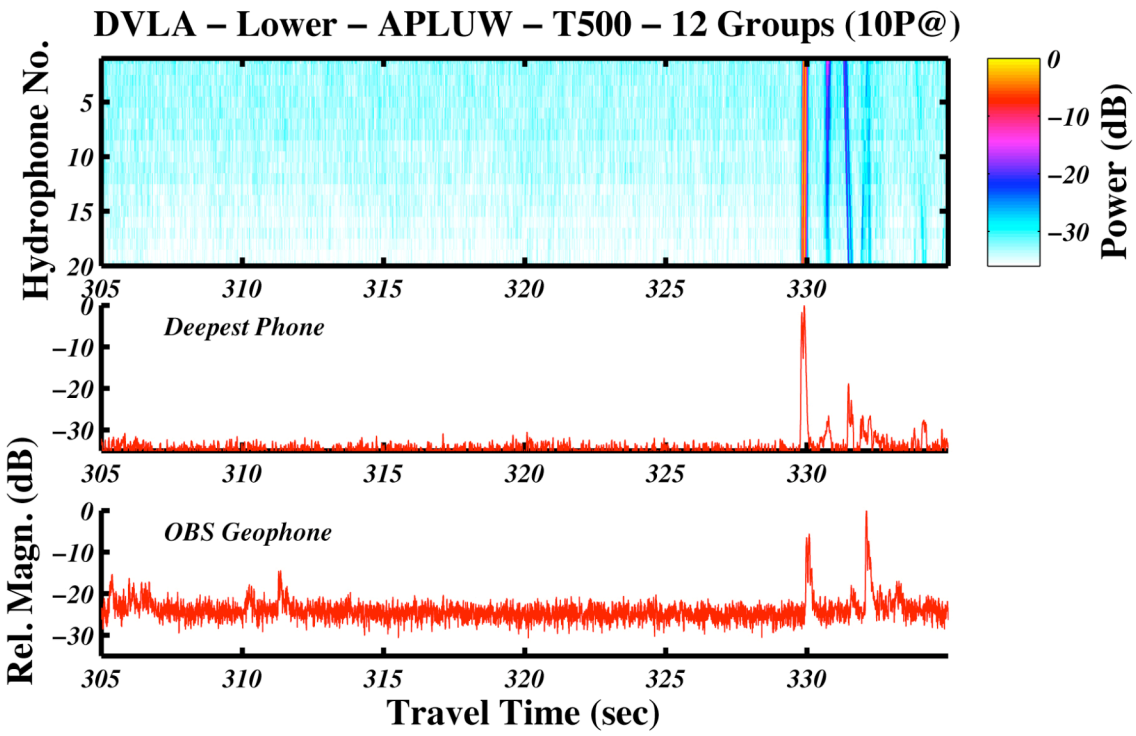

Figure 5-8: This figure compares data for the incoherent stack of 12 coherent stacks (groups of 10 periods) at T500. SNR improves even further. Late arrivals on OBS are wrapping around in the time window. There is no indication of the late OBS arrivals on the DVLA even though the DVLA hydrophones have better self noise characteristics. If the late arrivals are SRBR one would expect to see SRBR on the DVLA as well.

In Figures 5-6 to 5-8 for T500, the time axis for the OBS is totally independent of the time axis for the DVLA. The OBS time is based on the OBS clock and the WHOI processing. One would expect slightly different arrival times at the OBS (about 5000m deep) than at the lowest hydrophone of the DVLA (about 4250m) because of a slight difference in range but there are no gross errors (greater than a tenths of a second or so) in timing. [APLUW_T500_Fig_3.jpg]

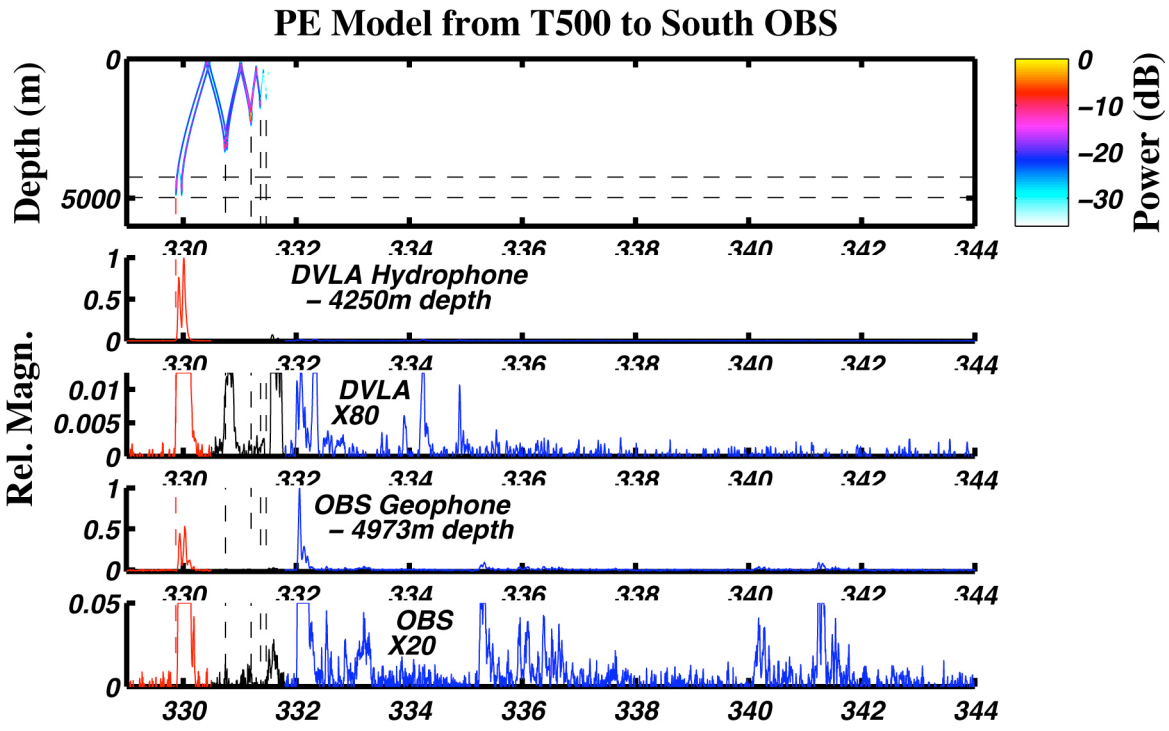

Figure 5-9: This version of Figure 4-1 with an extended time axis shows the very late arrivals, after 333sec on DVLA-L20-Hyd (second and third panels from the top) and OBS-S-Geo (bottom two panels). The overall arrival pattern on the OBS is about 12sec long. Since we do not see these very late arrivals at longer ranges we do not include them in our discussion of deep seafloor arrivals in section 4. [Fig_4b-500a.jpg]

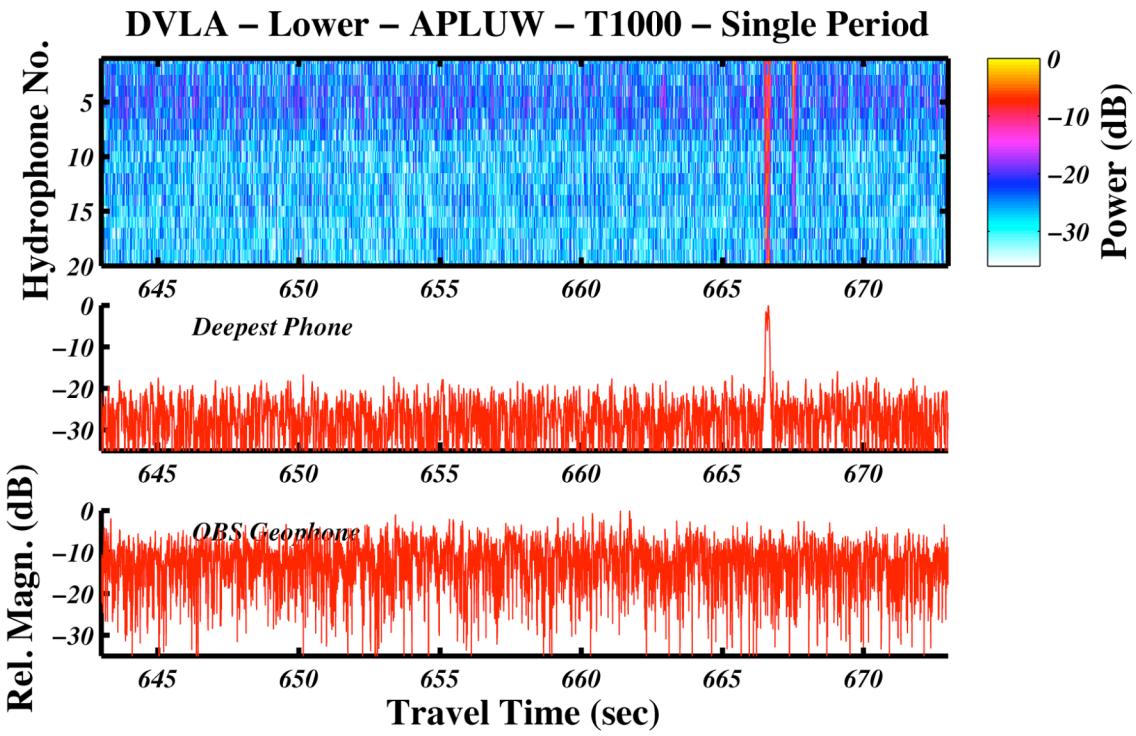

Figure 5-10: Same as Figure 5-6 but for T1000. OBS arrivals are not observable on this first period, but they are observed on some later periods for T1000. [APLUW_T1000_Fig_1.jpg]

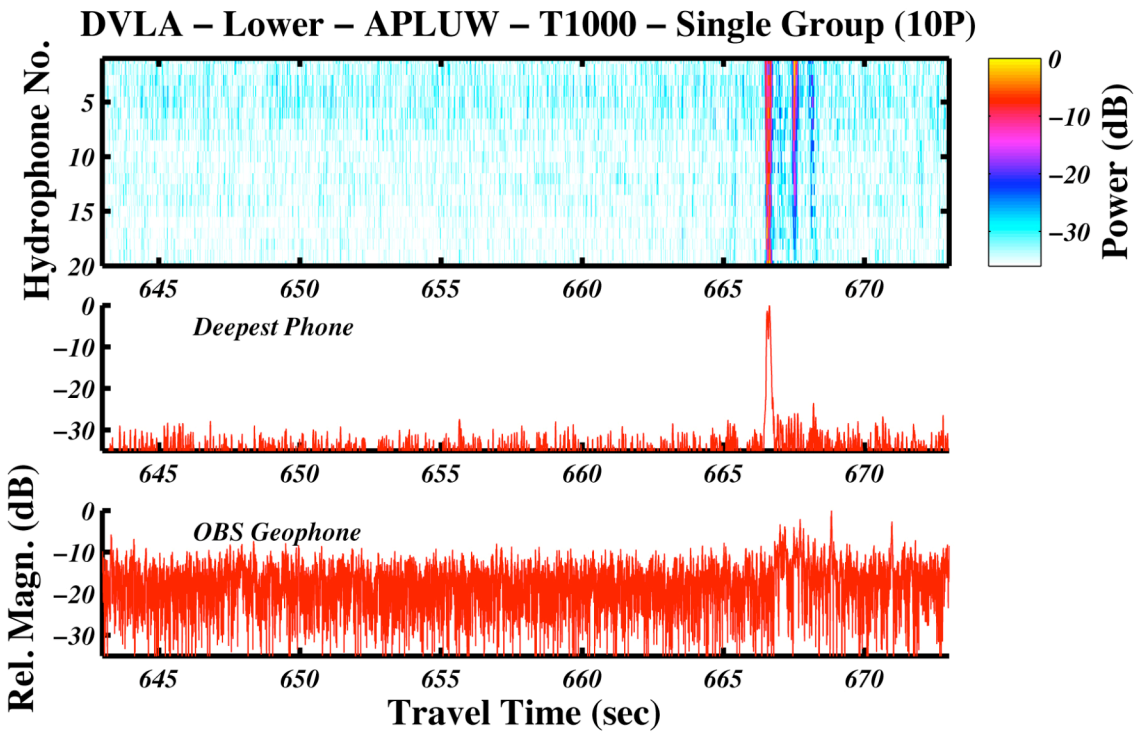

Figure 5-11: Same as Figure 5-7 but for T1000. Coherent stacking over ten periods brings out some late arrivals on the OBS that are not observed on the DVLA. [APLUW_T1000_Fig_2.jpg]

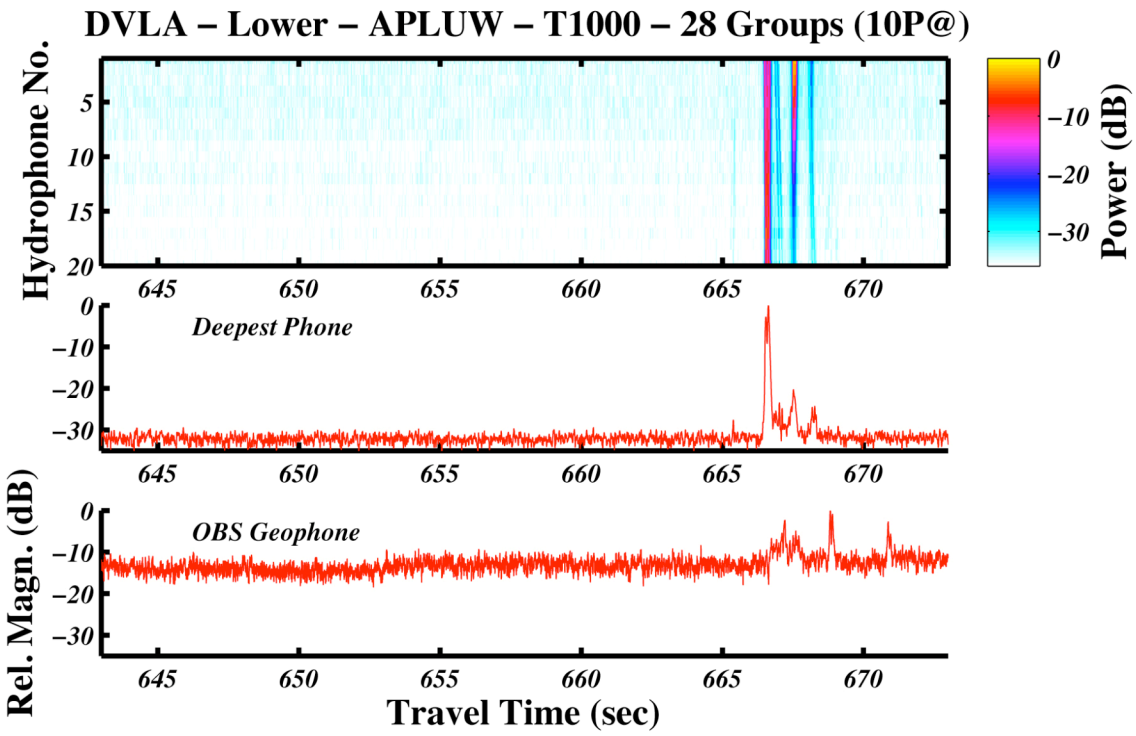

Figure 5-12: Same as Figure 5-8 but for T1000. The arrival structure on the OBS bears no resemblance to the structure on the lowest hydrophone of the DVLA. (I should add the trace from the LttE paper (incoherent stack of everything) to this figure and Figure 5-8). [APLUW_T1000_Fig_3.jpg]

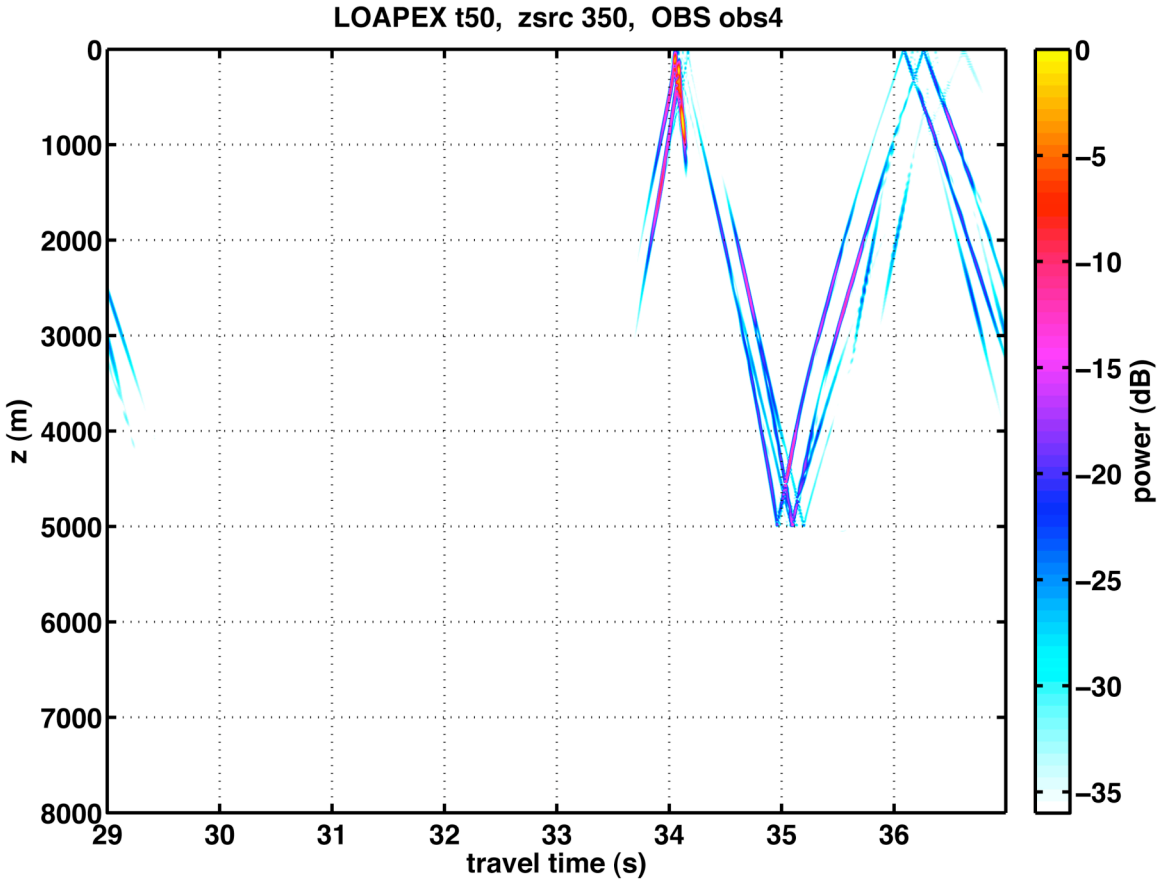

Figure 5-13: PE model time fronts with bottom interaction from T50 to the South OBS. At T50 there are clear surface-reflected bottom-reflected (SRBR) events and Ilya mentions seeing SRBR in his data at this range. [obstf.t50.z350.obs4.pdf]

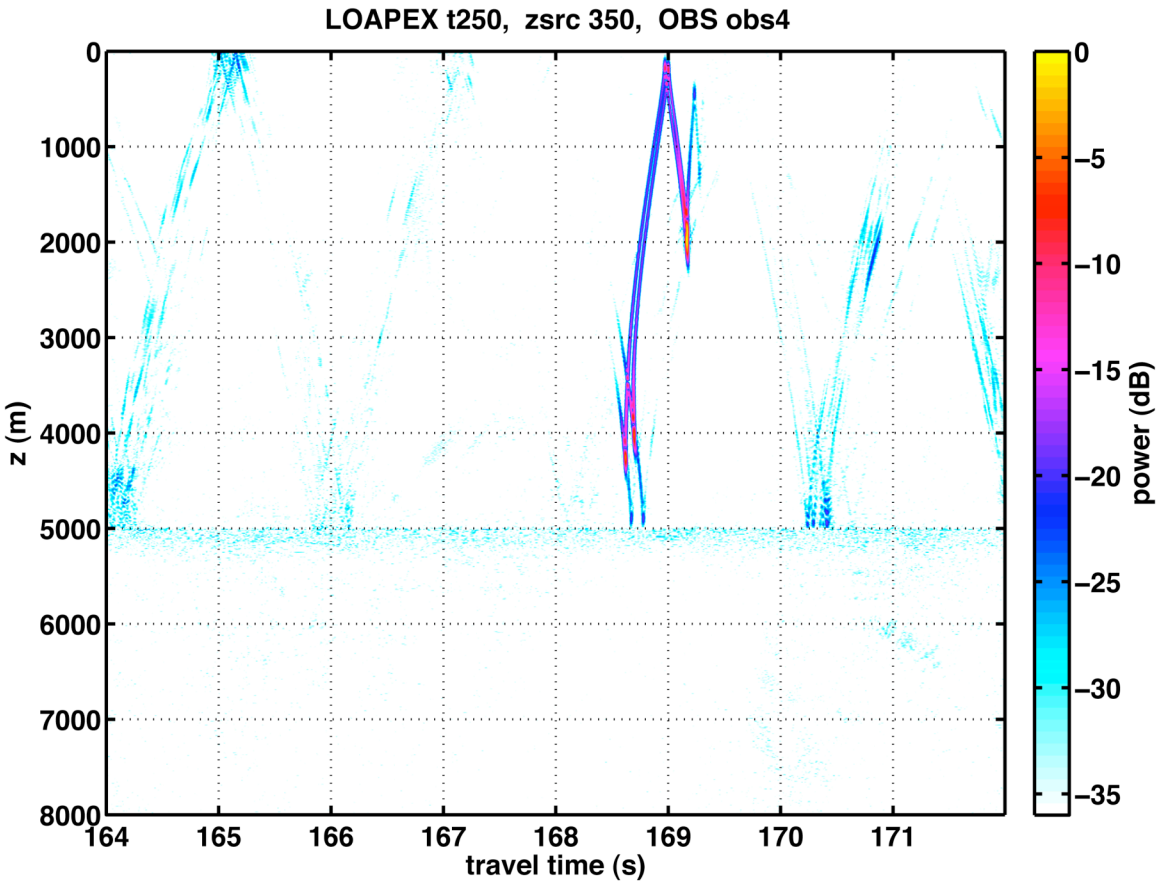

Figure 5-14: PE model time fronts with bottom interaction from T250 to the South OBS. One can see the bottom reflected energy (in cyan) below the RR and RSR paths (in blue and maroon) at about 168.8sec. Then three multiples are seen at the seafloor at about 170.3, 172.1 and 174sec (allowing for wrap-around). They are separated by about 1.5 to 1.9sec and the amplitude decays for subsequent arrivals. It is interesting that the amplitude seems to be enhanced by about 6dB near the seafloor. These events decay upward into the water column similar to the deep seafloor arrivals discussed in Section 4. [obstf.t250.z350.obs4.pdf]

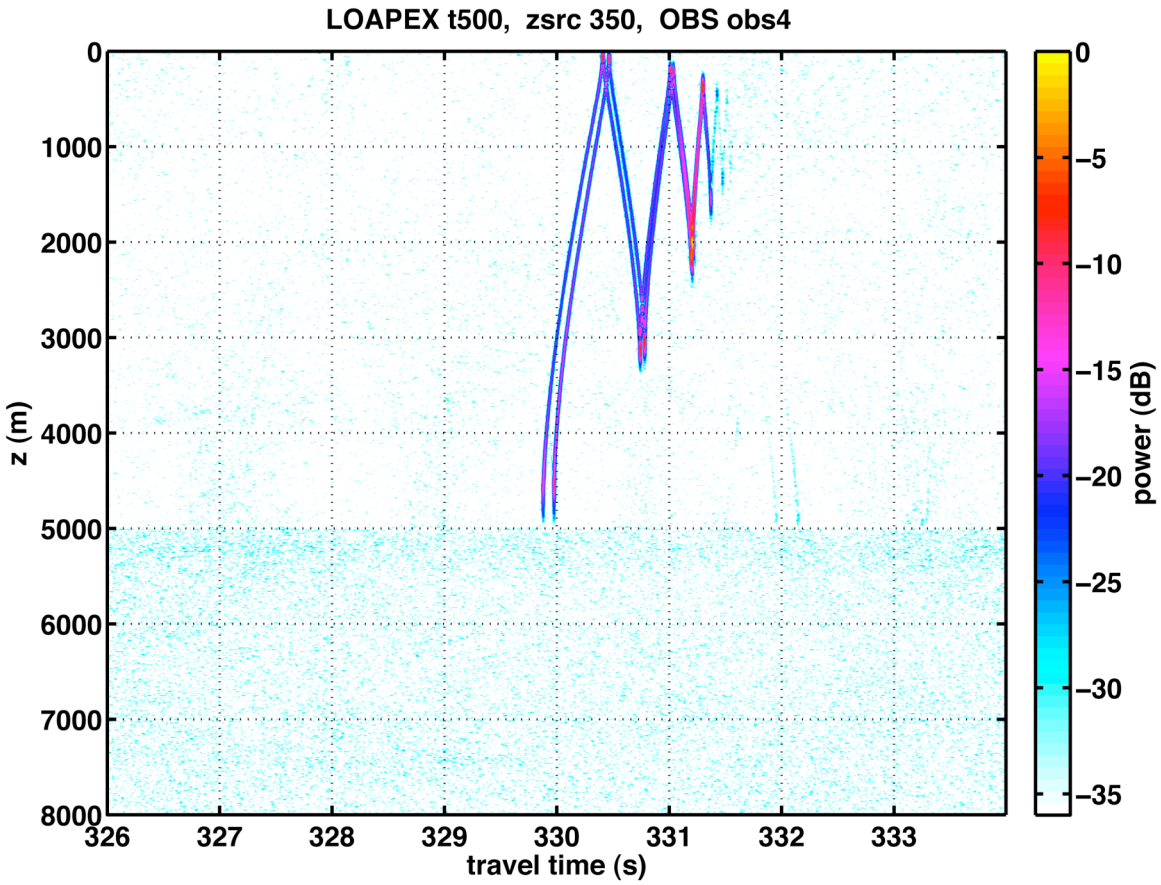

Figure 5-15: PE model time fronts with bottom interaction from T500 to the South OBS. The SRBR arrivals are relatively very weak at T500, but there is a very weak event near the seafloor just after 332sec which could be SRBR. [obstf.t500.z350.obs4.pdf]

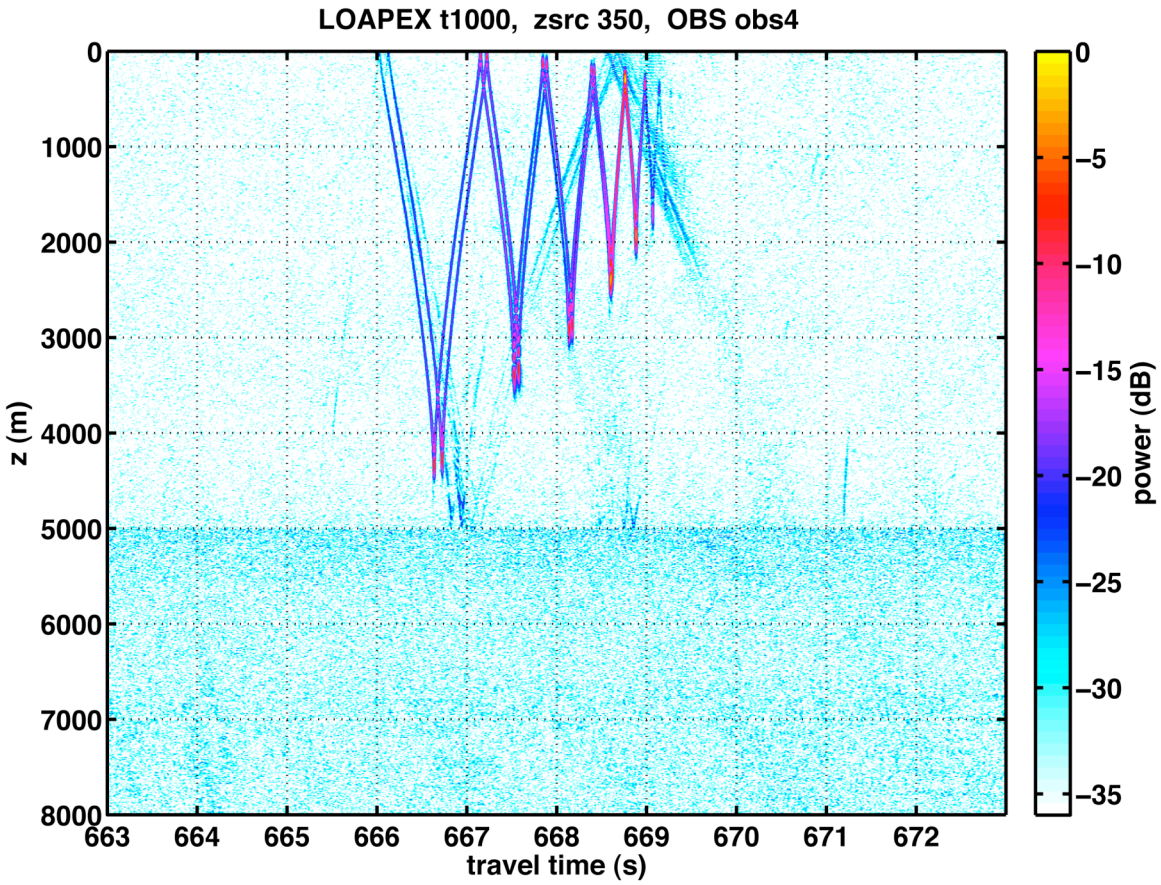

Figure 5-16: PE model time fronts with bottom interaction from T1000 to the South OBS. Two SRBR paths, separated by 2sec, can be seen at the seafloor and there are also clear time fronts shallower than about 3000m. There is also a weak indication of a possible SRBR arrival near the seafloor just after 671sec. [obstf.t1000.z350.obs4.pdf]

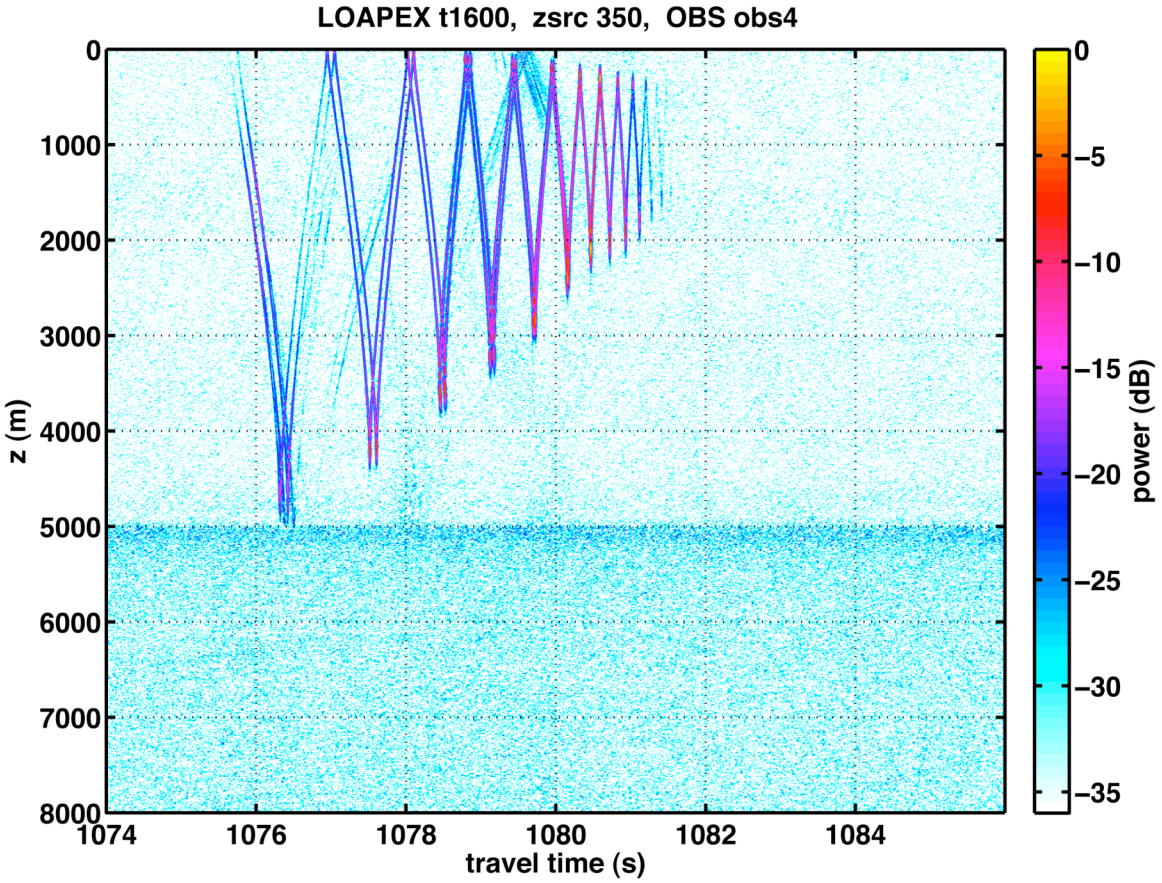

Figure 5-17: PE model time fronts with bottom interaction from T1600 to the South OBS. There is a slight indication of three seafloor SRBR arrivals separated by about 2sec. The latter two (near 1078 and 1080sec) are very weak compared with the first one (just after 1076sec). [obstf.t1600.z350.obs4.pdf]

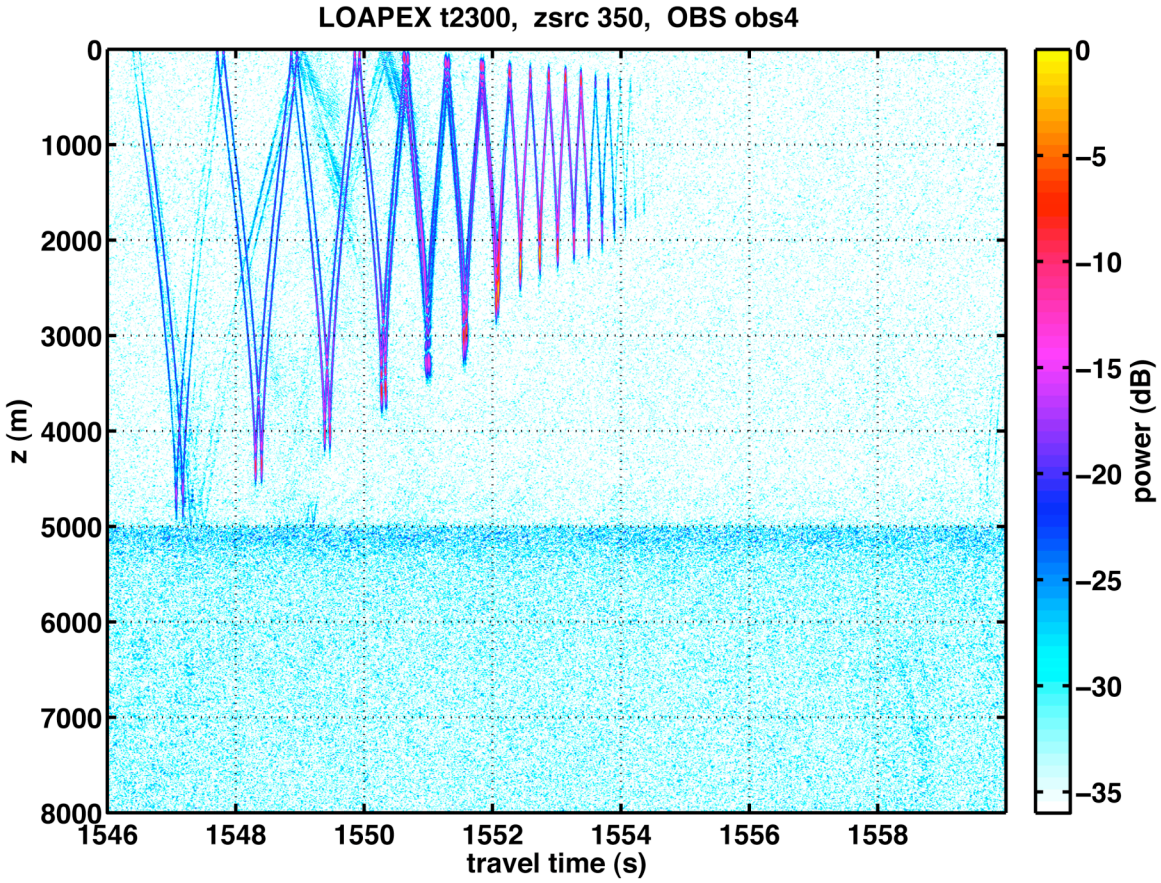

Figure 5-18: PE model time fronts with bottom interaction from T2300 to the South OBS. There are two SRBR arrivals separated by about 2sec. In the PE modeling SRBR arrivals at the seafloor are accompanied with clear time fronts shallower in the water column. [obstf.t2300.z350.obs4.pdf]

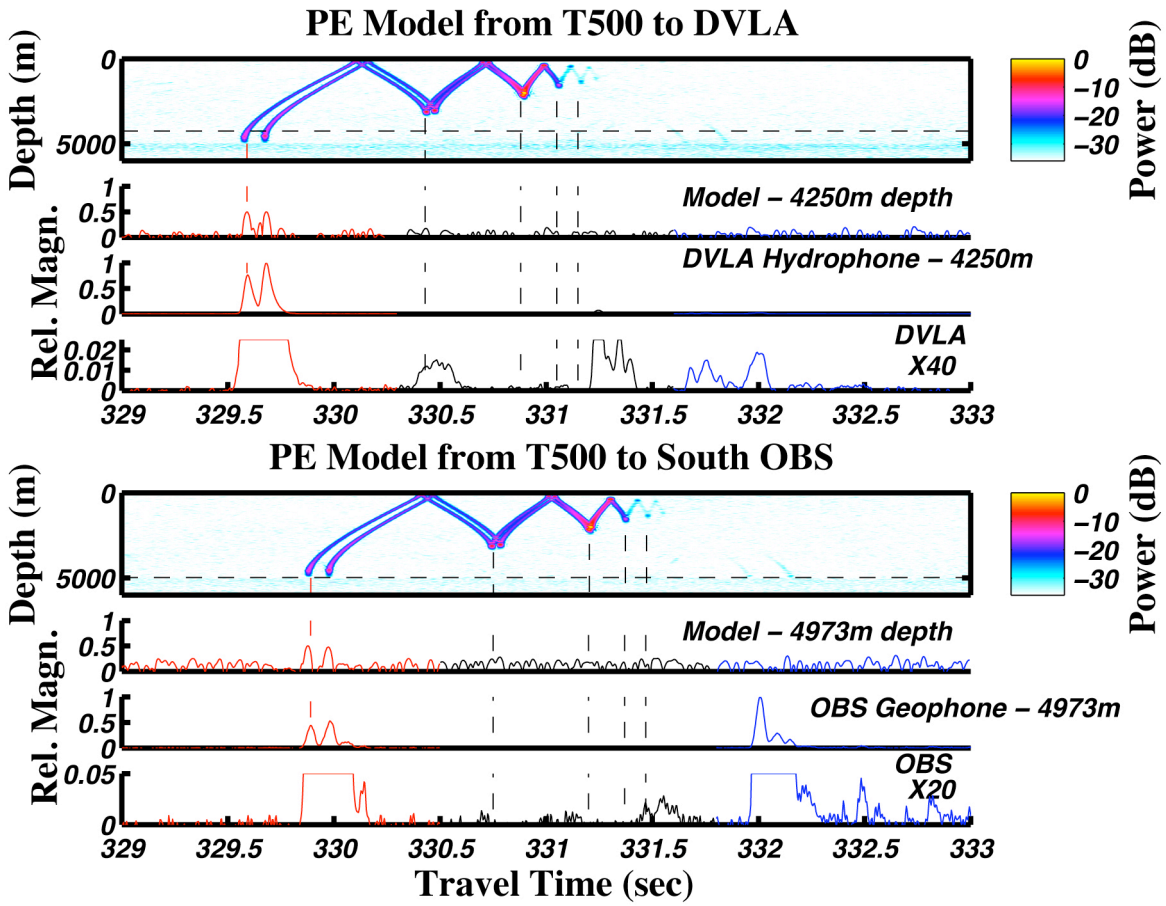

Figure 5-19: Figures 5-19 to 5-22 compare DVLA-L20-Hyd and OBS-S-Geo data (the incoherent stacks of all periods as in Figures 2-1 and -2) with the PE models including bottom interaction (Figures 5-13 to 5-18) for T500, T1000, T1600 and T2300, respectively. All four figures have the same format. The top group of four panels is the model-data comparison for DVLA-L20-Hyd and the bottom group is for OBS-S-Geo. Within each group of four, the top panel is the time front diagram, the second panel is the model trace at the receiver depth (indicated by a horizontal dashed line in the time front diagram), the third panel is the data trace normalized to its maximum amplitude and the bottom trace is an expanded view of the data trace.

The clear deep seafloor arrival at 332sec corresponds to a weak event in the model time front between 4000 and 5000m (it can be seen more clearly on Figure 5-15) and could be SRBR. [Fig_4c-500.jpg]

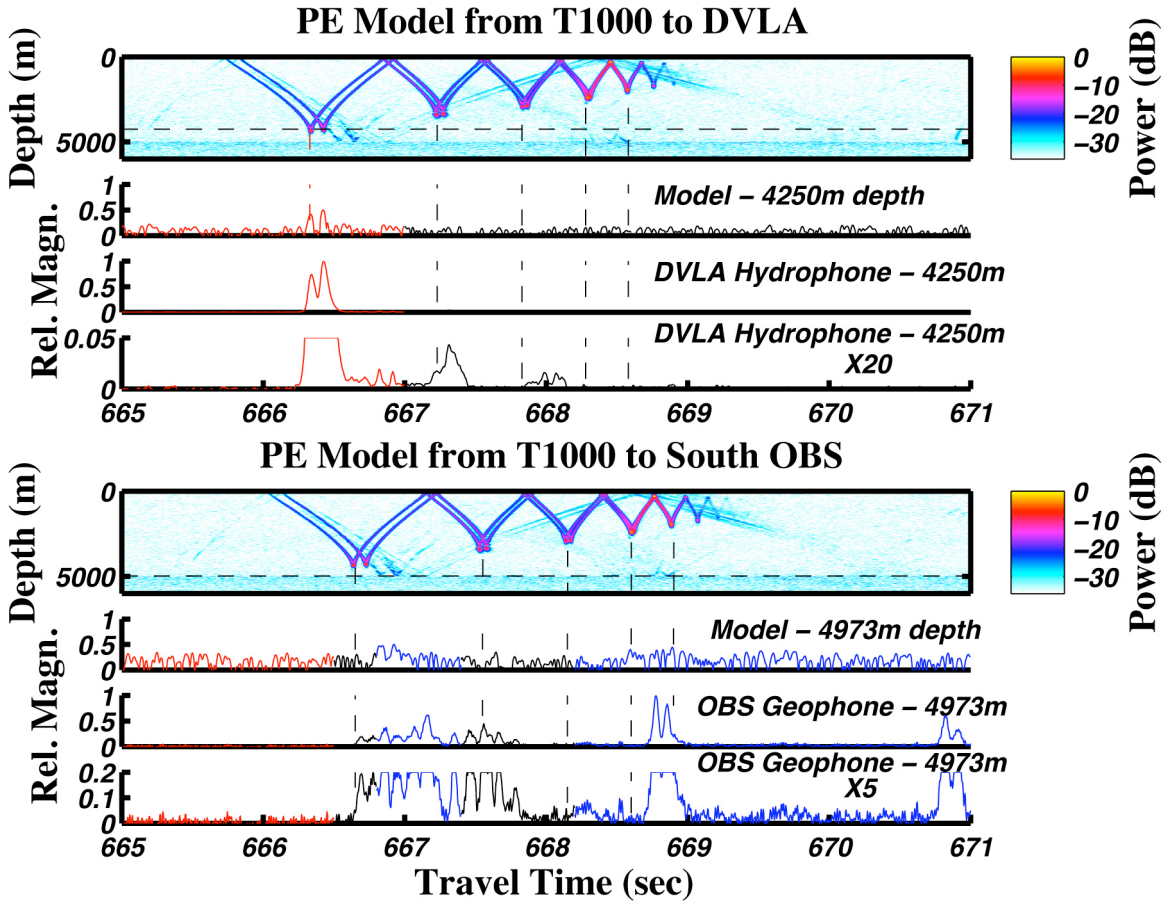

Figure 5-20: Same format as Figure 5-19 for T1000. The muddle of energy between the first two turning point times (from about 666.6 to 667.8see) on OBS-S-Geo corresponds to a weak concentration of energy near the seafloor in the PE model and this energy could be SRBR. The largest amplitude arrival on OBS-S-Geo occurs just before 669sec and corresponds to a weak concentration of energy near the seafloor in the PE model (this can be seen more clearly on Figure 5-16). This energy could be SRBR. The second largest amplitude arrival on OBS-S-Geo at T1000 occurs just before 671sec and arrives after the finale. Since this arrival is occurring about 0.5sec before a concentration of energy in the PE model, we are tentatively concluding that it is not SRBR. [Fig_4c-1000.jpg]

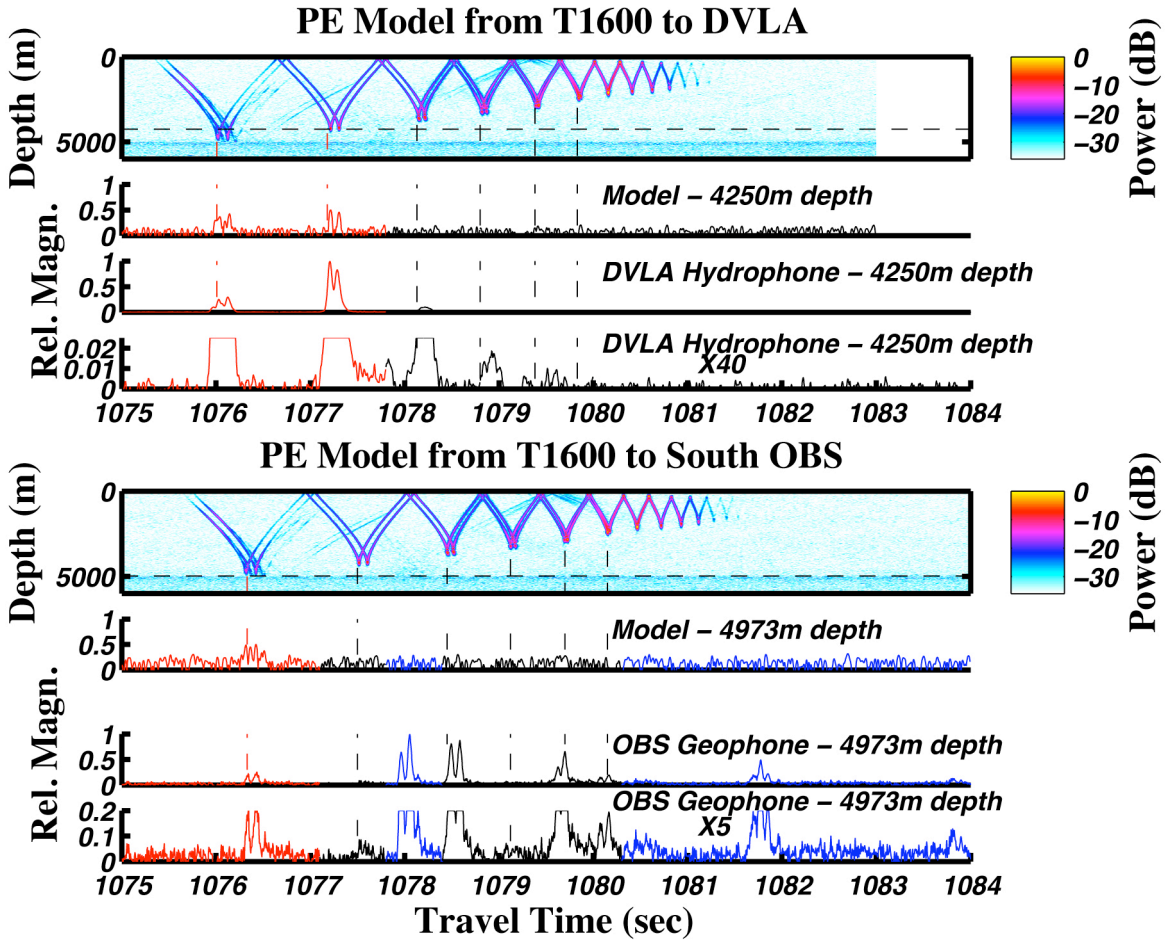

Figure 5-21: Same format as Figure 5-19 for T1600. The arrival structures are discussed in the text. [Fig_4c-1600.jpg]

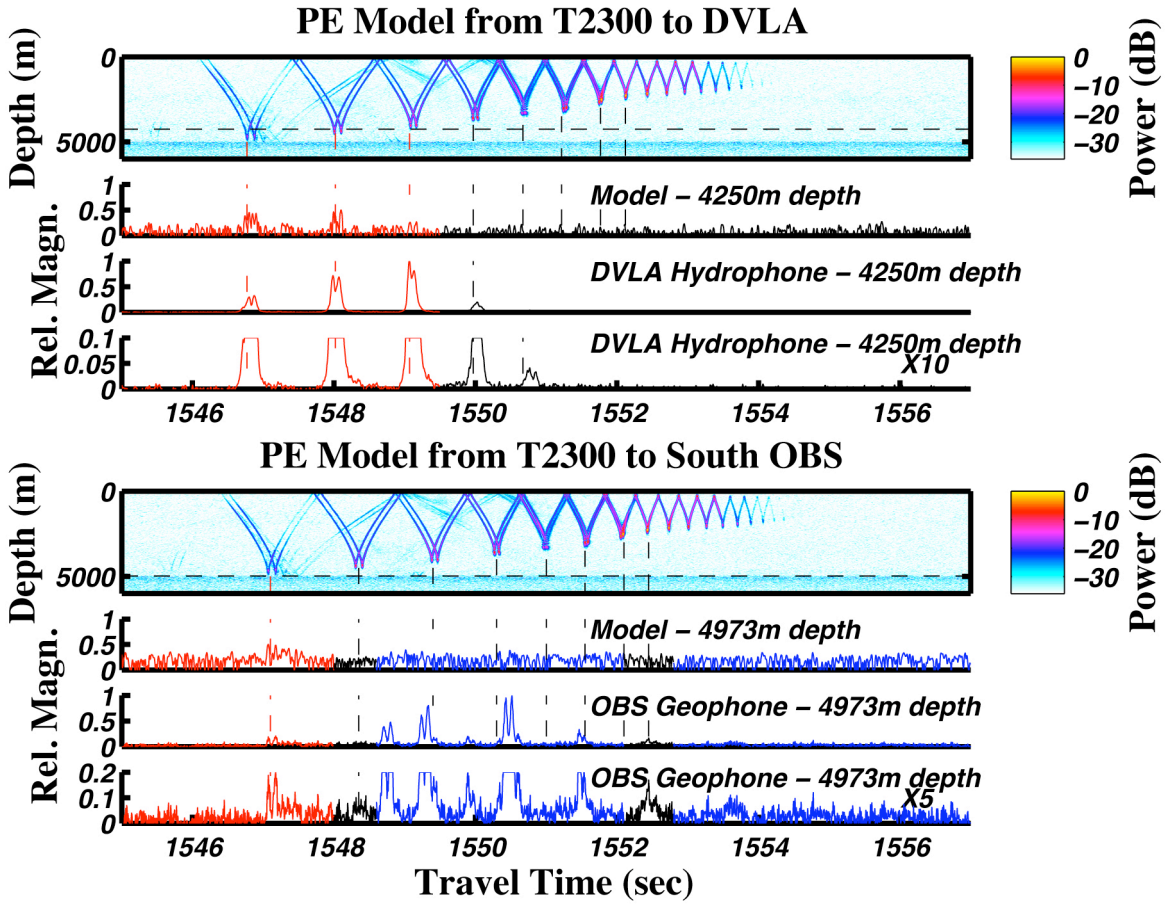

Figure 5-22: Same format as Figure 5-19 for T2300. The arrival structures are discussed in the text. [Fig_4c-2300.jpg]

Table 5-1: Summary of timing offsets and drifts.

	DVLA	South OBS	West OBS	East OBS
T500 - offset	-0.20	-0.05	-0.05	0.20
- drift	-0.02	-0.05	0.0	-2.15
T1000 - offset	-0.20	-0.05	-0.05	0.20
- drift	0.0	0.0	0.0	0.0
T1600 - offset	-0.20	-0.05	-0.05	(1)
- drift	0.0	0.0	0.0	(1)
T2300 - offset	-0.20	-0.05	-0.05	(1)
- drift	0.0	0.0	0.0	(1)

(1) The East OBS had the worst SNR on the geophone and the timing seemed flaky. Perhaps the poor SNR was a result of stacking traces with poor timing.

Table 5-2: New Output from the Range Code Using the "Bottom" Locations

Recievers	Dir	Source	Range	Angle Rec	Del	Diff
OBS 1	West	T50	48076.4137	103.063	1923.5863	-84.117
OBS 1	West	T250	248072.8677	102.4123	1927.1323	-82.2342
OBS 1	West	T500	488072.4151	102.3353	11927.5849	-82.0109
OBS 1	West	T1000	988072.3173	102.295	11927.6827	-81.8941
OBS 1	West	T1600	1598072.0094	102.2798	1927.9906	-81.8499
OBS 1	West	T2300	2298071.3811	102.2721	1928.6189	-81.8278
OBS 1	West	T3200	3198071.8271	102.2671	1928.1729	-81.8131
OBS 4	South	T50	50505.7999	104.7369	-505.7999	53.6676
OBS 4	South	T250	250468.6578	102.7654	-468.6578	48.603
OBS 4	South	T500	490464.0301	102.5216	9535.9699	47.9719
OBS 4	South	T1000	990461.7265	102.3928	9538.2735	47.6383
OBS 4	South	T1600	1600460.5848	102.3442	-460.5848	47.5122
OBS 4	South	T2300	2300459.537	102.3197	-459.537	47.4488
OBS 4	South	T3200	3200459.7053	102.3035	-459.7053	47.4068
OBS 3	East	T50	51664.0767	101.7403	-1664.0767	256.366
OBS 3	East	T250	251662.5663	102.1679	-1662.5663	257.104
OBS 3	East	T500	491662.3409	102.2218	8337.6591	257.1965
OBS 3	East	T1000	991662.3593	102.2505	8337.6407	257.2457
OBS 3	East	T1600	1601662.0959	102.2613	-1662.0959	257.2641
OBS 3	East	T2300	2301661.49	102.2667	-1661.49	257.2734
OBS 3	East	T3200	3201661.9505	102.2703	-1661.9505	257.2796
DVLA		T50	50001.1677	102.268	-1.1677	
DVLA		T250	250001.4669	102.268	-1.4669	
DVLA		T500	490001.4696	102.268	9998.5304	
DVLA		T1000	990001.6097	102.2681	9998.3903	
DVLA		T1600	1600001.3918	102.268	-1.3918	
DVLA		T2300	2300000.8088	102.268	-0.80881	
DVLA		T3200	3200001.2846	102.268	-1.2846	

6) Outstanding Issues

This is just a progress report and there is a lot more that can be done and a lot of other issues to consider. These include:

a) Late arrivals are also seen on the M75 (800m source depth) and M68.2 (500m source depth) data and two other OBSs (Figures 6-1 to 6-4). Although modeling the draft LttE arrivals would be a start, the other data could provide important constraints.

b) The seafloor results discussed above considered vertical particle velocity (geophones) but the water column DVLA results are acoustic pressure (hydrophones). It would be nice to know what the acoustic pressure is at the seafloor. Preliminary analysis shows that particle velocity and pressure at the seafloor are not simply related (for example by the acoustic impedance) as they are high in the water column. More work needs to be done on the hydrophone data from the OBSs (although this was badly self-noise limited)(Figures 6-5 to 6-7). Modeling work would also be useful to assess the role of rigidity in the seafloor.

c) Are the seafloor late arrivals just bottom reverberation? For a single bottom receiver these are discrete arrivals. But if one had an array of bottom receivers and did signal processing based only on acoustic theory (for example, sound speeds across the array of about 1.5km/s) these seafloor late arrivals (say with much slower local sound speed, 500m/s or less) would not coherently process and would appear as reverberation noise? We could get a handle on this by studying the other 2 OBSs (West and East).

d) We need a better description of the PE modeling (Collins and Westwood, 1991). These PE results use the range dependent ocean WOA2004 (World Ocean Atlas 2004). What is being done for the bathymetry? based on Smith & Sandwell? actual swath map data?

e) We should consider modeling approaches other than PE. If the late arrivals really do require propagating shear or interface waves I do not think that codes exist at the moment for these frequencies and ranges, especially if it requires bathymetry and other range dependent structure. The work of Park and Odom with modes might be a start.

f) Absolute amplitudes, range dependence (TL – transmission loss), instrument self noise, ambient field noise and SNRs should be quantitatively addressed.

g) Ray tracing might be useful to check for scattering from particular bathymetric features. There are interesting bathymetric features that lie off the geodesic.

h) What is happening with Jim's JOE (Journal of Oceanic Engineering) paper?

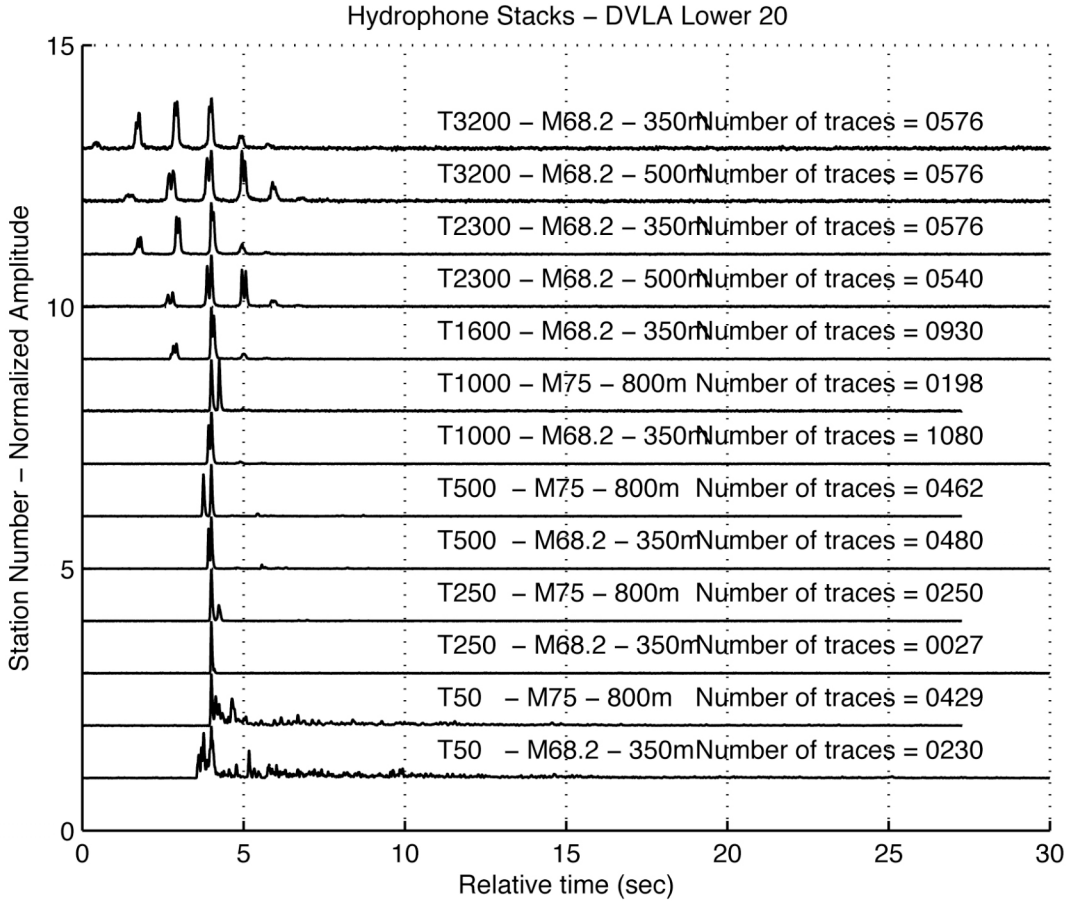

Figure 6-1: The incoherent stacks of the DVLA hydrophone data (lowermost sensor - DVLA-L20-Hyd) for all of the M-sequence source depth and range combinations. All traces have been time shifted so that the peak magnitude occurs at 4sec and all traces are amplitude normalized to the peak amplitude. The M68.2 at 350m depth stacks are the same "hydrophone" traces that were displayed in 2-2c and that were discussed in Sections 4 and 5e). The M68.2 at 500m depth stacks and the M75 at 800m depth stacks have not yet been studied in detail. [DVLA_20_Summary.jpg]

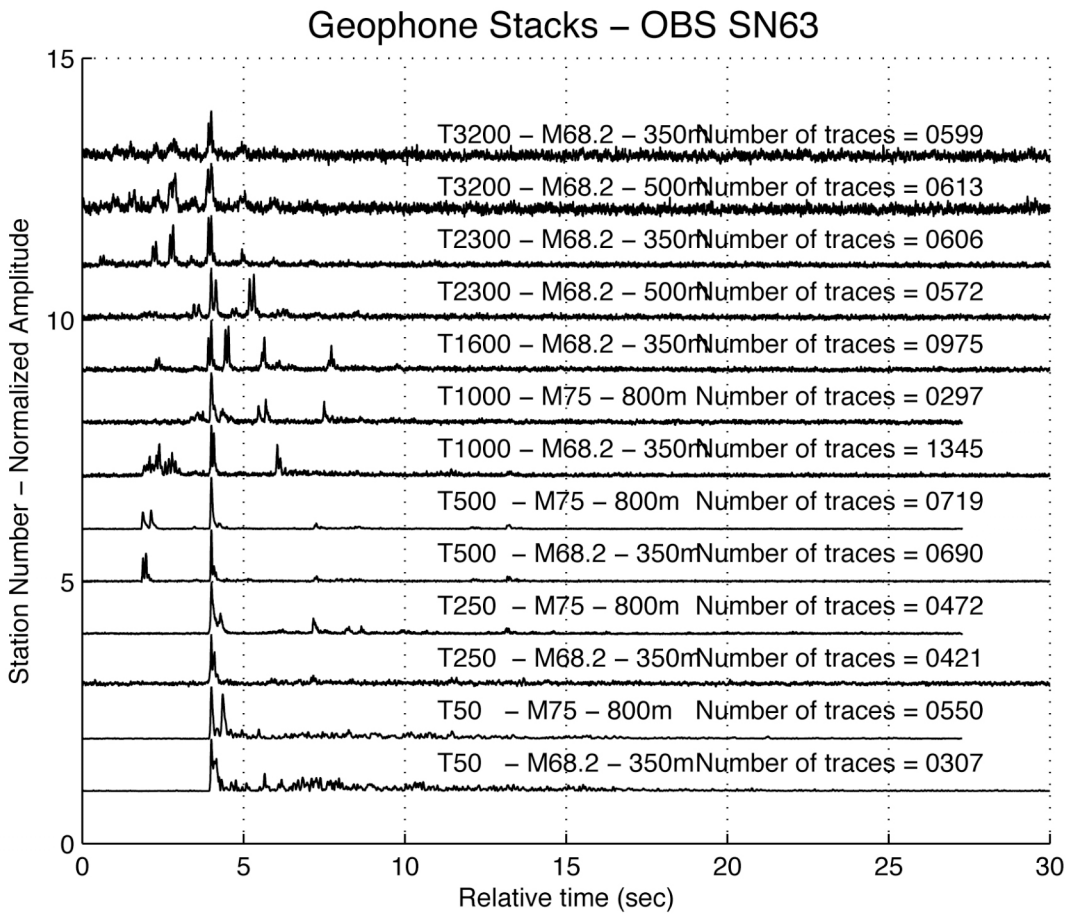

Figure 6-2: The incoherent stacks of the geophone data at the South OBS (SN63, OBS #4) for all of the M-sequence source depth and range combinations. All traces have been time shifted so that the peak magnitude occurs at 4sec and all traces are amplitude normalized to the peak amplitude. Detectable events are seen for all combinations. The M68.2 at 350m depth stacks are the same "geophone" traces that were displayed in Figures 2-1a and 2-2a and that were discussed in Sections 4 and 5e). The M68.2 at 500m depth stacks and the M75 at 800m depth stacks have not yet been studied in detail. A quick comparison with the DVLA stacks in Figure 6-1 shows that, in general, the seafloor geophone has more arrivals spread over a longer time than the DVLA hydrophone. [SN63_Summary.jpg]

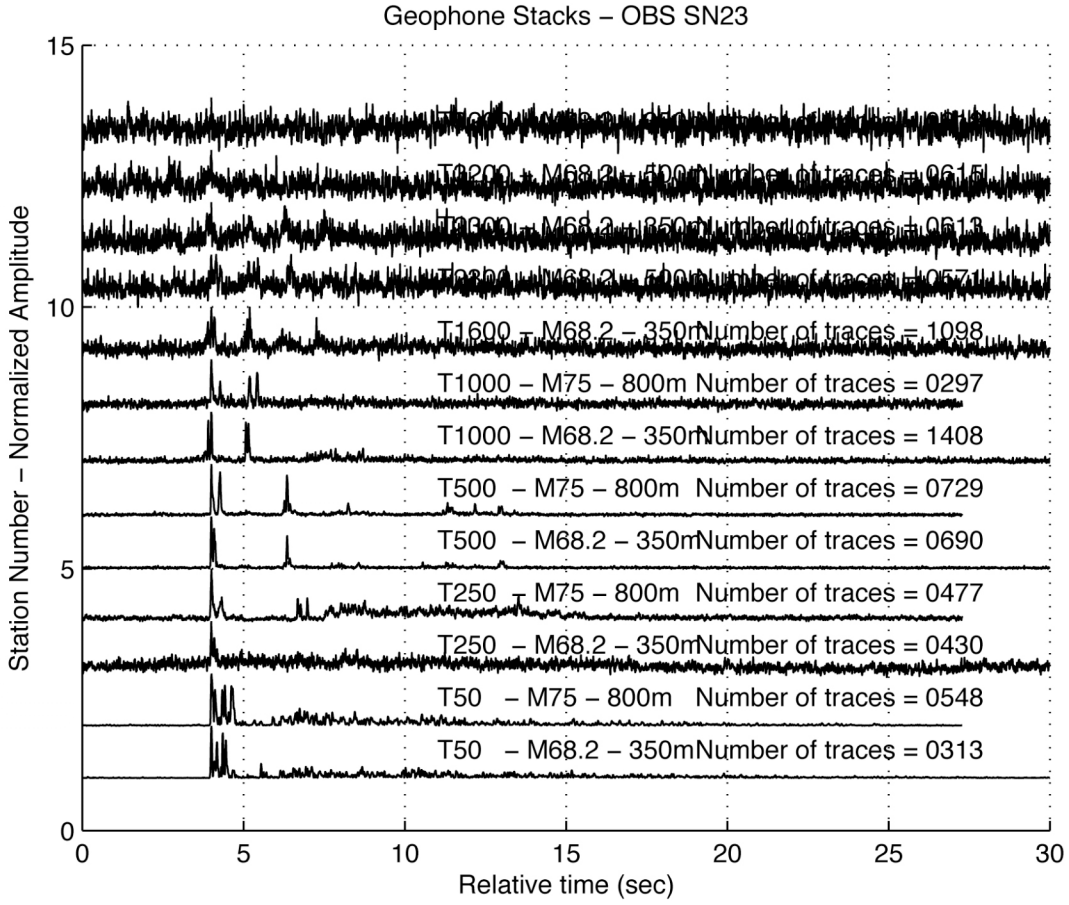

Figure 6-3: The incoherent stacks of the geophone data at the East OBS (SN23, OBS #4) for all of the M-sequence source depth and range combinations. The SNR is not as good as for the South OBS (Figure 6-2) but clear arrivals can still be identified out to T2300. All traces have been time shifted so that the peak magnitude occurs at 4sec and all traces are amplitude normalized to the peak amplitude. None of these stacks have been studied yet in detail. [SN23_Summary.jpg]

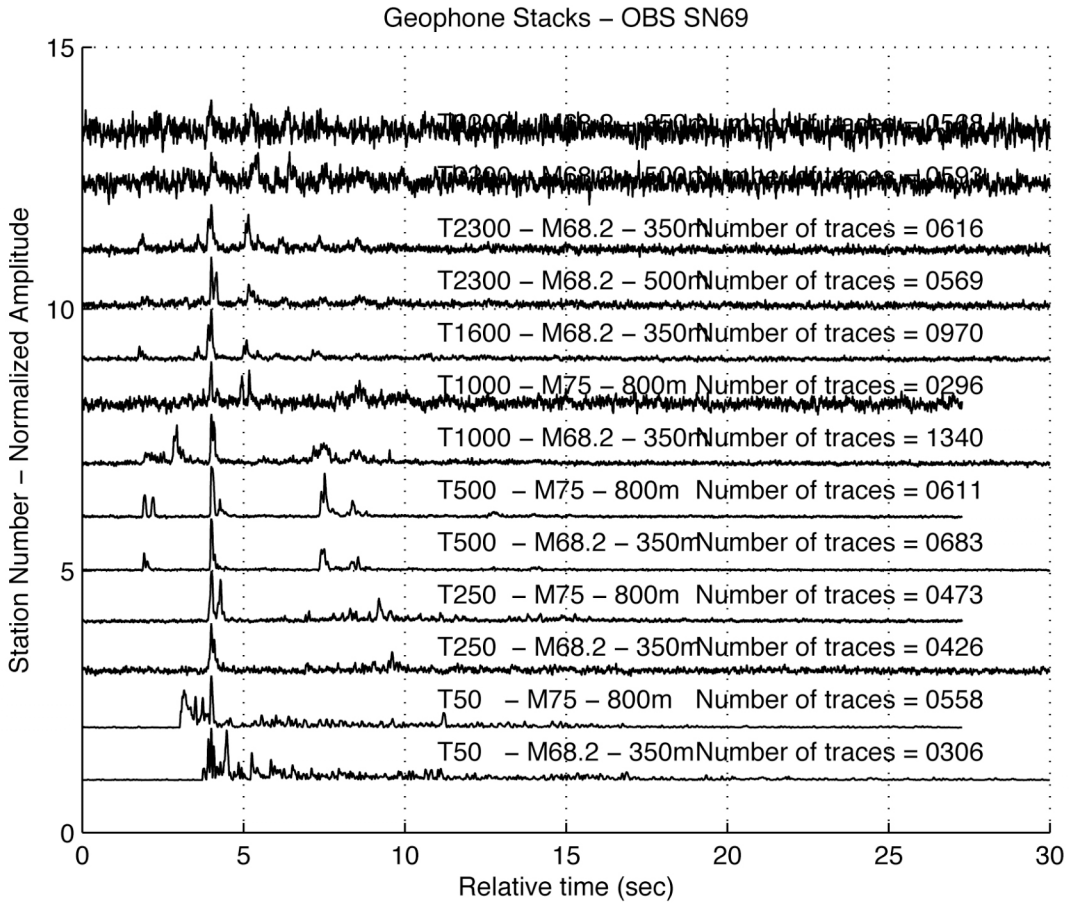

Figure 6-4: The incoherent stacks of the geophone data at the West OBS (SN69, OBS #1) for all of the M-sequence source depth and range combinations. The SNR is not as good as for the South OBS (Figure 6-2) but clear arrivals can still be identified out to T2300. All traces have been time shifted so that the peak magnitude occurs at 4sec and all traces are amplitude normalized to the peak amplitude. None of these stacks have been studied yet in detail. [SN69_Summary.jpg]

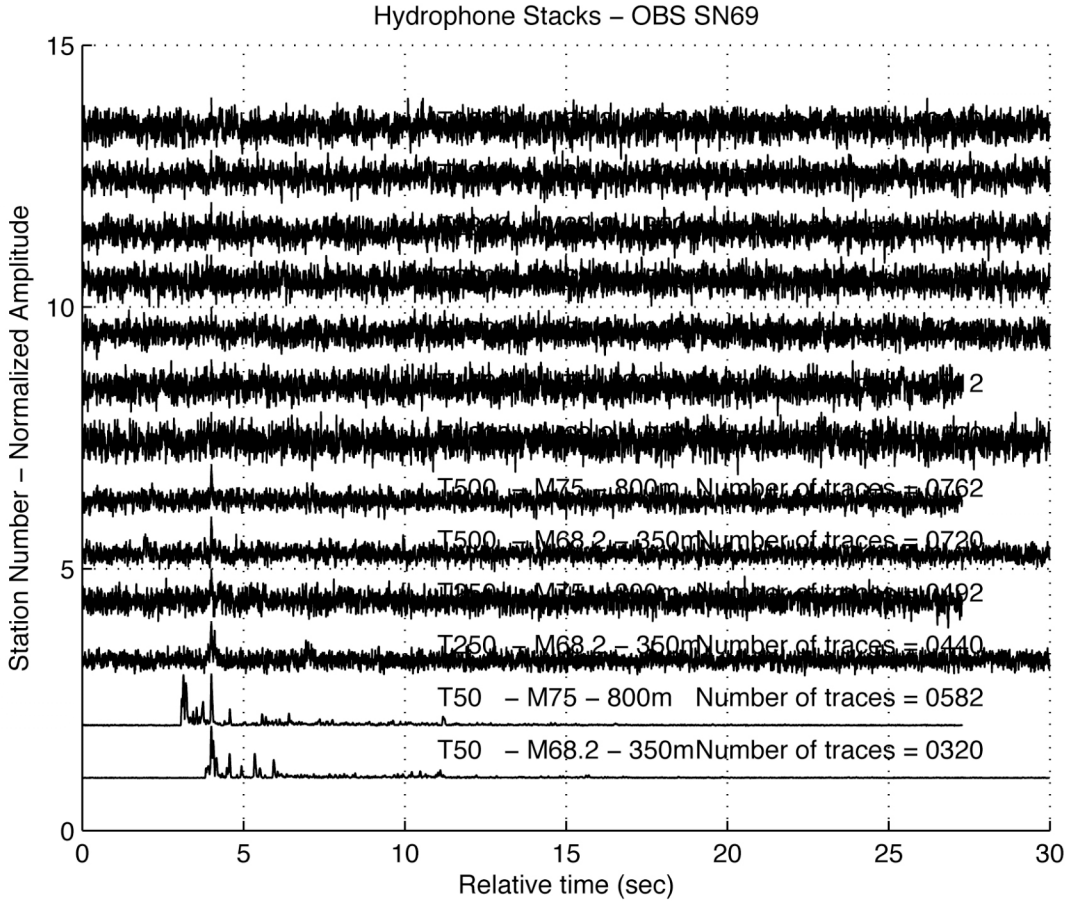

Figure 6-5: The incoherent stacks of the hydrophone data at the South OBS (SN63, OBS #4) for all of the M-sequence source depth and range combinations. The SNR on the OBS hydrophones is much worse than on the OBS geophones but clear arrivals can still be identified out to T500. All traces have been time shifted so that the peak magnitude occurs at 4sec and all traces are amplitude normalized to the peak amplitude. None of these stacks have been studied yet in detail. [SN63_Summary_hyd.jpg]

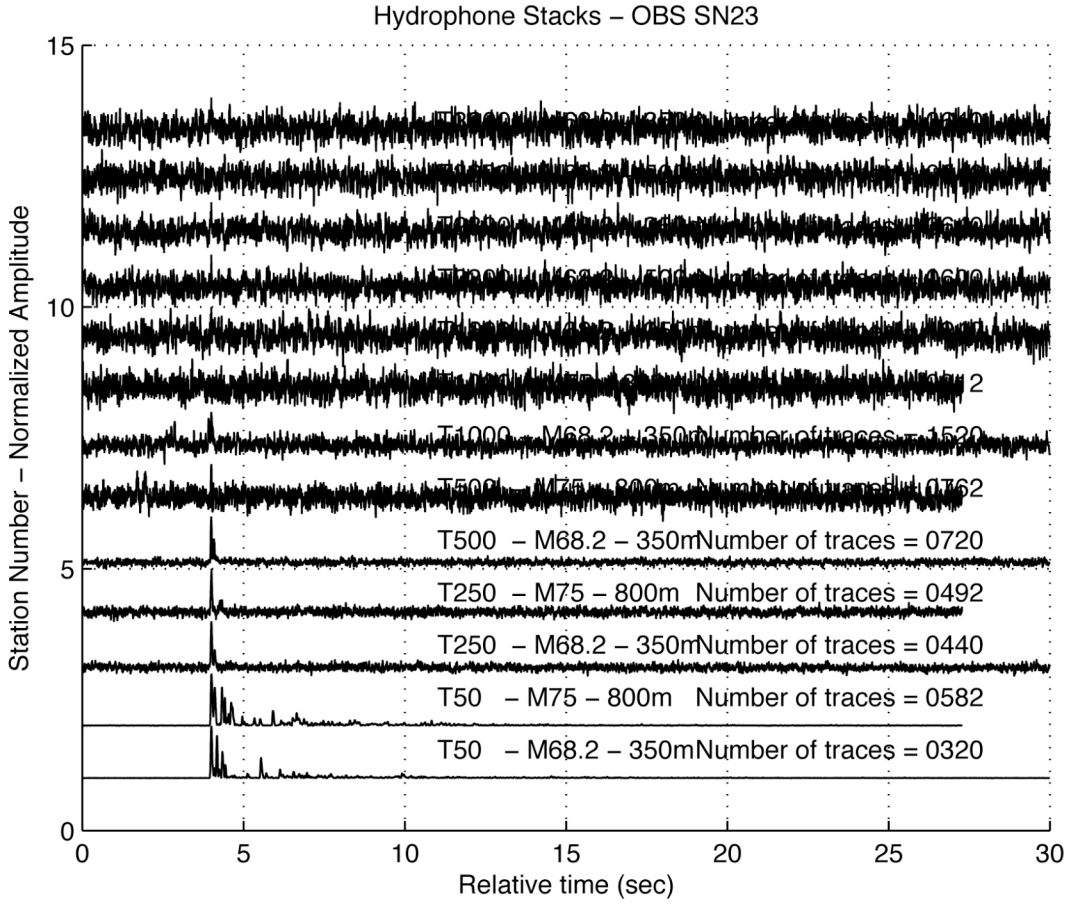

Figure 6-6: The incoherent stacks of the hydrophone data at the East OBS (SN23, OBS #4) for all of the M-sequence source depth and range combinations. The SNR on the OBS hydrophones is much worse than on the OBS geophones but clear arrivals can still be identified out to T1000. All traces have been time shifted so that the peak magnitude occurs at 4sec and all traces are amplitude normalized to the peak amplitude. None of these stacks have been studied yet in detail. [SN23_Summary_hyd.jpg]

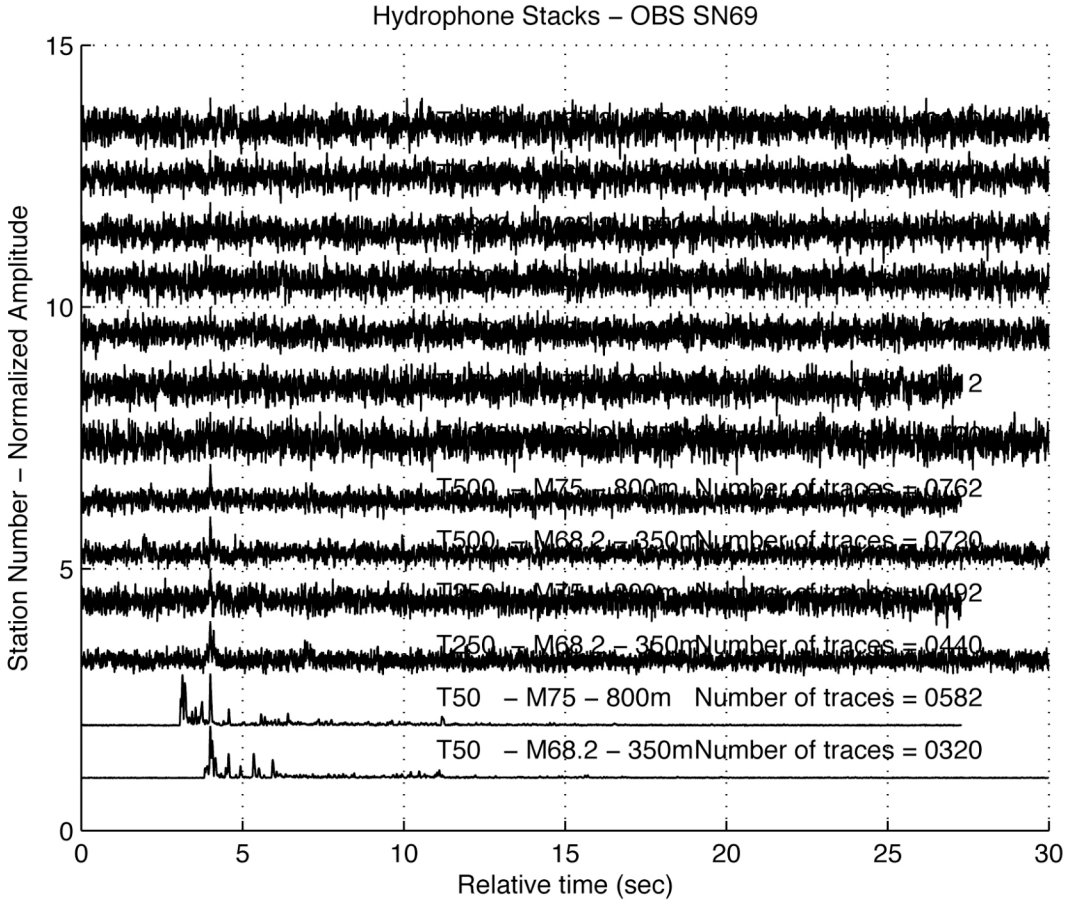

Figure 6-7: The incoherent stacks of the hydrophone data at the West OBS (SN69, OBS #1) for all of the M-sequence source depth and range combinations. The SNR on the OBS hydrophones is much worse than on the OBS geophones but clear arrivals can still be identified out to T500. All traces have been time shifted so that the peak magnitude occurs at 4sec and all traces are amplitude normalized to the peak amplitude. None of these stacks have been studied yet in detail. [SN69_Summary_hyd.jpg]

ACKNOWLEDGMENTS

The LOAPEX source deployments, the moored DVLA receiver deployments and some post-cruise data reduction and analysis were funded by the Office of Naval Research under Award Numbers N00014-1403-1-0181, N00014-03-1-0182 and N00014-06-1-0222. Additional post cruise analysis support was provided to RAS through the Edward W. and Betty J. Scripps Chair for Excellence in Oceanography. The OBS/Hs used in the experiment were provided by Scripps Institution of Oceanography under the U.S. National Ocean Bottom Seismic Instrumentation Pool (SIO-OBSIP - http://www.obsip.org). To cover the costs of the OBS/H deployments funds were paid to SIO-OBSIP from the National Science Foundation and from the Woods Hole Oceanographic Institution Deep Ocean Exploration Institute. The OBS/H data are archived at the IRIS (Incorporated Research Institutions for Seismology) Data Management Center.

REFERENCES

Andrew, R. K. (**2008**), LOAPEX DVLA Time Series, (APL-UW, Seattle, WA).

Collins, M. D., and Westwood, E. K. (**1991**). "A higher-order energy-conserving parabolic equation for range-dependent ocean depth, sound speed, and density " J. Acoust. Soc. Am. **89**, 1068-1075.

Dushaw, B. D., Howe, B. M., Mercer, J. A., and Spindel, R. (**1999**). "Multimegameter-range acoustic data obtained by bottom-mounted hydrophone arrays for measurement of ocean temperature," IEEE J. Ocean. Eng. **24**, 202-214.

Hamilton, E. L. (**1976**). "Sound attenuation as a function of depth in the seafloor," J. Acoust. Soc. Am. **59**, 528-535.

Mercer, J., Andrew, R., Howe, B. M., and Colosi, J. (**2005**), Cruise Report: Long-range Ocean Acoustic Propagation EXperiment (LOAPEX), pp 1-115, (Applied Physics Laboratory, University of Washington, Seattle, WA).

Mercer, J. A., Colosi, J. A., Howe, B. M., Dzieciuch, M. A., Stephen, R. A., and Worcester, P. F. (**submitted**). "LOAPEX: The Long-range Ocean Acoustic Propagation Experiment," IEEE J. Ocean. Eng.

Morse, P. M., and Feshbach, H. (**1953**). *Methods of theoretical physics*, (McGraw-Hill Book Co., Inc., New York).

Munk, W., Worcester, P., and Wunsch, C. (**1995**). *Ocean acoustic tomography*, (Cambridge University Press, Cambridge, U.K.).

Pierce, A. D. (**1989**). *Acoustics: An introduction to its physical principles and applications*, (Acoustical Society of America, Woodbury).

Smith, W. H. F., and Sandwell, D. T. (**1997**). "Global seafloor topography from satellite altimetry and ship depth soundings," Science **277**, 1956-1962.

Stephen, R. A., Bolmer, S. T., Dzieciuch, M. A., Worcester, P. F., Andrew, R. K., Buck, L. J., Mercer, J. A., Colosi, J. A., and Howe, B. M. (**submitted**). "Deep seafloor arrivals: A new class of arrivals in long-range ocean acoustic propagation," J. Acoust. Soc. Am.

Swift, S. A., Lizarralde, D., Hoskins, H., and Stephen, R. A. (**1998**). "Seismic attenuation in upper oceanic crust at Hole 504B," J. Geophys. Res. **103**, 27,193-127,206.

Van Uffelen, L., Worcester, P. F., and Dzieciuch, M. A. (2008), Absolute intensities of acoustic shadow zone arrivals, in *11th NPAL Workshop, Borrego Springs, CA*, edited, Scripps Institution of Oceanography, La Jolla, CA.

Van Uffelen, L. J., Worcester, P. F., Dzieciuch, M. A., and Rudnick, D. L. (**submitted**). "The vertical structure of shadow-zone arrivals at long range in the ocean," J. Acoust. Soc. Am.

Worcester, P. (**2005a**), North Pacific Acoustic Laboratory: SPICE04 Recovery Cruise Report, pp 1-20, (Scripps Institution of Oceanography, La Jolla, CA).

Worcester, P. (**2005b**), NPAL04 Long-Range Propagation Experiment: SPICE04 Plan, (Scripps Institution of Oceanography, La Jolla, CA).

Xu, J. (2007), Effects of internal waves on low frequency, long range, acoustic propagation in the deep ocean, PhD thesis, Woods Hole, MA.

50272-101

REPORT DOCUMENTATION PAGE	1. REPORT NO. WHOI-2008-03	2.	3. Recipient's Accession No.

4. Title and Subtitle
NPAL04 OBS Data Analysis Part 1: Kinematics of Deep Seafloor Arrivals

5. Report Date
December 2008

6.

7. Author(s)
Ralph Stephen et al.

8. Performing Organization Rept. No.

9. Performing Organization Name and Address
Woods Hole Oceanographic Institution
Woods Hole, Massachusetts 02543

10. Project/Task/Work Unit No.

11. Contract(C) or Grant(G) No.
(C)N00014-06-1-0222
(G)

12. Sponsoring Organization Name and Address
National Science Foundation

13. Type of Report & Period Covered
Technical Report

14.

15. Supplementary Notes
This report should be cited as: Woods Hole Oceanog. Inst. Tech. Rept., WHOI-2008-03.

16. Abstract (Limit: 200 words)

These notes provide supporting information for a JASA (Journal of the Acoustical Society of America) LttE (Letter to the Editor) manuscript, "Deep seafloor arrivals: A new class of arrivals in long-range ocean acoustic propagation" (Stephen *et al.*, submitted). It addresses five issues raised by the co-authors: 1) incorrect processing for the time-compressed traces at T2300 and T3200 that appeared in an early version of the LttE (T2300, T3200 … refer to transmissions at 2300, 3200km etc from the DVLA (Deep Vertical Line Array)), 2) processing issues, including the trade-offs between coherent and incoherent stacking and corrections for the effects of moving sources and receivers and tidal currents (Doppler), 4) the distinction between "deep shadow zone arrivals", which occur below the turning points in Parabolic Equation (PE) models, and "deep seafloor arrivals", which appear dominantly on the Ocean Bottom Seismometer (OBS) but are either very weak or absent on the deepest element in the DVLA and do not coincide with turning points in the PE model (some of these OBS late arrivals occur after the finale region), 4) the role of surface-reflected bottom-reflected (SRBR) paths in explaining the late arriving energy, and 5) generally reconciling the OBS analysis with work by other North Pacific Acoustic Laboratory (NPAL) investigators and Dushaw et al (1999).

17. Document Analysis a. Descriptors

ocean bottom seismology
ocean acoustic propagation
bottom interaction

b. Identifiers/Open-Ended Terms

c. COSATI Field/Group

18. Availability Statement
Approved for public release; distribution unlimited.

19. Security Class (This Report)
UNCLASSIFIED

20. Security Class (This Page)

21. No. of Pages
95

22. Price

(See ANSI-Z39.18) *See Instructions on Reverse* OPTIONAL FORM 272 (4-77)
(Formerly NTIS-35)
Department of Commerce